The Dissertation Committee for Vinod K. Valsalam

certifies that this is the approved version of the following dissertation:

Utilizing Symmetry in Evolutionary Design

Committee:

Risto Miikkulainen, Supervisor

Dana Ballard

Benjamin Kuipers

Matthew Campbell

Peter Stone

Utilizing Symmetry in Evolutionary Design

by

Vinod K. Valsalam, B.Tech., M.S.

Dissertation

Presented to the Faculty of the Graduate School of

The University of Texas at Austin

in Partial Fulfillment

of the Requirements

for the Degree of

Doctor of Philosophy

The University of Texas at Austin

August 2010

Acknowledgments

This dissertation was made possible by the excellent support and guidance of my advisor, Risto Miikkulainen. He has been a constant source of ideas and inspiration for pursuing exciting research. Working with him has been an invaluable educational experience.

I would not have started my doctoral studies without the encouragement of Robert van de Geijn. He has continued as a wonderful mentor, providing support and inspiration.

I am very grateful to my committee members, Dana Ballard, Matthew Campbell, Benjamin Kuipers, and Peter Stone for their insightful comments and constructive criticisms.

I wish to express my sincere gratitude to Greg Plaxton for productive discussions on sorting networks, including his suggestion to utilize the zero-one principle.

I am also very grateful to Hod Lipson for the opportunity to design and build a robot at his Cornell Computational Synthesis Laboratory. He and his team of researchers provided expert guidance, making it possible for me to complete the project in two weeks. In particular, I wish to thank Ricardo Garcia, Jonathan Hiller, Robert MacCurdy, Franz Nigl, and Michael Tolley for contributing design ideas and for helping me with unfamiliar tools.

I have benefited immensely from group discussions with the members of the UTCS Neural Networks research group. Their helpful comments shaped my research and their valuable feedback improved my presentations.

Finally, I am most grateful to my family for their love, patience, and support while I took my time to finish the dissertation.

VINOD K. VALSALAM

The University of Texas at Austin

August 2010

Utilizing Symmetry in Evolutionary Design

Publication No. _____

Vinod K. Valsalam, Ph.D.

The University of Texas at Austin, 2010

Supervisor: Risto Miikkulainen

Can symmetry be utilized as a design principle to constrain evolutionary search, making it more effective? This dissertation aims to show that this is indeed the case, in two ways. First, an approach called ENSO is developed to evolve modular neural network controllers for simulated multilegged robots. Inspired by how symmetric organisms have evolved in nature, ENSO utilizes group theory to break symmetry systematically, constraining evolution to explore promising regions of the search space. As a result, it evolves effective controllers even when the appropriate symmetry constraints are difficult to design by hand. The controllers perform equally well when transferred from simulation to a physical robot. Second, the same principle is used to evolve minimal-size sorting networks. In this different domain, a different instantiation of the same principle is effective: building

the desired symmetry step-by-step. This approach is more scalable than previous methods and finds smaller networks, thereby demonstrating that the principle is general. Thus, evolutionary search that utilizes symmetry constraints is shown to be effective in a range of challenging applications.

Contents

List of Tables

List of Figures

Chapter 1

Introduction

Imagine having to design a multilegged robot to explore Mars. Such a robot could navigate the rugged terrains of Mars better than a wheeled robot, but designing a controller for it is more challenging. The controller must coordinate its legs properly, generating robust gaits to navigate different terrains effectively while maintaining its stability. Moreover, the robot should be robust to different environmental conditions, wear and tear, and even failure like losing one or more legs, to reliably complete its mission.

Designing such controllers is an excellent example of the challenges faced in designing complex distributed systems in general. Hand-design is generally difficult and brittle because it is hard to anticipate all operating conditions. Therefore, automatic design utilizing learning techniques such as evolution would be desirable. However, the large design space of such systems often makes evolutionary search ineffective. This dissertation focuses on utilizing symmetry to constrain the search space in a way that makes evolutionary design possible in a range of interesting complex systems.
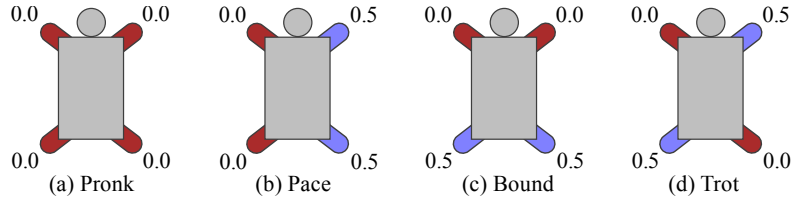
Figure 1.1: Phase relations between legs in the pronk, pace, bound and trot gaits of quadrupeds. The numbers as well as the colors indicate phase of leg movement. In the pronk gait, all four legs move synchronously, while in the other gaits pairs of legs are synchronous and a half-period out of phase with the other pair. These gaits are common in nature and can also be produced in a quadruped robot with appropriate controller symmetries.

1.1 Motivation

Distributed control systems can be modeled as interconnected components called *modules*. For example, the controller for a multilegged robot can be implemented as a system of interconnected neural network modules, each controlling a different leg (Beer et al., 1989). Some of these modules and interconnections may be identical, resulting in *symmetries*, i.e. permutations of modules that leave the solution invariant. Symmetries express constraints crucial for designing effective systems; for instance they determine the type of gaits that a multilegged robot controller can produce (Collins and Stewart, 1993).

In some cases, it is possible to design the appropriate symmetries by hand. For example, the controller symmetries required to produce the common quadruped gaits seen in nature, such as pronk, pace, bound, and trot (Figure 1.1) can be designed analytically (Collins and Stewart, 1993). These symmetries specify which controller modules and interconnections are identical, thus simplifying the design problem to optimizing only the set of modules and interconnections that are actually distinct.

However, it is difficult to design symmetries by hand and it may not even be possible in some cases. For example, if the robot has to walk on an incline, hand-designed solutions are no longer effective. In such cases, the symmetries of the system must be optimized together with the modules and interconnections. Since the system is not constrained by

known symmetries, its design is more challenging. Therefore, an approach to explore the space of symmetries efficiently is essential for designing such systems.

Such an approach has many applications. In addition to multilegged robots, the same approach can be used to design controllers for other distributed systems such as automated manufacturing processes, chemical plants, and electrical power grids. Multiagent systems in which teams of agents interact with each other can also be designed in the same way, i.e by modeling the agents as the modules of the system and their interactions as the connections between the modules. These teams may cooperate to achieve a common goal as in robotic soccer or compete to outdo each other as in online auctions. Moreover, since symmetry is a common phenomenon, an evolutionary approach based on symmetry can potentially be generalized to structural design, such as the sorting networks demonstrated in this dissertation.

1.2 Challenge

Approaches to designing symmetric modular systems have been actively pursued by researchers in the area of *generative and developmental systems* (Gruau, 1994b, Hornby and Pollack, 2002, Miller, 2004, Stanley and Miikkulainen, 2003). These approaches, called *indirect encodings*, combine evolutionary search with abstractions of embryo development, i.e. they evolve genotypes that undergo a developmental process to produce phenotype systems. As a result, they can have a compact search space and can produce symmetric phenotypes through gene reuse (Gruau, 1994b, Sims, 1994a). However, how effectively they can explore different symmetries depends on the genotype encoding, the evolutionary operators, and the genotype-phenotype mapping they use.

Traditionally, indirect encoding approaches simulate the developmental growth process, e.g. by modeling cellular interactions or by using grammatical rewrite rules (Stanley and Miikkulainen, 2003). The resulting mapping from genotype to phenotype is complex, which makes it difficult to evolve the desired phenotypic symmetries through genetic vari-

3

ation. Other approaches have been developed that abstract the developmental process. For example, *HyperNEAT* uses function composition to capture the essential characteristics of this process without implementing it explicitly (Stanley, 2007, Stanley et al., 2009). As a result, phenotypic symmetries can be encoded directly into the genotype as symmetric functions. However, composing a manually specified set of primitive functions may not be an effective way to explore the space of useful symmetries. For example, it was necessary to include external oscillations to quadruped controllers evolved with HyperNEAT to generate gaits, and even such external forcing could not produce the symmetric gaits illustrated in Figure 1.1 (Clune et al., 2009).

These approaches represent symmetry implicitly in the genotype, i.e. they rely on developmental processes and function compositions to produce symmetries in the phenotype. As a result, evolution cannot search for symmetries directly, making it difficult to optimize them. Addressing this issue, this dissertation develops an evolutionary approach that makes symmetry search effective by representing symmetry explicitly.

1.3 Approach

The main insight of this approach is that symmetry is an organizing principle, making it possible to define other essential characteristics of development such as reuse and modularity in terms of symmetry. This approach, called Evolution of Network Symmetry and mOdularity (ENSO), utilizes *group theory*, the mathematical theory of symmetry, to represent symmetries explicitly as the constraints between a given number of modules. The resulting genotype is compact, storing the parameters of identical modules only once, while allowing variations between them to evolve. It uses a simple genotype-phenotype mapping that makes the entire space of phenotype properties easily accessible to evolutionary search.

Group theory exposes the structure of the space of symmetries, making it possible to search for symmetries directly and also to constrain the search to promising regions of the space. ENSO performs this search by defining genetic variation (mutation) operators that

explore the space of symmetries systematically. It initializes evolution with a population of maximally symmetric solutions: They have the simplest possible structure, consisting of identical modules and interconnections. During evolution, mutations break their symmetries systematically, thus exploring less symmetric, more complex solutions with different types of modules and interconnections. As a result, evolution can optimize the modules and interconnections for simpler solutions first and elaborate them to create more complex solutions. Moreover, the systematic, symmetry-breaking mutations constrain search to promising symmetries, making evolution more effective than mutating symmetry unsystematically.

These features make it possible for ENSO to solve complex problems such as the design of distributed controllers and multiagent systems. For instance in this dissertation, ENSO evolves effective neural network controllers for a quadruped robot in physically realistic simulations. The resulting controllers produce robust gaits such as those in Figure 1.1. Moreover, they perform equally well when they are transferred to a physical robot. ENSO also evolves controllers that produce effective gaits for a robot on an incline and for a robot with a faulty leg, scenarios in which the appropriate symmetries are difficult to design by hand.

Thus evolving symmetries through symmetry breaking is effective when solving the problem requires finding the appropriate symmetries. In other problems the symmetries of the solution may already be known, and the challenge is to construct from scratch an optimal solution that possesses those symmetries. As shown in this dissertation, such problems may be amenable to a symmetry building approach. For example, the problem of designing minimal-size sorting networks (Knuth, 1998) can be made easier to solve utilizing this generalization. The source code implementing these approaches is available from the website `http://nn.cs.utexas.edu/?symmetry`.

1.4 Outline of the Dissertation

This dissertation is organized into four main parts: background (Chapters 1-3), symmetry breaking with multilegged robots (Chapters 4-6), symmetry building with sorting networks (Chapter 7), and discussion (Chapters 8-9).

Chapter 2 discusses the biological motivation for the symmetry-breaking principle of ENSO, reviews the fundamental concepts of group theory, and applies those concepts to describe the symmetries of multilegged locomotion and sorting networks.

Chapter 3 is a survey of previous approaches to evolving symmetric and modular systems, designing controllers for multilegged robots, and designing minimal-size sorting networks.

Chapter 4 lays the groundwork for the ENSO approach. It introduces the multilegged robot model used in the simulations, its neural network controller architectures, and shows how evolution constrained with hand-designed symmetries produces better controllers than unconstrained evolution and hand-coding.

Chapter 5 introduces the ENSO approach and describes its genotype, phenotype, and evolutionary mechanisms. ENSO is then utilized to evolve controllers for a quadruped walking on flat ground and a more challenging incline. They are compared with controllers evolved with random symmetry mutations and hand-designed symmetries and are shown to perform better.

Chapter 6 presents the design, manufacture, and experimental evaluation of a physical quadruped robot. ENSO is shown to be an effective method for designing controllers for such robots.

Chapter 7 extends the symmetry-based approach for constraining search to designing minimal-size sorting networks, improving on several previously known best results.

Chapter 8 discusses the implications of results presented in previous chapters and suggests ways to improve them. Several extensions and potential applications of ENSO and symmetry building are proposed.

Chapter 9 summarizes the contributions and concludes this dissertation.

Chapter 2

Foundations

Nature has evolved a variety of symmetric organisms, motivating a symmetry-based approach for the evolutionary design of artificial systems as well. This chapter begins by discussing this motivation and then reviews the group theory concepts required for utilizing symmetry in evolutionary algorithms. To make the approach concrete, these concepts are applied to represent the symmetries of controllers for multilegged robots and those of sorting networks. Representing symmetries in this manner makes it possible to constrain the design space to promising solutions. As a result, large and challenging design problems becomes more tractable, as demonstrated in later chapters.

2.1 Biological Motivation

Symmetry is the product of constraints between identical subsystems. For example, a bilaterally symmetric animal has identical left and right legs that are constrained to be equidistant from its plane of symmetry, and the symmetric neural circuitry controlling its locomotion has identical modules constrained by the nature of their interconnections (Collins and Stewart, 1993). Symmetry in such systems provides two benefits: (1) it can make evolutionary search easier by encoding identical subsystems compactly using a common set

8

of genes, and (2) it can produce useful phenomena such as patterned oscillations in neural circuits, e.g. for effective gaits.

How did organisms with different symmetries evolve in nature? Fossil evidence suggests that more symmetric organisms evolved into less symmetric organisms (Martindale and Henry, 1998, Palmer, 2004). For example, primitive, single-celled organisms like protozoans are highly symmetric with spherical shapes. They evolved into less symmetric organisms such as jelly fish, which have radial symmetry. And radially symmetric organisms in turn evolved into even less symmetric organisms, e.g. the bilaterally symmetric humans. Simply put, nature evolves symmetry through symmetry breaking.

Mutations that break symmetries produce novel phenotypic variations (Palmer, 2004). For example, fiddler crabs, whose males are asymmetric with an oversized claw, evolved from a bilaterally symmetric ancestor. Bilateral symmetry is the default in such organisms, i.e. the same developmental program creates paired, symmetric sides. Breaking this symmetry requires the genome to specify additional information on how one side is different from the other, thus increasing the complexity of the genome.

In fact, symmetry is fundamentally related to complexity, allowing complexity to be characterized as the lack of symmetry (Heylighen, 1999). Increase in complexity of organisms during evolution is accompanied by symmetry breaking at different levels of organization (Garcia-Bellido, 1996). Moreover, *complexification*, i.e. increasing complexity gradually, makes evolutionary search more effective because it allows evolution to start with low-dimensional genotypes, which are easy to optimize, and gradually add more dimensions (Stanley and Miikkulainen, 2004). Building complex systems by elaborating solutions in this manner is more likely to succeed than evolving solutions in the final high-dimensional space directly. Therefore, evolving complex systems from simple symmetric systems by breaking symmetry step-by-step might be a good way to design them.

This idea for focusing evolutionary search on promising solutions motivates the symmetry breaking approach of ENSO discussed in Chapter 5. ENSO represents solutions

as graphs and utilizes group theory to represent the symmetries of those graphs, as described next.

2.2 Symmetries and Group Theory

ENSO evolves modular solutions to design problems. It represents the modules as the vertices and the relationships between them as the edges of a complete graph $G = (V, E)$, where V is the vertex set and $E = \{(u, v) \mid u, v \in V; \ u \neq v\}$ is the edge set. Since G cannot have loops, it is possible to represent a vertex v by the pair (v, v), and thus represent both vertices and edges by the elements of the set $V \times V$. In order to represent the symmetries of G, ENSO assigns every element of $V \times V$ a color, producing a *complete coloring* (Bastert, 2001) of the vertices and edges of G. In practice, each color represents a particular combination of parameters associated with a vertex or an edge. A *symmetry* of G is defined as any permutation of its vertices that preserves the color of edges between them.

The symmetries of a graph can be represented mathematically as a group (Beineke et al., 2004, Chan and Godsil, 1997). A *group* is a set $\mathcal{G}$ of elements closed under a binary operation $\circ$ satisfying the following axioms:

Associativity: For all $g, h, k \in \mathcal{G}$, $(g \circ h) \circ k = g \circ (h \circ k)$.

Identity element: There exists an element $e \in \mathcal{G}$ such that for all $g \in \mathcal{G}$, $e \circ g = g \circ e = g$.

Inverse element: For each $g \in \mathcal{G}$, there is an element $g^{-1} \in \mathcal{G}$ such that $g \circ g^{-1} = g^{-1} \circ g = e$.

The operation $g \circ h$ is usually written more compactly as gh.

A *subgroup* $\mathcal{H}$ of a group $\mathcal{G}$, denoted $\mathcal{H} \leq \mathcal{G}$, is a subset of the group elements of $\mathcal{G}$ satisfying the group axioms under the same operation. If the subset is a proper subset of $\mathcal{G}$, then the subgroup is called a *proper subgroup* of $\mathcal{G}$. A *maximal subgroup* of $\mathcal{G}$ is any proper subgroup $\mathcal{S}$ such that no other proper subgroup $\mathcal{T}$ contains $\mathcal{S}$ strictly. If $\mathcal{G}$ represents the

10

symmetries of a graph G, then its proper subgroup $\mathcal{H}$ represents the symmetries of a less symmetric graph H. ENSO uses this fact to compare graph symmetries.

Two subgroups $\mathcal{S}$ and $\mathcal{T}$ are said to be *conjugate* if there exists an element $g \in \mathcal{G}$ such that $\mathcal{T} = g\mathcal{S}g^{-1}$, i.e. $\mathcal{T} = \{gsg^{-1} \mid s \in \mathcal{S}\}$. Conjugacy is an equivalence relation, partitioning the set of all subgroups of a group $\mathcal{G}$ into equivalence classes called *conjugacy classes*. The subgroups belonging to a given conjugacy class represent graphs with similar symmetries. Therefore, conjugacy classes are useful for characterizing the space of graph symmetries that ENSO has to search.

Figure 2.1 illustrates how the above definitions can be used to represent the symmetries of a completely colored graph with four vertices. Since all edges of graph G_A have the same color, any permutation of its vertices is a symmetry of the graph. In contrast, graph G_B has fewer symmetries because its edges have different colors. The permutation $g = (1\ 2)(3\ 4)$, which swaps vertices 1 and 2 as well as vertices 3 and 4, is a symmetry of G_B. Similarly, the permutation $h = (1\ 3)(2\ 4)$ is another symmetry and their composition hg obtained by performing the two permutations in sequence is yet another symmetry. The trivial permutation $e = ()$, which fixes each vertex of the graph, is also a symmetry. The set of all such symmetries of a graph G is closed under composition and inverse, i.e. it forms a group with composition as the group operation. This group is called the symmetry group or *automorphism group* of G, denoted as $\mathrm{Aut}(G)$.

The automorphism group of graph G_A, consisting of all 4! permutations of its vertex set $V = \{1, 2, 3, 4\}$, is called the *symmetric group* of degree four, denoted as $\mathcal{S}_4$. The automorphism group of the less symmetric graph G_B is a subgroup of $\mathcal{S}_4$ called the *dihedral group* $\mathcal{D}_2$ (and is isomorphic to the symmetries of a regular polygon with two sides, i.e. a line segment). More generally, the automorphism group of any graph G with vertex set $V = \{1, 2, 3, 4\}$ is a subgroup of $\mathcal{S}_4$, and is fully determined by the complete coloring of G. ENSO utilizes this observation to manipulate the symmetries of graphs by changing their coloring.
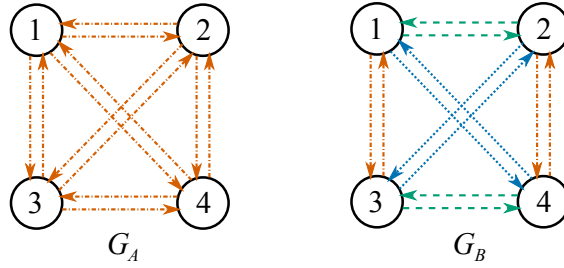
Figure 2.1: Representing graph symmetries using groups. Each vertex and edge has a color (indicated by both color and line style) representing a particular combination of parameters. A graph symmetry is any permutation of vertices under which the edge colors remain the same. Both graphs in this figure have vertices of the same color. All edges of graph G_A have the same color, while edges of graph G_B have different colors. Therefore, any permutation of the vertices of graph G_A is a symmetry. In contrast, only the permutations $g = (1\ 2)(3\ 4)$ and $h = (1\ 3)(2\ 4)$, and their compositions are symmetries of graph G_B. The set of all symmetries of a graph form a group, with composition as the group operation. Thus group theory is a natural way to represent symmetries.

Changing the coloring of a graph G such that its new automorphism group is a subgroup of its original automorphism group is said to *break the symmetry* of G. In order to implement symmetry breaking, ENSO defines a canonical complete coloring of G for any given automorphism group $\mathcal{G}$ using the concept of group action. Formally, the *action* of $\mathcal{G}$ on the vertex set V is a function $\mathcal{G} \times V \rightarrow V$, denoted $(g, v) \mapsto g \cdot v$ for each $g \in \mathcal{G}$ and each $v \in V$, which satisfies the following two conditions:

1. $e \cdot v = v$ for every $v \in V$, where e is the identity element of $\mathcal{G}$, and

2. $(gh) \cdot v = g \cdot (h \cdot v)$ for all $g, h \in \mathcal{G}$ and $v \in V$.

The set of all $w \in V$ to which v is mapped by the elements of $\mathcal{G}$ is called the *orbit* of v. Similarly, the coordinate-wise action of $\mathcal{G}$ on $V \times V$ is defined as $g \cdot (v, w) = (g \cdot v, g \cdot w)$ for any $(v, w) \in V \times V$. The orbits in this action are called *orbitals*, and they form a partition of $V \times V$ called an *orbital partition*. Assigning a different color to each part of this partition produces the desired canonical complete coloring of G.

If a graph G' is produced by breaking the symmetry of G, then the orbital partition ρ' under the action of $\mathrm{Aut}(G')$ is a *refinement* of the orbital partition ρ under the action of

$\mathrm{Aut}(G)$, i.e. each part of ρ' is a subset of a part of ρ. Therefore, the canonical complete coloring of G' can be obtained from that of G by assigning new colors to the parts of ρ' that are a proper subset of a part of ρ and retaining the colors of parts of ρ' that are also parts of ρ. ENSO represents this hierarchical relationship between the colors of G and G' by organizing the new colors of G' as the children of colors of G that they replace. This organization produces a tree of colors when symmetry is broken repeatedly during evolution.

Breaking symmetry in the above manner induces a partial ordering of the graphs based on the subgroup relation between their automorphism groups. More precisely, with subgroup as the partial order relation, the set of all subgroups of a group form a lattice. Figure 2.2 illustrates this lattice for the subgroups of $\mathcal{S}_4$. Nodes of this lattice represent conjugacy classes of subgroups. A group $\mathcal{G}_i$ is placed above another group $\mathcal{G}_j$ and connected by a line if and only if $\mathcal{G}_j$ is a maximal subgroup of $\mathcal{G}_i$. This lattice contains the automorphism groups of all completely colored graphs with vertex set $V = \{1, 2, 3, 4\}$. The most symmetric graphs with automorphism group $\mathcal{S}_4$ are at the top of the lattice, while the least symmetric graphs with the trivial automorphism group $\{e\}$ are at the bottom.

ENSO utilizes this ordering of graphs induced by the subgroup lattice to search the space of graph symmetries systematically. The above group theory concepts can also be utilized to explain the symmetries of the two applications considered in this dissertation: multilegged locomotion and sorting networks. For this purpose, multilegged locomotion is abstracted as coupled cell systems, as described next.

2.3   Locomotion Controllers

A coupled cell system consists of a set of dynamical systems, called cells, and a specification of how the cells are coupled, i.e. how the state of each cell affects the states of the other cells (Golubitsky and Stewart, 2002). Some or all of the cells and couplings may be identical, resulting in symmetries that correspond to permutations of the cells under which
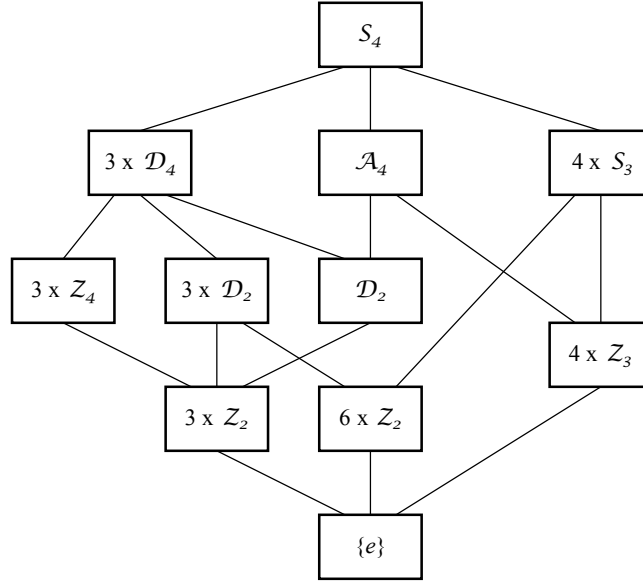
Figure 2.2: Lattice of subgroups of $\mathcal{S}_4$**.** This lattice was computed using the GAP (2007) software for computational group theory and shows the subgroups of the group $\mathcal{S}_4$, which is the symmetric group of degree four containing all $4!$ permutations of the set $V = \{1, 2, 3, 4\}$. Each node of the lattice represents an equivalence class of conjugate subgroups. There are four types of nodes. The node labeled $4 \times \mathcal{S}_3$ represents the four symmetric groups of degree three obtained by fixing each of the four elements of V and permuting only the other three elements. The node labeled $\mathcal{A}_4$ represents the alternating group of degree four, formed by the permutations of V that can be expressed as the composition of an even number of transpositions. The node labeled $\mathcal{D}_n$ represent the dihedral groups, formed by the permutations of V that are isomorphic to the symmetries of a regular polygon with n sides. The node labeled $\mathcal{Z}_n$ represent the cyclic groups, formed by the permutations of V that are isomorphic to the group of integers under addition modulo n. The automorphism groups of all graphs with vertex set V appear in this lattice, inducing a partial order of the corresponding graphs. Thus, the most symmetric graphs with automorphism group $\mathcal{S}_4$ appear at the top and the least symmetric graphs at the bottom of the lattice, with the trivial automorphism group $\{e\}$ at the very bottom. This order makes it possible for ENSO to search the space of graph symmetries systematically by traversing the lattice from top to bottom.

the behavior of the system is invariant. Such symmetric, coupled cell systems can exhibit synchronous and phase-related periodic patterns in their state. Collins and Stewart (1993) showed that this patterned behavior can be used to model animal locomotion and to explain gait symmetries.

Following their method, the modular controllers in this dissertation are also modeled as symmetric coupled cell systems. The patterned oscillatory behavior produced by these symmetries is independent of the model parameters, i.e. the details of the internal dynamics of the cells do not matter. Therefore, analyzing the symmetries of a coupled cell system can give insights into the high-level qualitative behavior of the system.

This analysis is illustrated below for a coupled cell system due to Pinto and Golubitsky (2006). While they used this system to understand biped locomotion, it is adapted in this review to model quadruped gaits. This system consists of four identical cells, described by the following system of ordinary differential equations (ODEs):

$$\begin{cases} \dot{\mathbf{x}}_1 = F(\mathbf{x}_1, \mathbf{x}_2, \mathbf{x}_3, \mathbf{x}_4) \\ \dot{\mathbf{x}}_2 = F(\mathbf{x}_2, \mathbf{x}_1, \mathbf{x}_4, \mathbf{x}_3) \\ \dot{\mathbf{x}}_3 = F(\mathbf{x}_3, \mathbf{x}_4, \mathbf{x}_1, \mathbf{x}_2) \\ \dot{\mathbf{x}}_4 = F(\mathbf{x}_4, \mathbf{x}_3, \mathbf{x}_2, \mathbf{x}_1), \end{cases} \tag{2.1}$$

where $\mathbf{x}_i \in \mathbf{R}^k$ are the k state variables of cell i, and $F : (\mathbf{R}^k)^4 \rightarrow \mathbf{R}^k$ encapsulates the internal dynamics of each cell and its coupling with other cells. Thus, this system of ODEs describes how the state variables of each cell change in time as a function of the cell's own state and the state of the other cells.

This system can be represented by the graph in Figure 2.3, which helps visualize its symmetries. The vertices of the graph represent cells and the edges represent coupling between the cells. Each edge color represents a different type of coupling, corresponding to a different argument position in the function F. This graph is the same as the graph G_B of Figure 2.1 in Section 2.2, where its symmetries were analyzed. In particular, its
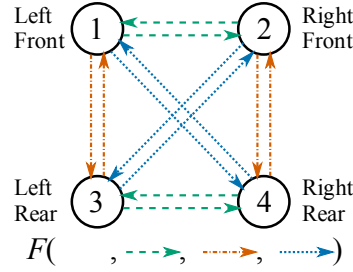
Figure 2.3: Graph corresponding to the coupled cell system in equation (2.1). The vertices, numbered 1 through 4, represent cells and the edges represent coupling between the cells. The different edge colors (also indicated with different line styles) represent different couplings, corresponding to different argument positions in function F as shown in the legend. This graph helps visualize the symmetries of the coupled cell system and shows how the cells may be assigned to control the legs of a quadruped robot to produce different gaits (Figure 1.1). For example, these symmetries can constrain cells 1 and 2 to oscillate synchronously with phase opposite to that of similarly synchronous cells 3 and 4, producing the bound gait.

automorphism group is $\mathcal{D}_2$, consisting of the symmetric permutations $g = (1\ 2)(3\ 4)$, $h = (1\ 3)(2\ 4)$, and their composition hg.

Each symmetry of the graph induces a symmetry of the associated system of ODEs, i.e. a transformation γ such that $\gamma \mathbf{x}(t)$ is a solution whenever $\mathbf{x}(t)$ is a solution. For example, suppose $\mathbf{x}(t)$ is a solution to (2.1). Applying the permutation g to (2.1) produces an equivalent system of ODEs for which $g\mathbf{x}(t)$ is a solution. Thus, the system of ODEs inherits the symmetry g from the corresponding graph.

In particular, periodic solutions of the system are interesting because they model gaits. Let $\mathbf{x}(t)$ be a T-periodic solution to (2.1) and γ be a symmetry. Then $\gamma \mathbf{x}(t)$ is also a solution. Because solutions to the same initial conditions are unique, if $\mathbf{x}(t)$ and $\gamma \mathbf{x}(t)$ are the same trajectory, then their phases must be different, i.e. $\gamma \mathbf{x}(t) = \mathbf{x}(t + \theta)$ where $\theta \in [0, T)$ for all t. Since applying either g twice or h twice to a solution is equivalent to applying the identity, $2\theta \equiv 0 \pmod{T}$ for both symmetries. Therefore, the possible values of phase shift θ is either 0 or $\frac{T}{2}$ for both symmetries.

Such phase shifts impose constraints on the components of the solution $\mathbf{x}(t) = (\mathbf{x}_1(t), \mathbf{x}_2(t), \mathbf{x}_3(t), \mathbf{x}_4(t))$, producing specific patterned behavior for the system. For ex-

	Pronk	Pace	Bound	Trot
θ_g	0	$\frac{T}{2}$	0	$\frac{T}{2}$
θ_h	0	0	$\frac{T}{2}$	$\frac{T}{2}$

Table 2.1: Gaits corresponding to different combinations of phase shifts θ_g and θ_h associated with two permutation symmetries g and h of the coupled cell system in Figure 2.3. Thus, this system can have solutions modeling a variety of common quadruped gaits.

ample, the bound gait pattern results from the following constraints. The symmetry g is first applied to $\mathbf{x}(t)$ with a phase shift of $\theta_g = 0$, resulting in the constraints $\mathbf{x}_2(t) = \mathbf{x}_1(t)$ and $\mathbf{x}_4(t) = \mathbf{x}_3(t)$. Consequently, the solution has the form $\mathbf{x}(t) = (\mathbf{x}_1(t), \mathbf{x}_1(t), \mathbf{x}_3(t), \mathbf{x}_3(t))$, implying that cells 1 and 2 are synchronous and cells 3 and 4 are synchronous, but their synchrony is independent, i.e. it does not yet produce an interesting gait. However, applying the symmetry h to this solution with a phase shift of $\theta_h = \frac{T}{2}$ results in a further constraint $\mathbf{x}_3(t) = \mathbf{x}_1(t + \frac{T}{2})$. Now, the solution has the form $\mathbf{x}(t) = (\mathbf{x}_1(t), \mathbf{x}_1(t), \mathbf{x}_1(t + \frac{T}{2}), \mathbf{x}_1(t + \frac{T}{2}))$, implying that cells 1 and 2 are synchronous, while cells 3 and 4 are also synchronous with the same periodic trajectory as cells 1 and 2, but half-period out of phase. Assigning these cells to control the legs of a quadruped robot as illustrated in Figure 2.3 produces a bound gait (Figure 1.1c).

Other common quadruped gaits (such as those depicted in Figure 1.1) can be obtained similarly by selecting different combinations of values for θ_g and θ_h as shown in Table 2.1. Although these gaits are possible solutions of the system, whether any particular gait can be obtained in an instance of the system depends on the details of the cell dynamics and the couplings, i.e. on the function F in the ODEs. Chapter 4 shows that this function F can be designed effectively by utilizing modular neuroevolution, i.e. by representing each cell as a neural network module and evolving its weights. The resulting controllers produced all four gaits listed in Table 2.1.

The above theoretical results make the gait-production capabilities of such modular controller networks easy to understand. Consequently, in contrast to other approaches, these

controllers are easy to design and scale well to robots with more legs and more complex legs (Chapter 4). Moreover, neuroevolution is an effective alternative to designing coupled cell system ODEs manually such as was done, e.g. by Collins and Stewart (1993),Kimura et al. (1999), Seo and Slotine (2007), and Righetti and Ijspeert (2008). In Chapter 5, the ENSO approach extends modular neuroevolution by also evolving the symmetries of the system. As a result, ENSO can evolve controllers that produce effective gaits even when such gaits are unknown and manual design of the required symmetries is difficult.

The ENSO approach is useful in problems such as distributed control and multiagent systems for which the appropriate symmetries are unknown. In other design problems, the appropriate symmetry of the solution may be known, and a better approach may be to construct an optimal solution with that symmetry. The next section discusses an application for such an approach, i.e. designing minimal-size sorting networks.

2.4 Sorting Networks

A sorting network of n inputs is a fixed sequence of comparison-exchange operations (comparators) that sorts all inputs of size n (Knuth, 1998). For example, Figure 2.4 illustrates a 4-input sorting network. The horizontal lines of the network receive the input values $\{x_1, x_2, x_3, x_4\}$ at the left. Each vertical line represents a comparison-exchange operation that takes two values and exchanges them if necessary such that the larger value is on the lower line. As a result of these comparison-exchanges, the output values appear at the right side of the network in sorted order: $\{y_1 \leq y_2 \leq y_3 \leq y_4\}$.

Since the same fixed sequence of comparators in a sorting network can sort any input, it represents an oblivious or data-independent sorting algorithm, i.e. the sequence of comparisons does not depend on the input data. Their resulting fixed communication pattern makes them desirable in parallel implementations of sorting, e.g. on graphics processing units (Kipfer et al., 2004). For the same reason, they are also simpler to implement in hardware and are useful as switching networks in multiprocessor computers (Batcher,
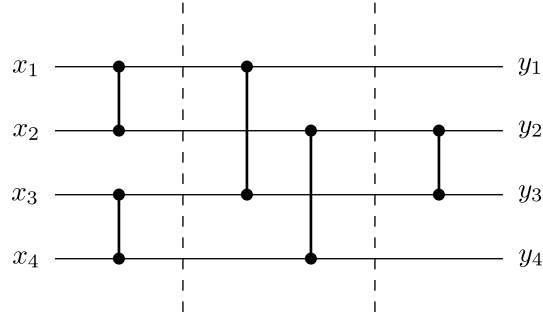
Figure 2.4: A 4-input sorting network. The input values $\{x_1, x_2, x_3, x_4\}$ at the left side of the horizontal lines pass through a sequence of comparison-exchange operations, represented by vertical lines connecting pairs of horizontal lines. Each such comparator sorts its two values, resulting in the horizontal lines contain the sorted output values $\{y_1 \leq y_2 \leq y_3 \leq y_4\}$ at the right. Those comparators that are non-overlapping are grouped into parallel steps separated by the vertical dashed lines. This network is minimal in terms of both the number of comparators and parallel steps. But such minimal networks are not known in general for other input sizes and designing them is a challenging optimization problem.

1968). Driven by such applications, sorting networks have been the subject of active research since the 1950's (Knuth, 1998). Of particular interest are minimal-size networks that sort utilizing a minimal number of comparators and minimal-delay networks that sort in minimal number of (parallel) time steps. Designing such networks is a hard combinatorial optimization problem, which this dissertation shows how to make more tractable utilizing their symmetries.

The outputs of any n-input sorting network are invariant to any of the $n!$ permutations of its inputs because the sorted order at its outputs remains the same. Therefore, it has symmetry group $\mathcal{S}_n$ with respect to permutations of its input variables. Moreover, swapping the outputs of every comparator in the network to move the larger values to their respective upper lines creates a dual network producing outputs in reversed sorted order. This duality can also be expressed formally as symmetries by utilizing the *zero-one principle* (Knuth, 1998) to represent the network outputs as Boolean functions. According to this principle, if the network sorts all 2^n binary sequences correctly, then it will also sort any arbitrary

sequence of n numbers correctly. Therefore, it is possible to represent the network inputs as Boolean variables and its outputs as Boolean functions of those variables.

The symmetries of the network can then be defined as the symmetries of its set of output functions. Since the output functions are known, the network symmetries are also known, making it possible to develop an approach for minimizing the number of comparators in the network by building its symmetries step by step. This approach will be discussed in Chapter 7.

2.5 Conclusion

Symmetry is ubiquitous in nature and in engineering, imposing constraints on system design. Nature utilizes these constraints with evolution to search the design space effectively. A similar approach may be useful with artificial evolution to design complex engineered systems. This dissertation explores this hypothesis in two domains: (1) designing controllers for multilegged robots, and (2) designing sorting networks with minimal number of comparators. The next chapter reviews previous research on these topics.

Chapter 3

Related Work

Nature utilizes a developmental process to construct organisms from the information encoded in their genomes. Constraints for producing regularities and symmetries are encoded in the genome as well as in the developmental process itself. Most computational approaches for evolving symmetry, including ENSO, are based on abstractions of this developmental paradigm. This chapter begins with a review of these approaches, called *indirect encodings*. It is followed by a review of previous research on designing controllers for multilegged robots, a challenging problem that is used in later chapters to evaluate ENSO's capabilities to evolve symmetric solutions. The problem of minimizing the size of sorting networks is also reviewed since it is later used to demonstrate that symmetry constraints can make combinatorially hard search problems easier to solve.

3.1 Indirect Encodings

Most indirect encodings were developed for evolving artificial neural networks. Kitano (1990) evolved matrix rewrite rules that produce the adjacency matrix of neural networks through a series of rewrite steps. His method was based on *L-systems*, that is, grammatical string rewrite rules first developed by Lindenmayer (1968) to model the biological growth

of plants, yielding complex tree-like structures that resemble fractals. Kitano's scheme produced such structures from an initial 2×2 matrix, whose symbols were rewritten iteratively with other 2×2 matrices, creating larger and larger matrices. Repeating the symbols in the matrix creates regularities and symmetries. The rewriting stopped when the current matrix contained only numerical values, and the result was then interpreted as a neural network's adjacency matrix. Kitano evolved such networks to solve encoder/decoder problems. However, because their size is exponential in the number of rewrite steps, these networks were typically very large. Evolving detailed connectivity between network units were also difficult.

Boers and Kuiper (1992) used a different L-system to evolve the topology of modular neural networks. Their system was based on context-sensitive graph rewriting to describe neural network topologies. Rule strings were repeated and rules applied recursively to obtain modular network architectures with symmetries. Boers and Kuiper evolved only the architecture of the networks in this manner; the connection weights were subsequently optimized using the backpropagation algorithm (Chauvin and Rumelhart, 1995, Rumelhart et al., 1986). Using this method, they evolved solutions for problems such as XOR and shape recognition. Because backpropagation was used for learning the connection weights, the networks were limited to feed-forward architectures.

Sims (1994a) used another type of generative graph-based encoding to evolve virtual creatures in simulated physical environments. He used directed graphs as genotypes to encode developmental instructions for constructing the morphology of the creatures. The nodes of the graph contained information on synthesizing body parts, while its edges specified the order in which to synthesize them. Multiple edges to the same child node resulted in reuse of body parts, which is useful for creating multiple instances of limbs and symmetries. Recursive edges were also possible, producing repetitive, fractal-like morphologies. The neural network control circuitry of the creature was embedded in the genotype graph and evolved along with its morphology. Although the developmental mechanism in this

method was elementary, the resulting creatures were significantly regular and often symmetry and capable of a variety of interesting locomotive behaviors.

Gruau (1994b), Gruau and Whitley (1993) and Gruau et al. (1996) also used graphs as genotypes in a method called *cellular encoding* (CE), which was inspired by the way biological development occurs through cell division. The genotype encodes a program tree for constructing a neural network from a single ancestral cell. These program trees were then evolved using standard techniques for genetic programming (Koza et al., 1996). The nodes of the tree contained cellular developmental instructions, such as for splitting a cell into two, deleting a connection between two cells, or changing the weight of a connection. A full neural network was built by executing these instructions in the sequence specified by the edges of the program tree. Gruau et al. showed that networks with repeated structures can be produced by using a recursion instruction that transfers control of development back to the root of the program tree. He evolved such networks to solve problems with regularity such as finding the parity and symmetry of a set of binary digits.

Luke and Spector (1996) identified several weaknesses in CE and proposed *edge encoding* (EE) as an alternative to address many of those concerns. For example, crossover in CE can produce drastic changes in the phenotype of an offspring, which may be problematic for evolution in many domains. Moreover, the networks produced by CE tend to be highly interconnected because they are grown by splitting cells into two or more interconnected cells. Such networks are a disadvantage in domains where such high connectivity is not required, requiring the extra weights to be optimized. CE also does not provide a convenient mechanism to tune connection weights because cells, not connections, are the target of its development instructions. In contrast, EE grows networks by modifying edges rather than cells, thereby avoiding these problems of CE and making it more effective in many domains. However, although both CE and EE are expressive enough to produce all possible graphs, it is not clear how their particular biases affect their performance on any given problem.

In a domain similar to Sims' simulated 3D virtual creatures, Hornby and Pollack (2002) combined ideas of CE and EE with L-systems to evolve the body and brain of such creatures simultaneously. They used strings of build commands to construct the neural network brains instead of the trees as in CE. These build commands operate on connections in the network as in EE. They defined a different set of commands for building body parts of the creatures. The separate command languages for building the body and brain were then combined using an L-system, and evolved. The resulting creatures were more complex, having more parts and regularity, and they were able to walk faster than similar creatures evolved using a non-developmental encoding. They were also more complex than the creatures produced by Sims.

Bongard and Pfeifer (2001) also evolved similar virtual creatures, but by using an abstraction of *genetic regulatory networks* (GRNs) for encoding bodies and neural networks. GRNs model gene expression inside biological cells, i.e. the interactions between genes as they regulate each other during the production of proteins (Kauffman, 1993). In Bongard and Pfeifer's work, the creature begins development as a single spherical unit. Depending on the concentrations of gene products inside this unit, it grows in size and eventually divides into two child units. These units are attached to each other by a joint. Each unit contains a small neural network, which develops according to a variant of the CE method. In this variant, different gene products trigger different operations that modify the local network. The development continues until a fixed number of time steps is reached. Using this method, the authors produced creatures with hierarchical repeated structures in the task of pushing a block.

Dellaert and Beer (1996) had previously used an abstraction of GRNs called *random Boolean networks* (RBNs) to evolve simulated agents capable of following curved lines. In their method, cells representing the body of the agent developed first. A neural network developed on top of the arrangement of these cells when specialized cells sent out axons, making connections with other cells within its range. A similar neural network developmental

model was used by Cangelosi et al. (1994) to create organisms that seek out food and water. Their networks grew in a two-dimensional space using processes such as cell division and axon growth. Kodjabachian and Meyer (1998) also used connection growth mechanisms in their geometry-oriented version of CE called SGOCE. Utilizing similar ideas of development, Miller (2004) evolved developmental programs that could construct the French flag (i.e. adjoining rectangular regions of blue, white, and red colors) and repair damages in it.

In the above methods, small changes in the genotype often produce unpredictable changes in the phenotypes. Steiner et al. (2009) proposed to reduce this effect by manipulating the phase space of the dynamic system of the GRN directly. Moreover, GRN-based approaches abstract biological development at levels lower than those of graph-based methods by modeling biological growth processes in varying detail. However, detailed simulation of biological processes are computationally expensive, and may be unnecessary or even counterproductive (Dellaert and Beer, 1996). Therefore, determining the right level of developmental abstraction for indirect encodings is an important research topic.

Addressing this issue of abstraction, Stanley (2007) proposed an indirect encoding called *Compositional Pattern Producing Networks* (CPPNs) that eliminates the traditional local interaction and temporal unfolding mechanisms of developmental systems. Instead, he argued that the effects of such mechanisms can be obtained by composing specific functions in the appropriate order, i.e. by constructing a CPPN. The patterns produced by a CPPN are interpreted as the spatial connectivity patterns of a neural network using a method called *HyperNEAT*. Stanley et al. (2009) applied this method to tasks having a large number of inputs and regularities, such as robot food gathering and visual object discrimination.

All the above methods provide mechanisms for reuse of genes and repetition of phenotypic substructures, thus encouraging modularity. The developmental process also sometimes produces symmetries in the modular phenotypes, especially if symmetric and periodic functions are used in the encoding. In contrast, the ENSO approach presented in this dissertation utilizes symmetry as an organizing principle to constrain other character-

istics of development such as reuse and modularity automatically (Chapter 5). As a result, it can search the space of symmetric solutions effectively by breaking symmetry systematically. This claim is evaluated in the task of evolving robust locomotion controllers for multilegged robots. Previous research on this task is reviewed next.

3.2 Multilegged Locomotion

Efforts to build legged machines began more than a century ago. Early designs required humans to control the machines, but in the 1970s computer control became a viable alternative to human control. In the 1980s, Raibert and his coworkers built legged hopping and running machines (Raibert, 1986, Raibert et al., 1986). They started with a single-legged algorithm that alternates between a support phase and a flight phase. This algorithm was generalized to control biped running by alternating support and flight between the two legs. The same approach was then extended to quadruped gaits in which pairs of legs move in unison (in pace, bound and trot), by applying the biped algorithm to the paired legs. Thus these early hand-designed controllers also had symmetric designs with algorithmic modules.

Brooks (1989), another pioneer in robotics, constructed controllers for a six-legged robot named Genghis incrementally. These controllers were completely decentralized networks of augmented finite state machines (AFSMs), some of which were repeated in the network to replicate the functionality for each leg. Each step of the incremental construction produced viable controllers for increasingly complex behaviors such as standing up, walking, and following moving objects. His work also showed that robust walking behaviors can be produced by distributed sensorimotor control units with limited central coordination. The controllers that ENSO evolves implement the same idea: Each module produces control signals for a leg through proprioceptive sensing of joint angles without central coordination.

The distributed nature of legged locomotion has also been observed in insects. Such observations inspired the distributed neural network hexapod controller hand-designed by

Beer et al. (1989). The network uses leaky integrator neurons, each with a different functionality such as sensing and producing rhythmic signals. The controllers produced stable gaits that are resistant to damage, such as the loss of a sensor or some connections in the neural network. In another approach, they used a genetic algorithm to find parameter values for the controller network (Beer and Gallagher, 1992). As in the ENSO approach, the evolutionary search space was shrunk by organizing the controller into subnetworks, producing a reduced set of parameters for evolution to optimize.

Other approaches to controller design for legged robots typically have a similar flavor, i.e. implementing controllers as continuous-time recurrent neural networks (CTRNNs) organized into distributed modules. For example, Billard and Ijspeert (2000) hand-designed CTRNN networks for controlling Aibo robot dogs. Their networks, consisting of oscillator modules for each joint, were able to walk, trot and gallop. More recently, Téllez et al. (2006) evolved CTRNNs in the same task. Because of the difficulty of evolving walking behaviors, network modules were evolved in stages, using more complex fitness evaluations in each successive stage. Each stage represented a different abstraction of the task, resulting in a distributed and hierarchical architecture for the controller.

Bull et al. (1995) evolved gaits for their wall-climbing quadruped robot using an extreme version of distributed control, in which controllers for each leg were modeled as communicating agents in a multiagent system. They found that such controllers performed better than a single-agent controller that was responsible for moving all four legs of the robot. Thus their experiments showed that modular, distributed control (similar to the controllers that ENSO evolves) can be more effective than monolithic control in some domains.

Another approach to evolving modular controllers is based on utilizing the modularity and symmetry produced by indirect encodings. During development of the controller, the same parts of the program may be read multiple times, once for each module instantiation. When modules are represented intrinsically in the genotype in this manner, evolution can discover them automatically. Gruau (1994a,b) demonstrated this capability by evolving

CTRNN controllers for hexapod locomotion using his cellular encoding (CE) method. Subsequently, Filliat et al. (1999) used SGOCE, the geometry-oriented version of CE, to evolve CTRNN controllers incrementally for a hexapod, although their scheme required that the precursor cells for module subnetworks be specified explicitly.

In the above evolutionary methods, fitness of controllers was evaluated by simulating the physical behavior of robots and their environments. Such experiments are useful because they allow testing a range of conditions effectively. However, simulation may not always produce accurate enough results when the evolved controller needs to be transferred to a physical robot (Jakobi, 1998). In such cases, fitness evaluation must be done using real robot hardware. Hornby et al. (1999, 2000) for instance did so for the quadruped robot Aibo. They evolved locomotion parameters for different Aibo gaits by measuring how fast the robot walked inside a pen. Similarly, Kohl and Stone (2004a,b) obtained faster gaits for the Aibo by also performing evaluations on physical robots to optimize walk parameters, and Zykov et al. (2004) used hardware evaluations to evolve controller parameters for a nine-legged robot equipped with pneumatic actuators. In contrast, Miglino et al. (1995) showed that controllers evaluated using a realistic simulation of the Khepera robot transferred well to the actual physical Khepera.

The conclusion is that evolution using simulated fitness evaluations can be highly productive if the simulation is realistic enough and the evolved controllers are robust enough. Therefore, ENSO evolves robust controllers based on physically realistic simulations. This approach makes it possible to test a wide range of designs in a wide range of conditions, and thereby can potentially come up with creative solutions. Moreover, the evolved controllers produced the same gaits and performed well when they were transferred to a physical robot.

Recent progress in building sophisticated physical robots was summarized by Holmes et al. (2006). They also discussed the role of mathematical models of body-limb and environment dynamics, central pattern generators, and proprioceptive and environmental sensing in the design of a very agile six-legged robot called RHex. The sprawled posture and

compliant legs of RHex, inspired by characteristics found in insects, allows the robot to be stable and operate dynamically even on rocky and uneven terrain (Koditschek et al., 2004). The stability is achieved through open-loop control utilizing only proprioceptive feedback. Similarly, the Sprawl hexapedal robot uses open-loop control for stable running (Clark, 2004). Along the same lines, the modular controllers that ENSO evolves perform well utilizing only proprioceptive sensing of joint angles.

In nature, the control systems of animals evolved together with their body morphology, resulting in tightly integrated, efficient agents. Inspired by this observation, several researchers have evolved both the controller and the robot morphology concurrently. Examples of such body-brain evolution include the virtual block creatures of Sims (1994b), the generative representations used by Hornby and Pollack (2002), and the genetic regulatory networks developed by Bongard and Pfeifer (2003). Although not necessarily legged creatures, the agents produced by such methods may also have modular controllers, and may be able to walk in a synchronized manner.

Most of the above approaches are motivated by the biological central pattern generators (CPGs), i.e. groups of neurons that produce oscillatory signals for locomotion (Ijspeert, 2008, Shastri, 1997). They typically implement CPGs as CTRNNs, using leaky integrator neurons. The modular controller networks that ENSO evolves also function as CPGs, but they are based on simpler, sigmoidal neurons. Patterned oscillations are still possible in these networks because they are in essence symmetric, coupled cell systems (Section 2.3). Theoretically, such systems are CPGs, and in practice, they generate various gaits for legged robots (Collins and Stewart, 1993). Many researchers have previously hand-designed such systems using group-theoretic and dynamical systems analysis (Collins and Stewart, 1993, Kimura et al., 1999, Righetti and Ijspeert, 2008, Seo and Slotine, 2007). In contrast, ENSO utilizes evolution to design coupled cell systems for multilegged robots automatically.

As discussed in Section 2.3, the symmetries of the coupled cell system determine the gaits it can produce, making it is necessary to evolve the symmetry together with the

n	1	2	3	4	5	6	7	8	9	10	11	12	13	14	15	16
m	**0**	**1**	**3**	**5**	**9**	**12**	**16**	**19**	25	29	35	39	45	51	56	60

Table 3.1: The least number of comparators m **known to date for sorting networks of input sizes** $n \leq 16$. Such networks have been studied extensively, but these values of m have been proven to be minimal only for $n \leq 8$ (shown in bold; Knuth, 1998). Such small networks are interesting because they optimize hardware resources in implementations such as multiprocessor switching networks.

weights of the neural network that implements it. In order to search this combined space of symmetries and network weights effectively, ENSO utilizes symmetry breaking to focus the search on promising symmetries. While this approach to constraining the search space may also work in other similar domains, such as distributed controllers and multiagent systems, another approach may be more appropriate in other domains. For example, the opposite concept of symmetry building is useful in the challenging problem of finding minimal-size sorting networks as demonstrated in Chapter 7. Previous research on such networks is discussed next.

3.3 Sorting Networks

Sorting networks with $n \leq 16$ have been studied extensively with the goal of minimizing their sizes. The smallest sizes of such networks known to date are listed in Table 3.1 (Knuth, 1998). The number of comparators has been proven to be minimal only for $n \leq 8$ (Knuth, 1998). These networks can be constructed using Batcher's algorithm for odd-even merging networks (Batcher, 1968). The odd-even merge iteratively builds larger networks from smaller networks by merging two sorted lists. The odd and even indexed values of these two lists are first merged separately using small merging networks. Comparison-exchange operations are then applied to the corresponding values of the resulting small sorted lists to obtain the full sorted list.

Finding the minimum number of comparators required for $n > 8$ remains an open problem. The results in Table 3.1, for these values of n, improve on the number of com-

30
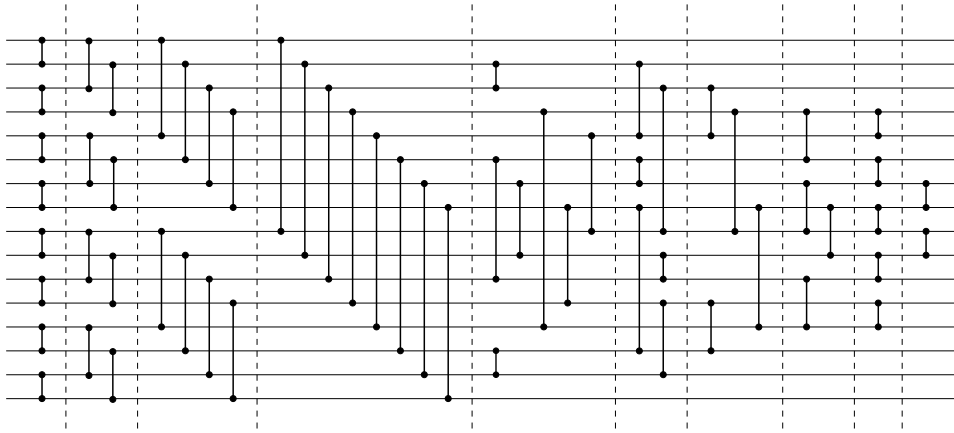
Figure 3.1: The 16-input sorting network found by Green. This network has 60 comparators, which is the fewest known for 16 inputs (Knuth, 1998). The network sorts the inputs in 10 parallel steps, which are separated by dashed vertical lines. The comparators in such hand-designed networks are often symmetrically arranged about a horizontal axis through the middle of the network. This observation has been used by some researchers to bias evolutionary search on this problem (Graham and Oppacher, 2006) and is also used as a heuristic to augment the symmetry-building approach described in Chapter 7.

parators used by Batcher's method, and were discovered separately using specialized techniques. For example, the 16-input case, for which Batcher's method requires 63 comparators, was improved by Shapiro who found a 62-comparator network in 1969. Soon afterwards, Green found a network with 60 comparators (Figure 3.1), which still remains the best in terms of the number of comparators.

In Green's construction, comparisons made after the first four levels (i.e. the first 32 comparators) are difficult to understand, making his method hard to generalize to larger values of n. For such values, the savings in the number of comparators relative to Batcher's method is potentially large. For example, the best known 256-input sorting network due to Van Voorhis requires only 3651 comparators, compared to 3839 comparators required by Batcher's method (Knuth, 1998). Asymptotically, Batcher's method requires $O(n \log^2 n)$ comparators and $O(\log^2 n)$ parallel steps. In comparison, the *AKS network* by Ajtai et al. (1983) produces better upper bounds, requiring only $O(n \log n)$ comparators and $O(\log n)$ parallel steps. However, the constants hidden in its asymptotic notation are so large that

n	17	18	19	20	21	22	23	24	25	26	27	28	29	30	31	32
m	73	80	88	93	103	110	118	123	133	140	150	157	166	172	180	185

Table 3.2: The least number of comparators m known to date for sorting networks of input sizes $17 \leq n \leq 32$. Networks for these values of n were obtained by merging the outputs of two smaller networks from Table 3.1 using Batcher's odd-even merging network (Baddar, 2009). Methods used to optimize networks for $n \leq 16$ are intractable for these values of n because of the explosive growth in the size of the search space. As a solution, the symmetry-building approach described in Chapter 7 mitigates this problem by constraining search to promising solutions and improves these results for input sizes 17, 18, 19, 20, and 22.

these networks are impractical. In contrast, Leighton and Plaxton (1990) have shown that small constants are actually possible in networks that sort all but a superpolynomially small fraction of the $n!$ input permutations.

Therefore, in order to create networks that sort all $n!$ input permutations for large values of n, Batcher's odd-even merging algorithm is often used in practice, despite its non-optimality. For example, such networks for $17 \leq n \leq 32$ listed in Table 3.2 were obtained by merging the outputs of two smaller networks from Table 3.1 using an odd-even merging network (Baddar, 2009).

The difficulty of finding such minimal sorting networks prompted researchers to attack the problem using evolutionary techniques. In one such study by Hillis (1991), a 16-input network having 61 comparators and 11 parallel steps was evolved. He facilitated the evolutionary search by initializing the population with the first four levels of Green's network, so that evolution would need to discover only the remaining comparators. This (host) population of sorting networks was co-evolved with a (parasite) population of test cases that were scored based on how well they made the sorting networks fail. The purpose of the parasitic test cases is to nudge the solutions away from getting stuck on local optima.

Juillé (1995) improved on Hillis' results by evolving 16-input networks that are as good as Green's network (60 comparators in 10 levels), from scratch without specifying the first 32 comparators. Moreover, Juillé's method discovered 45-comparator networks for the 13-input problem, which was an improvement of one comparator over the previously

known best result. His method, based on the Evolving Non-Determinism (END) model, constructs solutions incrementally as paths in a search tree whose leaves represent valid sorting networks. The individuals in the evolving population are internal nodes of this search tree. The search proceeds in a way similar to beam search by assigning a fitness score to internal nodes and selecting nodes that are the most promising. The fitness of an internal node is estimated by constructing a path incrementally and randomly to a leaf node. This method found good networks with the same number of comparators as in Table 3.1 for all $9 \leq n \leq 16$.

Motivated by observations of symmetric arrangement of comparators in many sorting networks (Figure 3.1), Graham and Oppacher (2006) used symmetry explicitly to bias evolutionary search. They compared evolutionary runs on populations initialized randomly with either symmetric or asymmetric networks for the 10-input sorting problem. The symmetric networks were produced using symmetric comparator pairs, i.e. pairs of comparators that are vertical mirror images of each other. Although evolution was allowed to disrupt the initial symmetry through variation operators, symmetric initialization resulted in higher success rates compared to asymmetric initialization. A similar heuristic is also utilized to augment the symmetry-building approach in Chapter 7.

Evolutionary approaches must verify that the solution network sorts all possible inputs correctly. A naive approach is to test the network on all $n!$ permutations of n distinct numbers. A better approach requiring far fewer tests utilizes the zero-one principle (Section 2.4) to reduce the number of test cases to 2^n binary sequences. However, the increase in the number of test cases remains exponential and is a bottleneck in fitness evaluations. Therefore, some researchers have used FPGAs to mitigate this problem by performing the fitness evaluations on a massively parallel scale (Korenek and Sekanina, 2005, Koza et al., 1998). In contrast, the symmetry-building approach in this dissertation utilizes Boolean lattices to evaluate fitness efficiently.

3.4   Conclusion

Previous research on utilizing symmetry in evolutionary search have focused on indirect encodings, which are abstractions of development in nature. However, searching large design spaces efficiently by utilizing symmetry to constrain search has been difficult because symmetries are difficult to specify formally in such systems. The ENSO approach will addresses this issue by utilizing group theory to represent symmetry mathematically. This capability will then be utilized to evolve robust controllers for multilegged robots, a hard engineering problem that has been investigated since the 1970s. Moreover, the general principle of utilizing symmetries to constrain search will be demonstrated on another challenging problem that has received considerable attention in the literature, i.e. designing minimal-size sorting networks.

Chapter 4

Evolving Modular Controllers

It is sometimes possible to constrain large search spaces by hand-designing symmetries. For example, the symmetries of modular neural network controllers for multilegged locomotion on flat ground can be designed in this way (Sections 2.3 and 3.2). This chapter evaluates how effective the resulting search is by evolving walking behaviors for a simulated quadruped robot. Three types of controllers were tested: (1) hand-designed controllers that serve as a baseline for performance comparisons, (2) non-modular controllers unconstrained by symmetry (i.e. the parameters of the entire neural network are evolved at once), and (3) modular controllers constrained by symmetry (i.e. only one module is evolved and duplicated four times to produce the complex neural network controller).

4.1   Quadruped Robot Model

The robot model resembles a table with a rectangular body supported by legs at the four corners (Figure 4.1). The legs are cylindrical with capped ends, and attached to the body by a hinge joint that has a full 360° freedom of rotation. The axis of rotation of the joint is tilted to the side, causing the rotating leg to trace a cone. The leg makes contact with the ground when it is at one edge of the cone. Forward or backward locomotion is achieved
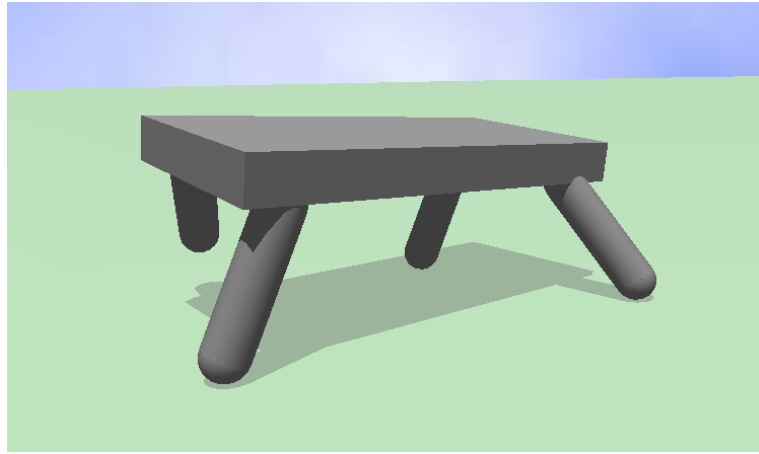
Figure 4.1: The quadruped robot model. The legs are attached to the body by hinge joints with axes of rotation tilted sideways, allowing the legs to make full circular rotation. Locomotion is achieved by coordinating the circular movements of the legs. This model is a simple but physically realistic platform that also allows scaling up to more complex robots by adding more legs or by increasing the legs' degrees of freedom.

by coordinating the circular movements of the leg. The controller activates the simulated servo motor attached to each joint by specifying either the desired joint angle or the angular velocity (in different experiments).

This model can be generalized and made more complex by adding more legs to the table or by using joints that have more degrees of freedom, such as a universal joint. Such more complex robots will be used to test the scale-up properties of the approach in Sections 4.8 and 4.9.

4.2   Hand-Designed Controller

The hand-designed controller specifies the desired angular positions of the legs as functions of time, coordinated so as to obtain a trot gait (Figure 1.1d). Plotted over time, the leg angles for the quadruped robot model produce sawtooth waveforms that all have the same period (Figure 4.2). The waveforms of the diagonal leg pairs are synchronous, and a half-
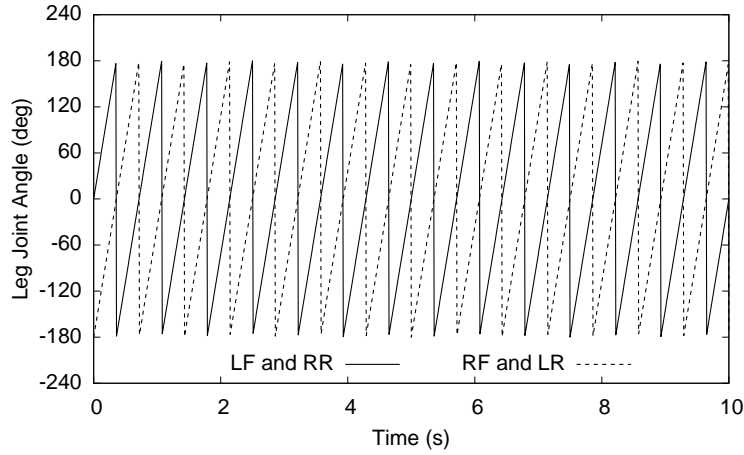
Figure 4.2: Leg angles specified by the hand-designed controller. Plotted over time, these leg angles produce sawtooth waveforms, i.e. the legs rotate with constant angular velocity. The diagonal pairs of legs move in unison, but each pair moves a half-period out of phase with the other pair, producing a trot gait.

period out of phase with the other pair. This gait is an effective base gait that occurs often in nature, and the evolved gaits can be compared with it.

4.3 Non-modular Controller

Figure 4.3a illustrates the non-modular neural network controller for the quadruped robot. Although a variety of architectures are possible, this simple two-layer architecture was chosen to make a fair comparison to the symmetric modular controller. The inputs are the angular positions of the leg joints, and the outputs are the desired angular velocities of the legs. Each input unit is connected to all hidden units, but each output unit is connected only to two hidden units, which in turn send their activation exclusively to that output unit. The hidden and output units have sigmoidal activation functions with a bias and slope as parameters; the input units do not perform any computation. Since the genotype of the non-modular controller represents the entire network, all parameters of the network will have to be optimized through evolution.

37
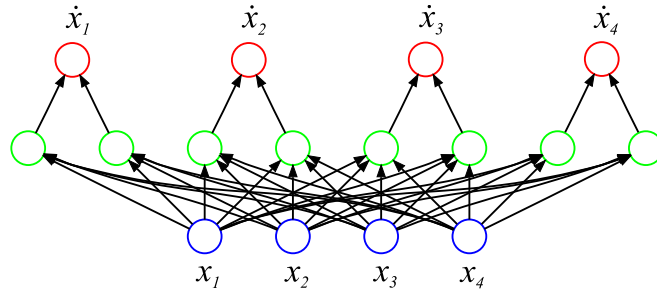
(a) Non-modular controller network
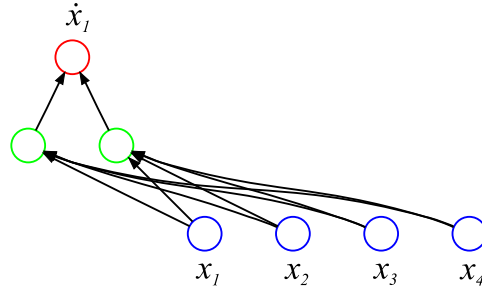
(b) First module of the modular controller network

Figure 4.3: Genotypes of the non-modular and modular controller networks for the quadruped robot model. Inputs are the leg angles and outputs are the desired angular velocities. Both the non-modular and modular networks have the same architecture. However, the genotype of the non-modular network contains the entire network while that of the modular network contains only the first module. The full modular network is constructed by replicating the first module with different permutations of the inputs.

A more general robot model having additional joint angles requires a network with additional inputs and outputs to represent those angles. The number of hidden nodes will also need to be increased to achieve better performance on more complex robots, thus increasing the search space and making the controller more difficult to optimize.

4.4   Modular Controller

The non-modular network can be decomposed structurally into four subnetworks (modules), each containing one of the output units, the two hidden units from which the output unit receives activation, and all the input units. Constraining these subnetworks to be identical with the same interconnection pattern as in Figure 2.3 results in a modular neural network with the same symmetries. Only the first subnetwork is used as the genotype (Figure 4.3b), making the evolutionary search space one-fourth of that for non-modular evolution. The full modular network is obtained by instantiating the other subnetworks with copies of the first subnetwork and with appropriate permutations of the inputs. As a result, the output unit of each subnetwork computes the time derivative of the joint angle it controls as a function of all the joint angles.

Such a construction allows the modular network to be modeled as a coupled cell system. The modules correspond to cells, and the input connections of modules correspond to couplings. Since the modules are identical, the cells are also identical. The permutations of module inputs determine how cells are coupled to each other. These permutations are chosen such that the system of ODEs corresponding to the resulting coupled cell system has the same form as equation (2.1). In this formalism, $\mathbf{x}_i$ represents the joint angles for leg i, and F represents the functional equivalent of each neural-network module.

Analysis of the symmetries of equation 2.1 and its corresponding graph (Figure 2.3) in Section 2.3 showed that this coupled cell system can have periodic solutions that correspond to synchronous and phase-related oscillatory behavior of the cells. When these cells (i.e. module outputs) are assigned to control robot legs, symmetric and regular gaits are

39

obtained. With such a setup, neuroevolution can exploit the symmetries and discover an appropriate F that produces effective gaits.

This coupled cell system models the behavior of the controller only; it does not take into account the dynamical effects of the robot and the environment in which the robot operates. Such effects may be thought of as perturbations to the state variables of the system, and the evolved controllers must be robust against them. Evolution can also discover a controller that utilizes such perturbations as feedback for switching to more suitable gaits on difficult terrains, as observed in Section 4.7.

Experiments comparing the controllers produced by the above three methods were run on flat ground and on terrain with obstacles, and on robots with different number of legs and different number of joint degrees of freedom. Visualization videos of the walking behaviors produced in these experiments can be seen at the website `http://nn.cs.utexas.edu/?modularne`.

4.5 Experimental Setup

The experiments were implemented utilizing a number of open source tools. The neuroevolution code was implemented as a library layer on top of the Open BEAGLE (2007) evolutionary computing framework, taking advantage of its generic programming interface. The physics simulation was programmed using OPAL (2007), an abstraction library on top of the Open Dynamics Engine (ODE, 2007). The Object-Oriented Graphics Rendering Engine (OGRE, 2007) library was used for 3D visualization of the simulation.

The initial population of networks was created with connection weights chosen randomly from the range $[-2, 2)$, neuron biases set to 0, and neuron sigmoid slopes set to 1. Three types of mutations were used, one for each of the above parameter types: (1) weight mutations, (2) bias mutations, and (3) slope mutations. All three types were implemented as Gaussian perturbations (with $\sigma = 0.2$), acting with a specified probability (0.5) on each of the parameters belonging to that type. In each generation, an offspring was created by

first selecting a parent in a two-way tournament and then applying exactly one of the three mutation types, chosen with equal probability. In addition, the network with the best fitness was copied without change to the next generation. A population size of 200 was used in all experiments.

Each network was evaluated in a physically realistic simulation in which the network controlled the locomotion of a robot. When the robot was initially placed in the simulation environment, its longitudinal and lateral axes were aligned with the coordinate directions of the ground plane. The simulation was then carried out for one minute of simulated time with step size 0.01s, after which the fitness of the controller network was calculated as the maximum distance traveled by the robot along either of the two coordinate dimensions (i.e. the Chebyshev distance; Murtagh, 2002). This fitness measure ensured that the evaluation of controller networks was fair even on the terrain with bumps arranged in concentric squares (Section 4.7). Although appropriate as a quantitative measure of performance, this measure does not capture how good the controllers are qualitatively. Therefore, the resulting gaits were also visualized and evaluated manually at the end of evolution to confirm that the champion controller networks had good locomotive properties.

For all experiments, evolution was run for 500 generations and repeated 10 times, each time with a different random number seed. The average and standard deviation of champion network fitness over all experiments are plotted in Figure 4.4. The fitness of the hand-designed controller is also plotted for comparison. This controller was obtained by manually implementing domain knowledge as well as by experimenting with gait periods similar to those produced by the modular controllers. The following sections discuss the results of each experiment in detail.

4.6 Walking on Flat Ground

In the first experiment, networks were evolved to control the simulated quadruped robot on flat terrain. The modular networks performed significantly better than the non-modular
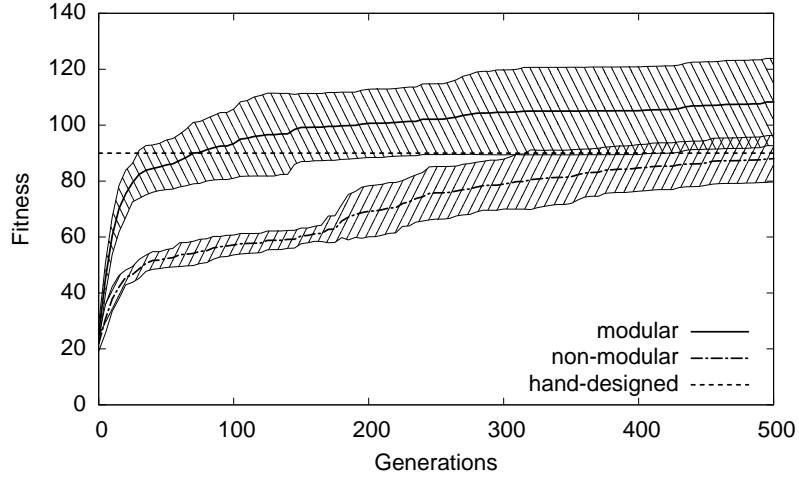
(a) Quadruped robot with hinge joints on flat terrain.
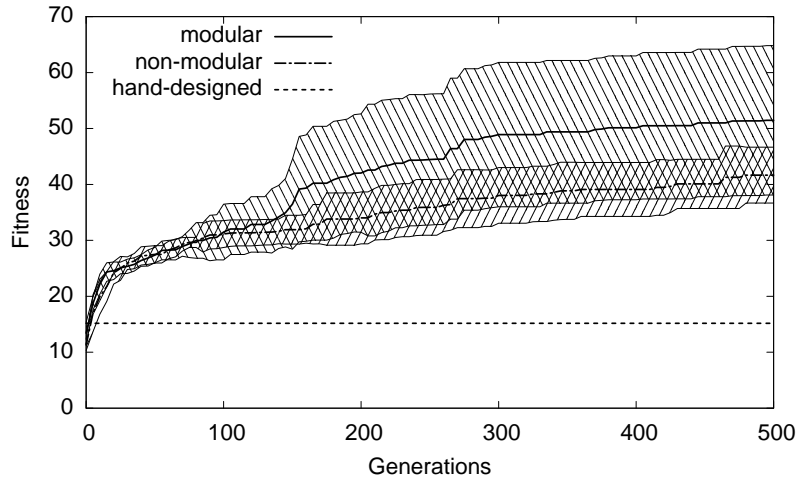
(b) Quadruped robot with hinge joints on obstacle terrain.

Figure 4.4: Performance of hand-designed, modular, and non-modular neuroevolution controllers on different terrains and robot models. Bold lines are averages and the shaded regions on either side are standard deviations obtained over 10 trials of evolution. The fitness of the hand-designed controller is also shown for reference. (a) Modular controllers perform significantly better than both non-modular and hand-designed controllers in the baseline experiment. (b) Performance gap between modular controllers and hand-designed controllers increases significantly when obstacles are added to the environment.

42
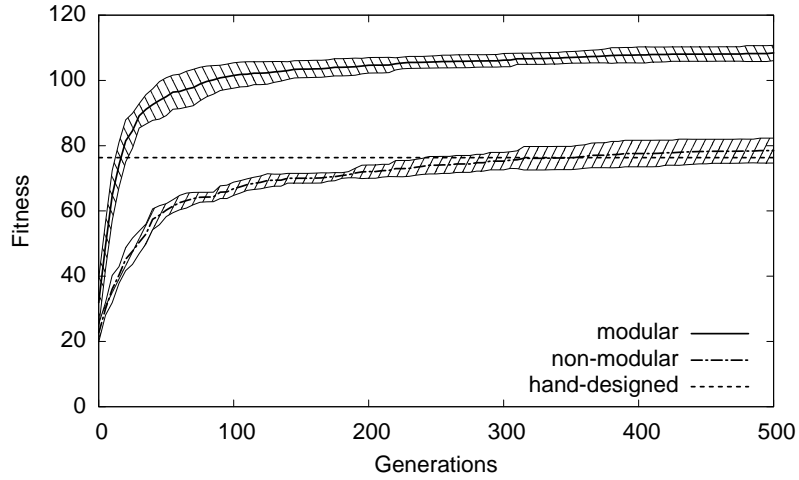
(c) Hexapod robot with hinge joints on flat terrain.
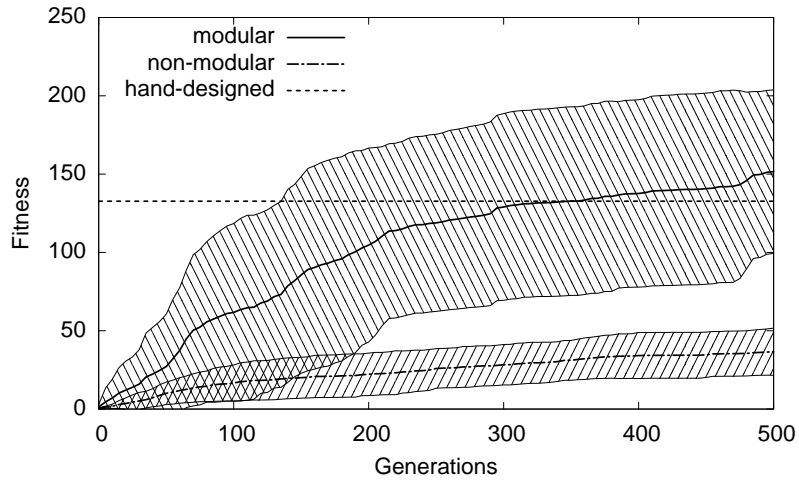
(d) Quadruped robot with universal joints on flat terrain.

Figure 4.4: (cont.) (c) Similarly, the performance gap increases significantly when number of legs is increased to six. (d) Likewise, performance gap increases significantly when an angular degree of freedom is added to each leg joint. These results demonstrate the advantage of modular evolution, i.e. search constrained by symmetries, over non-modular evolution and hand-design in discovering controllers for multilegged robots.

networks through all generations, as illustrated in Figure 4.4a. This result implies that the robots with modular controllers are able to travel farther than those with non-modular controllers. Figure 4.4a also shows that the modular controllers have higher fitness than the hand-designed controller. This result means that through evolution it was possible to discover more efficient or better tuned gaits than could be designed by hand.

When the locomotion of champion networks were visualized, another important benefit of modular evolution was revealed. The modular controllers produce regular gaits, such as pronk, pace, bound and trot, similar to those found in animals. Its hand-designed symmetries constrain the search space, making it easy to evolve such gaits (Section 2.3). In contrast, the non-modular networks typically produce asymmetric gaits in which one or two legs have limited mobility, resembling the gaits of crippled animals.

These results establish a baseline for comparisons involving more difficult terrain and more complex robots, as described next.

4.7   Negotiating Obstacles

In the next experiment, obstacles in the form of bumps (or walls, or fences) were placed on the ground at regular intervals to make the task of the controller more difficult (Figure 4.5). Five bumps were used in each coordinate direction, together forming concentric squares aligned with the coordinate directions of the ground plane. The first bump was at 10 units from the center, and the remaining bumps were at every 5 units outward. The robot was initially placed at the center. Note that although moving in a skewed direction can cover more distance without encountering the bumps, it does not increase the Chebyshev distance measure that is used as fitness.

As in the experiment on flat terrain, the modular controllers have a clear advantage over non-modular and hand-designed controllers because of their symmetry (Figure 4.4b). The hand-designed controller has a particularly hard time: It is unable to get past the first or second bump, depending on how the legs initially hit the bumps. This result further
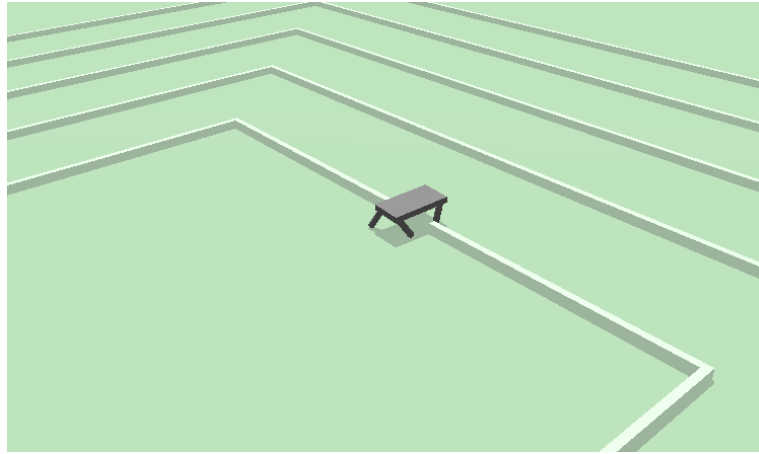
Figure 4.5: Robot negotiating a terrain with obstacles. The obstacles consist of five equally spaced bumps forming concentric squares around the robot. Moving on this terrain by stepping over the bumps is a difficult task: The symmetries of the modular controller make it possible to perform this task effectively, whereas the non-modular and hand-designed controllers struggle. Visualization videos of such behaviors can be seen at `http://nn.cs.utexas.edu/?modularne`.

demonstrates how evolution can discover more effective behavior than can be achieved through hand design.

The bumps perturb the dynamics of the modular controller more than the flat ground does. As a result, evolution often discovers controllers that utilize these perturbations to transition to a more favorable gait for stepping over the bumps. An example of this phenomenon is shown in Figure 4.6, where the robot changes from bound to trot when it hits the first bump, allowing it to get over it more easily. Such behaviors can potentially be generalized to arbitrary environments by evolving modular controllers with additional sensors, e.g. for obstacles, that can signal the need for gait transitions more reliably than perturbations of controller dynamics. In contrast, non-modular evolution fails to evolve gait transitions most likely because it does not have any symmetry constraints.
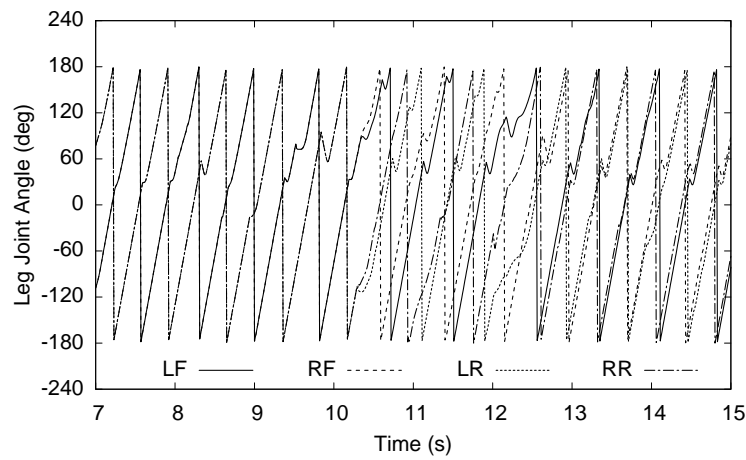
Figure 4.6: Gait changes produced by an evolved modular controller on a terrain with obstacles. As in Figure 4.2, the plot shows angular positions of the four legs of the robot over time. Initially, the front pair of legs (LF and RF) move out of phase from the rear pair (LR and RR), i.e. the robot has a bound gait (Figure 1.1c). The robot encounters the bumps at about 10 seconds. As it tries to move forward, its legs hit the bumps repeatedly, perturbing the dynamics of the controller. These perturbations cause the controller to transition to a trot gait in which the diagonal pairs of legs move out of phase (Figure 1.1d). This change of gait makes it easier for the robot to step over the bumps. Thus modular neuroevolution can evolve controllers that have the flexibility to negotiate difficult terrain.

46
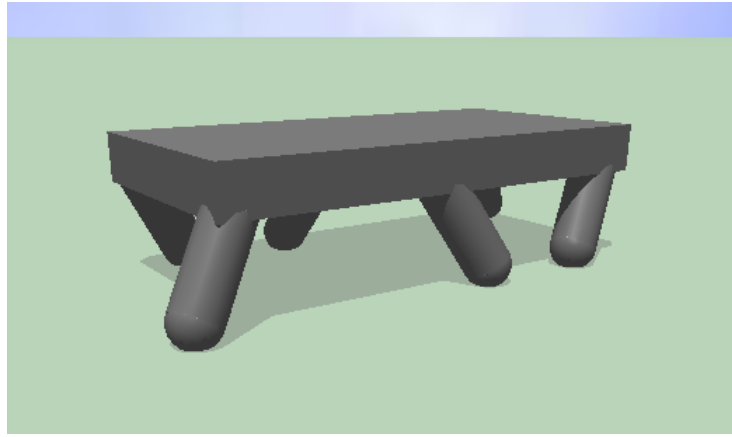
Figure 4.7: The hexapod robot model. This model is obtained by extending the quadruped in Figure 4.1 with a third row of legs. It is used to test how well the different methods for designing controllers scale-up to robots with more legs.

4.8 Scaling to a Hexapod

Because of the symmetries of the modular controller, only one module needs to be encoded, receiving input from all legs. Therefore, when more legs are added to the robot model, only a few more parameters need to be added to the modular genotype. In contrast, the non-modular genotype needs significantly more parameters because it encodes all modules separately. Consequently, evolutionary search is likely to be harder for the non-modular method than for the modular method when the number of legs is increased.

This hypothesis was tested by evolving controllers for a hexapod robot that had equally spaced rows of legs along its longitudinal axis (Figure 4.7). A hand-designed controller was also built by generalizing the trot gait of the quadruped into a tripod gait, in which the front and rear legs of one side are in phase with the middle leg of the other side. The coupled cell system associated with the hexapod modular controller extends the quadruped system of Figure 2.3, and is obtained by adding a third row of cells and connecting them with the other cells using bidirectional links (Figure 4.8). The resulting cell system has two types of symmetries: (1) swapping of the left and right columns of cells, and (2) cycling of the rows of cells either up or down.
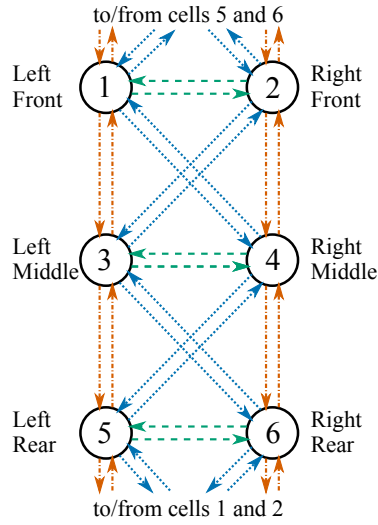
Figure 4.8: Graph of the coupled cell system for the hexapod robot in Figure 4.7. This system extends the quadruped system of Figure 2.3 by adding a third row of cells and connecting them with the other cells using bidirectional links. The resulting symmetries make the graph invariant to (1) swapping the left and right columns of cells and (2) cycling the rows of cells up or down. These symmetries constrain the oscillations of the system, making it possible to evolve effective hexapod gaits similar to those in nature.

Fitness of the modular and non-modular controllers in this experiment are plotted in Figure 4.4c. The modular controllers now outperform the non-modular and hand-designed controllers with a wider performance gap than in the quadruped case in Figure 4.4a. The non-modular controllers perform at the same level as the hand-designed controllers, possibly because they only have to get a few legs moving in a coordinated fashion to make reasonable progress. On the other hand, the modular controllers produce gaits with symmetric leg movements, typically producing a longitudinal wave pattern with same-row legs in phase or a half-period out of phase, which is much more effective and similar to the hexapod gaits in nature. Thus the symmetry constraints of modular evolution make it possible to scale up better than non-modular evolution when more legs are added to the robot.

4.9　Scaling to Universal Joints

The robot can also be made more complex and more difficult to control by increasing the number of angles that has to be controlled in each leg. That is, while the legs trace a cone in the previous robot models, a more challenging model would require controlling the forward-backward (longitudinal) and sideways (lateral) rotations of the legs separately. Since the controller inputs are the joint angles, the number of input connection weights increases correspondingly. This increase is limited to the single genotype module for modular networks, while it gets multiplied by the number of joints for non-modular networks. Again, because of the large number of extra parameters that non-modular evolution has to search, finding a good controller is likely to be harder for non-modular than for modular evolution.

The final experiment tested this hypothesis by replacing each hinge joint of the quadruped robot with a universal (hip) joint. This change in the robot model doubles the number of degrees of freedom of each joint and, consequently, the number of controller inputs. The forward-backward rotation is limited to 30° in both directions and the sideways rotation from vertical to 45° outwards. The hand-designed controller is generalized to this setup by adding signals for the lateral angle of each leg such that it is a quarter-period out of phase with its longitudinal angle, producing a trot gait.

The above hypothesis is confirmed by Figure 4.4d. The performance gap between modular and non-modular evolution has widened significantly: Modular evolution now performs nearly four times better than non-modular evolution, and also slightly better than the hand-designed controller. Visualizing the gaits reveals that non-modular controllers typically produce gaits resembling severely crippled animals, with nearly all their legs appearing disabled and poorly coordinated. These robots often have sideways moving gaits and may have certain joint angles locked in a fixed position. The modular controllers, on the other hand, typically produce regular trot gaits that achieve high fitness.

Thus unlike non-modular evolution, modular evolution scales up well when the robot legs are made more complex. These results demonstrate that utilizing symmetries to constrain the search space makes it possible to scale up evolutionary search to more complex robots.

4.10   Conclusion

This chapter showed how the symmetries of modular controllers constrain evolutionary search, reducing the number of parameters that need to be optimized and thus making it possible to find effective solutions. These symmetries were hand-designed to make it possible to evolve common quadruped gaits found in nature such as pronk, pace, bound, and trot. The modular controllers also evolved the ability to change gaits in response to changes in the environment and to scale well to more complex robot morphologies. In contrast, the unconstrained search of non-modular evolution failed to evolve effective controllers. However, designing symmetries by hand to constrain search in this manner is not always possible, making it necessary to evolve the symmetries as well, as will be discussed in the next chapter.

Chapter 5

Evolving Controller Symmetries

As the last chapter demonstrated, utilizing symmetries to constrain the search space makes it possible to evolve effective solutions that are otherwise difficult or impossible to find. However, it is not always possible to determine the appropriate symmetry analytically. For example, the hand-designed symmetries utilized in the last chapter are no longer appropriate when the robot is walking on an incline, because the physics is different. Continuing in the robot control domain, this chapter extends modular neuroevolution to evolve symmetries as well. The key insight is to utilize group theory to keep the search space constrained to promising solutions while making it possible for evolution to explore different symmetries by breaking symmetry systematically.

5.1   Symmetry-Breaking Approach (ENSO)

This approach, called Evolution of Network Symmetry and mOdularity (ENSO), evolves both the symmetries and the weights of modular neural networks simultaneously. ENSO represents the modules and the connections between the modules as vertices and edges of a completely colored graph (Section 2.2). Since such graphs have an ordering induced by the subgroup lattice of their automorphism groups, ENSO evolves symmetries by traversing

this lattice from top to bottom. As a result, it searches the space of symmetries systematically from the most symmetric to the least symmetric, breaking symmetry minimally in each step to constrain search to promising graphs. Moreover, ENSO searches the space of network weights for each subgroup visited in the lattice. Therefore, evolving the graph representations of such modular networks consists of two components: (1) evolving the symmetries of the module interconnection graph and (2) evolving the connection weights within and between modules. These components are described below.

5.1.1 Symmetry Evolution

In order to evolve a network with n modules, ENSO initializes a population of maximally symmetric, completely colored graphs with vertex set $V = \{1, 2, \ldots, n\}$, that is, graphs of automorphism group $\mathcal{S}_n$. These graphs have only two colors: All vertices are of one color while all edges are of the other color. Vertices and edges with the same color have the same set of neural network parameters and are therefore considered identical. Therefore, each graph in the initial population represents a modular neural network with identical modules and identical connections between the modules.

ENSO computes the subgroup lattice of $\mathcal{S}_n$ and the orbital partitions for each subgroup in the lattice at the beginning of evolution using the GAP (2007) software. During evolution, ENSO utilizes this lattice to mutate the coloring of graphs, thus breaking their symmetry. Each such color mutation creates a new graph coloring from the orbital partition of a randomly chosen successor in the subgroup lattice; that is, the automorphism group of the mutated graph is a random maximal subgroup of the automorphism group of the original graph.

ENSO organizes the colors created by successive color mutations as a tree. Each tree is a genotype for evolution. The leaf colors of the tree specify the complete coloring of a graph, which is the phenotype that is constructed from the genotype. Each genotype tree of the initial population has two leaf nodes, one representing the color of vertices and the

other representing the color of edges (Figure 5.1a). These two leaf nodes are the children of a root node that represents a dummy color.

Thus each node in the genotype tree represents a particular color c. Second, it represents the set Q of elements of $V \times V$ (i.e. the set of vertices or edges of the phenotype graph) that have the color c. This representation is a bit string of length n^2, where the bit position $(i-1)n + j$ is set to 1 if and only if the pair (i, j) is in Q. Third, the node stores the neural network parameters of these elements, i.e. the biases and connection weights of the module network (for each vertex) or the connection weights between modules (for each edge).

The effect of a color mutation on the genotype tree is to partition the set of vertex and edge elements associated with one or more leaf nodes, creating a new child color for each part of the partition (Figure 5.1b). As a result, the colors of these elements change correspondingly in the phenotype graph, i.e. some of the elements that were identical before the mutation are no longer identical: A new (initially random) set of neural network parameters is associated with each new color. These color changes break the symmetry of the phenotype graph, i.e. it loses its color invariance under a subset of permutations that were its symmetries prior to the mutation.

Since the automorphism group of the mutated graph is a maximal subgroup of the automorphism group of the original graph, color mutations break symmetry in minimal increments. As a result, evolution searches the space of symmetries systematically by exploring more symmetric graphs before less symmetric ones. Creating new colors and parameters in the genotype tree during this process increases the complexity of the genotype, that is, evolution searches in a low-dimensional space before it complexifies into a higher dimensional space. This approach allows evolution to optimize solutions in a small search space, and elaborate on them by adding more dimensions. Such complexification has been demonstrated to be useful in other methods for evolving neural networks (Siebel and Sommer, 2007, Stanley and Miikkulainen, 2004). Complexification also means that simpler
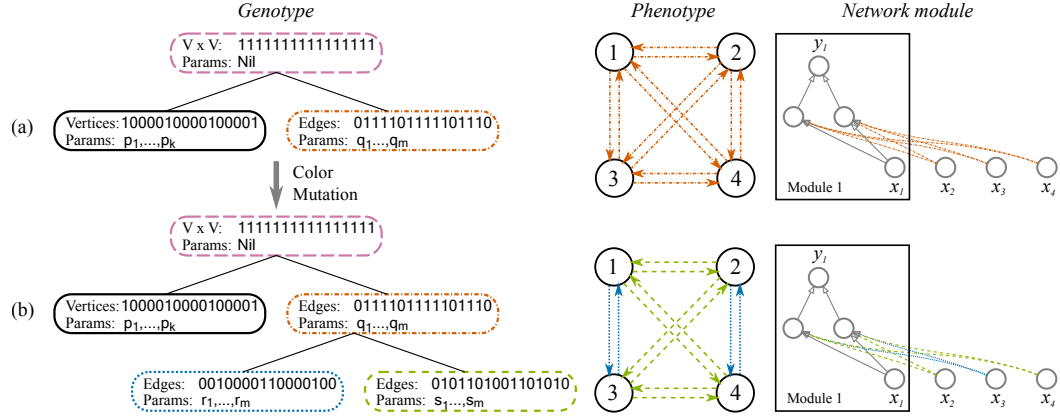
Figure 5.1: Examples of genotype, phenotype, network module, and color mutation. ENSO uses a tree of colors as genotype (left). Each leaf of this tree has a unique color, and represents a set of vertices or edges of the phenotype graph (middle) that have the same parameter values. The vertices and edges of the phenotype graph represent the modules of a neural network and the connections between them (right). Their parameters (stored in the genotype) consist of node biases and connection weights for each module network (vertex) and weights for each connection between modules (edge). Each module has a fixed architecture with a layer of hidden nodes fully connected to its inputs and outputs. A connection from another module (not shown) is implemented by fully connecting its input layer to the hidden layer of the target module. (a) At the beginning of evolution, each genotype in the population represents a maximally symmetric phenotype graph with automorphism group $\mathcal{S}_4$. All vertices of this graph have the same color (solid black, represented by the leaf on the left) and all its edges have the same color (orange with alternating dots and dashes, represented by the leaf on the right), implying that all modules are identical and all connections between them are also identical. (b) A color mutation breaks the phenotype graph symmetry to $\mathcal{D}_4$, which is a maximal subgroup of $\mathcal{S}_4$ (Figure 2.2). As a result, two child nodes are created for the node representing the set of edges, i.e. the set of edges is partitioned into two and each part is colored differently (dotted blue and dashed green). Since each color is associated with a different combination of parameter values, the mutated phenotype graph represents two types of connections between network modules. Such color mutations constrain symmetry search, and together with parameter mutations, make it possible to evolve symmetric modular neural networks efficiently.

solutions are preferred over more complex solutions, thus conforming to the principle of Occam's razor, which often results in more robust neural networks (Fahlman and Lebiere, 1990, le Cun et al., 1990).

For each phenotype graph that ENSO produces in the above manner, it also evolves the neural network parameters associated with its colors to optimize the functionality of the network modules and their interconnections. The structure of these modules and the evolution of network parameters are described next.

5.1.2 Module Evolution

A fixed architecture is used for the neural network modules, each module consisting of a layer of hidden nodes that are fully connected to inputs and outputs (Figure 5.1). Evolution optimizes two kinds of network parameters: (1) the scalar parameters of these modules, i.e. the connection weights and node biases, which form the vertex parameters of the phenotype graph, and (2) the weights of connections between modules, which form the edge parameters of the phenotype graph. Module interconnections are implemented by fully connecting the input layer of one module to the hidden layer of the other module (for instance, in a legged locomotion controller, such interconnections allow the control module of one leg to receive the state of another leg as input). If modules are not connected, then the corresponding graph edges are disabled using special binary edge parameters.

The vertex and edge parameters of the phenotype graph are stored in the genotype leaf nodes. In the initial population, these parameters are initialized with random values in parameter-specific ranges specified by the experimenter. During evolution, ENSO mutates each of these parameters probabilistically by perturbing them with Gaussian noise. When a parameter in a particular genotype node is mutated, it affects all vertices and edges with that color. Thus, representing identical elements by a single node in the genotype tree allows evolution to search the parameter space efficiently by making coordinated changes to the phenotype.

Symmetry and modules must be evolved together to find solution networks, making it necessary to mix parameter and color mutations. However, color mutations produce severe changes in the phenotype, resulting in sudden changes in fitness that may cause the phenotype to be removed from the population. It is possible to determine how effective such structural changes are only after enough parameter mutations have accumulated over evolutionary time. Therefore, color mutations are given the opportunity to be optimized by creating population niches, similar in spirit to speciation in the NEAT algorithm (Stanley and Miikkulainen, 2004) and to the evolution of structure and parameters at different time scales in the EANT/EANT2 algorithm (Siebel and Sommer, 2007). Individuals occupying a niche have the same phenotype symmetry and remain in the niche for a certain number of generations before they compete with the rest of the population. This number is a linear function of the size of the genotype, allowing individuals with more parameters to stay in their niches longer. Protecting symmetry mutations using this niching mechanism improves evolutionary performance significantly.

Evolving the symmetries and parameters of modular neural networks in the above manner constrains search to explore promising regions of the subgroup lattice and corresponding parameter combinations. As a result, ENSO can find solutions to modular problems effectively, as demonstrated next.

5.2   Quadruped Controller

ENSO evolved modular controllers for the quadruped robot model described in Section 4.1. Although robots with more legs and complex legs can be used, this chapter focuses on symmetry evolution in challenging environments, and therefore uses only this simple model. As discussed in Section 4.4, the quadruped controller can be constructed using four modules, each with the same network architecture (Figure 5.2a). Each module's input is the joint angle of the leg it controls. It can be represented by the angle itself, or by the sine and cosine of the angle; the sine and cosine are actually more robust (because they are contin-

(a) Network module and initial phenotype graph

(b) Full controller network consisting of four modules
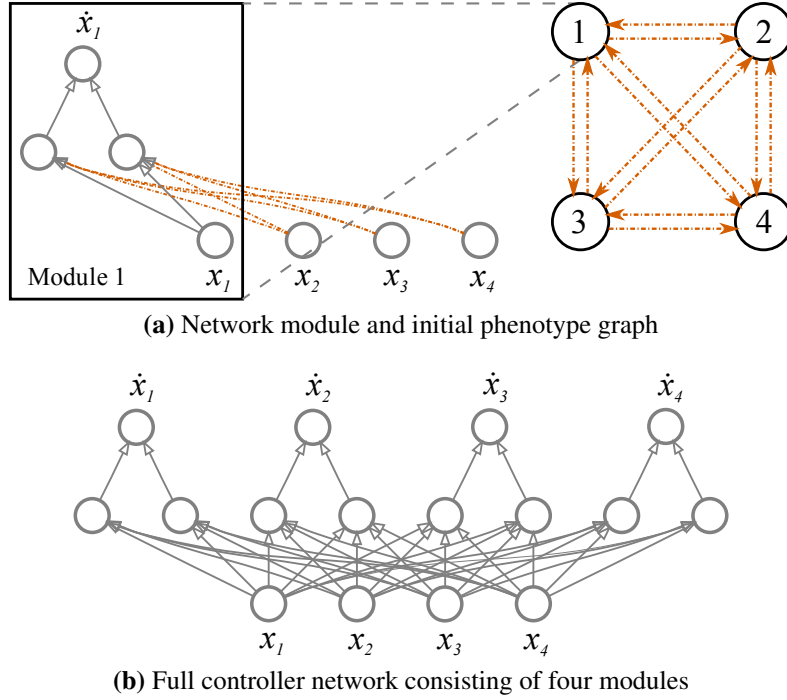
Figure 5.2: Modular controller network for the quadruped robot model. The input to each module is the angle (or its sine and cosine) of the leg it controls, and the output is the desired angular velocity of that leg. The full controller network consists of four such modules, each module receiving input from all the other modules. The phenotype graph represents these modules and their connectivity. At the beginning of evolution, this graph has identical vertices (modules) and edges (interconnections), i.e. all vertices and edges have the same combination of network parameters. Evolution discovers effective controllers by breaking symmetry to create new types of vertices and edges, and by optimizing the initially random vertex and edge parameters.

uous), and will be used in the experiments on inclined ground. The module's output is the desired angular velocity of that leg. The bias and slope of the hidden and output units and the weights of the internal connections of the module are the mutable vertex parameters of the phenotype graph (Section 5.1.2).

The phenotype graph represents the full controller network. It is obtained by connecting the four modules to each other such that each module receives input from all the other modules (Figure 5.2b). The weights of these connections are the edge parameters of the phenotype graph.

The phenotype graph also represents the coupled cell system corresponding to the controller (Section 2.3). As a result, its symmetries determine the types of gaits the controller can produce. The ENSO approach makes it possible to evolve these symmetries together with the network parameters, producing effective controllers even when the appropriate symmetry is difficult to determine analytically. The experimental methods used in demonstrating this result are described next.

5.3   Experimental Methods

In order to demonstrate the benefit of ENSO, four experimental methods for evolving the above modular controller were compared: (1) Evolving its symmetry systematically using ENSO, (2) evolving its symmetry randomly without the group-theory mechanisms of ENSO, (3) using fixed $\mathcal{S}_4$ symmetry during evolution (i.e. maximal symmetry), and (4) using fixed $\mathcal{D}_2$ symmetry during evolution (as was done in Chapter 4). Although the four methods differ in how they evolve symmetry, they all evolve controller parameters in the same way as ENSO.

The first method (ENSO) initializes evolution with a population of maximally symmetric phenotype graphs (graph G_A in Figure 2.1, having an $\mathcal{S}_4$ symmetry). Since they have identical vertices and edges, their genotype trees have only two leaf colors, one representing vertex parameters and the other representing edge parameters. During evolution, color mutations break the initial graph symmetry minimally to create new types of vertices and edges, and parameter mutations optimize the initially random vertex and edge parameters.

The second method (random symmetry) initializes evolution in the same way as above, but color mutations change the color of vertices and edges of the phenotype graph randomly. Each such mutation chooses a random number of genotype leaf colors with probability proportional to the size of the set of vertex or edge elements associated with those colors. Each of these colors is then split into a random number of child colors corresponding to the subsets of elements produced by recursively partitioning the original set of elements.

Like ENSO, these color mutations break graph symmetry, but unlike ENSO, they do not use group theory and therefore do not explore the subgroup lattice systematically (Figure 2.2). Consequently, the resulting symmetry break may not be minimal, producing larger changes in symmetry than ENSO. Therefore, this method is likely to be less evolvable and is likely to perform worse than ENSO, i.e. it is unlikely to constrain symmetry search as effectively as ENSO.

The third method initializes evolution in the same way as the above two methods, i.e. with graphs of $\mathcal{S}_4$ symmetry. However, it does not break this initial symmetry during evolution, and applies only parameter mutations to the phenotype graphs. Therefore, it is a good baseline for comparing with the above methods, making it possible to identify performance improvements due to symmetry evolution.

The fourth method also evolves only parameters, keeping the symmetry of the phenotype graphs fixed, but these graphs have $\mathcal{D}_2$ symmetry (graph G_B in Figure 2.1) instead of $\mathcal{S}_4$. This symmetry is the same hand-designed symmetry utilized in Chapter 4 to evolve quadruped controllers. Thus this experiment forms a second comparison baseline for determining whether symmetry evolution can find more appropriate symmetries than those found through mathematical analysis.

Experiments comparing these four methods for evolving quadruped controllers were performed on flat ground and on inclined ground, as described next. The source code for these experiments is available from the website `http://nn.cs.utexas.edu/?enso-code`.

5.4 Experimental Setup

As with the experiments in Chapter 4, the initial population of controllers had connection weights set randomly from the range $[-2, 2)$, neuron biases set to 0, and neuron sigmoid slopes set to 1. Parameter mutations were implemented as Gaussian perturbations (with $\sigma = 0.2$) acting with a specified probability (0.5) on each parameter. All edges were

enabled in the phenotype graphs of the initial controllers, and mutations toggled them with a specified probability (0.1). In each generation, an offspring was created by first selecting a parent in a two-way tournament, and then applying either a parameter mutation, an edge-toggle mutation, or a color mutation. Parameter mutations were 100 times more likely, and edge-toggle mutations were ten times more likely, than color mutations. Each color mutation created five offspring, all having the same symmetry, and the parameters in their newly created child colors were initialized randomly. In addition to the offspring created by mutations, the network with the best fitness was copied without change to the next generation. A population size of 200 was used in all experiments.

Each controller network was evaluated in a physically realistic simulation as described in Chapter 4. At the end of the simulation, the fitness of the controller network was calculated as a function of how far the robot traveled. This function was different on flat ground and on inclined ground (as will be explained later). The average fitness of champion networks in these experiments is shown in Figure 5.3. The following sections discuss the results of each experiment in detail.

5.5   Walking on Flat Ground

In the first set of experiments, the four methods reviewed in Section 5.3 were used to evolve modular controller networks for the quadruped robot on flat ground. These experiments use the Euclidean distance that the robot travels as the fitness measure. All four methods produce similar fitness through all generations, as illustrated in Figure 5.3a (their differences at the end of evolution are not statistically significant according to the Student's t-test, with $p > 0.23, df = 18$). This result implies that $\mathcal{S}_4$ symmetry is sufficient for controllers to produce fast gaits on flat ground, that is, breaking that symmetry manually or through evolution does not improve performance.

However, differences between ENSO and random symmetry evolution are evident in the symmetries of champion phenotype graphs they evolve. Although both methods mu-
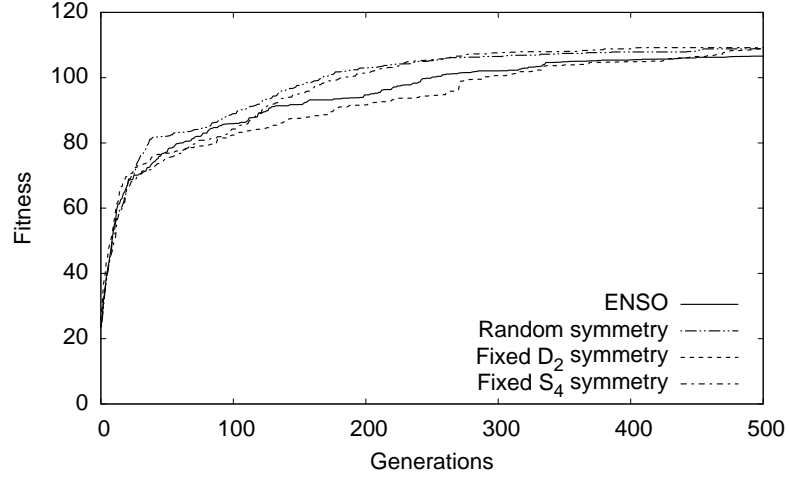
(a) Quadruped robot on flat ground
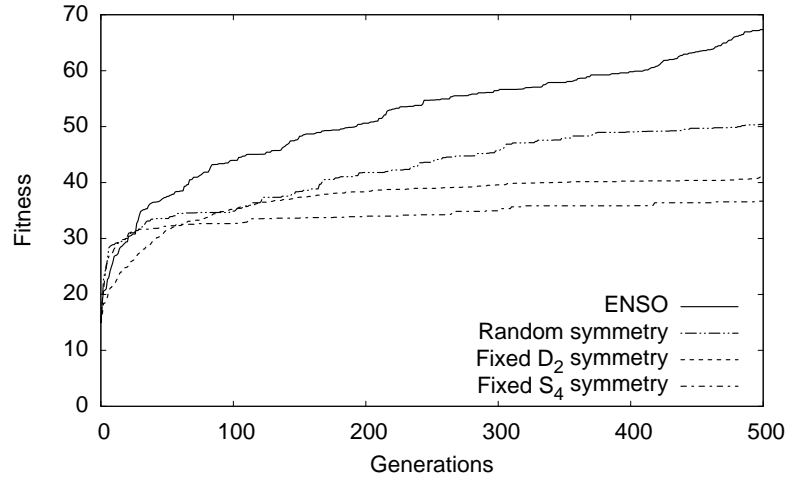
(b) Quadruped robot on inclined ground

Figure 5.3: Performance of controllers evolved using ENSO, random symmetry breaking, fixed $\mathcal{S}_4$ symmetry, and fixed $\mathcal{D}_2$ symmetry methods on flat and inclined ground. The plots are averages over ten trials of evolution. (a) On flat ground, all four methods perform similarly and achieve the same high level of fitness because many symmetries (including the hand-designed ones) can produce effective gaits in this case. (b) On inclined ground, however, both symmetry evolution methods perform better than the hand-designed symmetries because the best symmetries are difficult for humans to conceive. Moreover, the group-theoretic search approach of ENSO constrains search to more promising symmetries than the random search approach, thereby finding significantly better solutions.

61

tate symmetry at the same rate, champions in many runs of random symmetry evolution have the same $\mathcal{S}_4$ symmetry with which they were initialized, while ENSO evolved a variety of effective symmetries. This result implies that the unsystematic and large breaks in symmetry resulting from random symmetry mutations often produce graphs with low fitness that do not survive, and those that do survive have low symmetry (Figure 5.4b). In contrast, ENSO produces graphs with higher symmetry consistently because it uses group theory to break symmetry minimally (Figure 5.4a). While both approaches are equally good on flat ground, on more complex conditions they differ significantly, as will be shown in Section 5.6.

The evolved symmetries also impact the quality of gaits the controllers produce, as observed in visualizations of the locomotion of champion networks. The more symmetric champions evolved by ENSO produce smooth gaits with well-coordinated legs, while the less symmetric champions from random symmetry evolution produce stumbling gaits because legs are less coordinated. Both fixed symmetry methods also produce smooth and well-coordinated gaits, resembling common quadruped gaits such as pronk, bound, and trot seen in animals. Visualization videos of such behaviors can be seen at the website `http://nn.cs.utexas.edu/?enso-robots`.

The gaits of champion networks evolved by the different methods can also be assessed by plotting the leg joint angles of the robot as functions of time. Figure 5.5 shows typical plots for the first eight seconds of simulated time. Initially, all legs are in the same angular position, and they remain synchronous when they start moving. For gaits such as bound and trot that have pairs of legs moving half-period out of phase, this phase difference emerges early on. Thereafter, the controllers maintain synchronicity and phase relations between the legs. Well-coordinated gaits result for ENSO and the two fixed symmetry methods. However, random symmetry evolution typically produces gaits that have the following two flaws: (1) legs are not well synchronized (e.g. the two rear legs in Figure 5.5b) and (2) phase difference between legs does not divide the period evenly (e.g. phase differ-

(a) ENSO (minimal symmetry breaking)

(b) Random symmetry breaking evolution
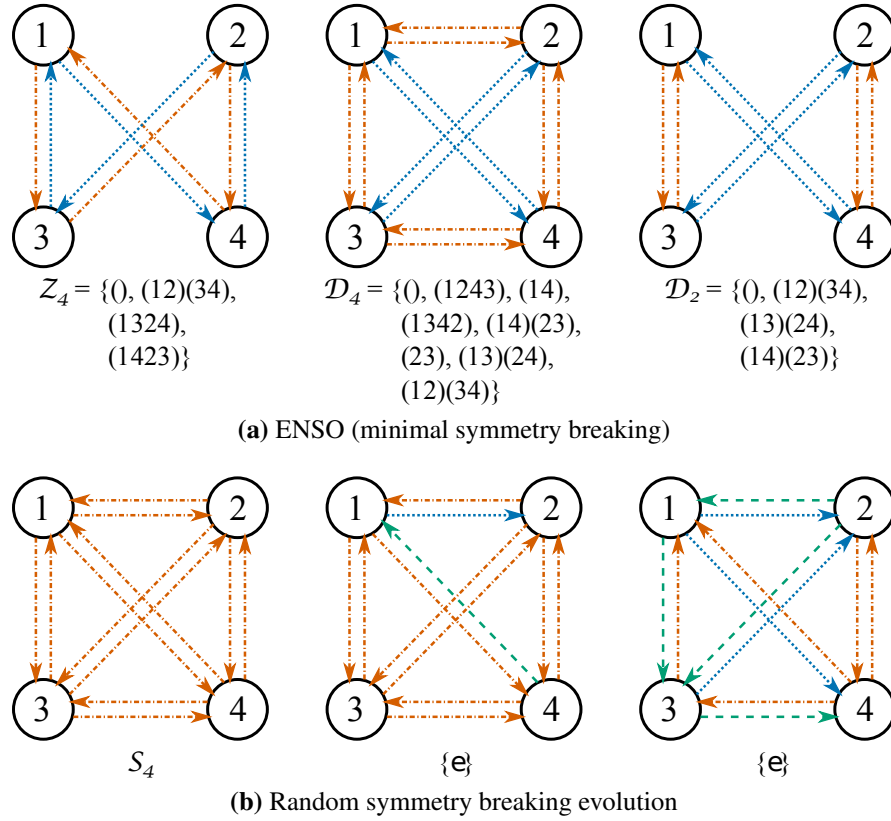
Figure 5.4: Phenotype graphs of typical champion networks evolved by ENSO and random symmetry evolution on flat ground. (a) The group theory mechanisms used in ENSO for minimal symmetry breaking biases evolution to produce phenotype graphs with high symmetry. Consequently, the robots they control have well-coordinated legs and smooth gaits. (b) In contrast, breaking symmetry randomly often produces large changes in symmetry that are deleterious and therefore do not survive. As a result, the champions of many evolutionary runs retain their initial $\mathcal{S}_4$ symmetry (left graph). Other champions such as the middle and right graphs have low symmetry that produce less coordinated, stumbling gaits.

ence between the front and rear leg pairs in Figure 5.5b). The resulting weak coordination of the legs produces the stumbling effect mentioned above, and seen in the videos.

To sum, although all methods produce gaits that are equally effective, ENSO's solutions are more symmetric and more smooth. Such a bias is a major advantage in more challenging environments, as described next.

5.6   Walking on Inclined Ground

In the second set of experiments, the ground was rotated about the longitudinal coordinate direction of the robot by $20°$ to make the task of the controller more difficult. The fitness measure is the distance the robot travels along the longitudinal coordinate minus the distance it travels along the lateral coordinate. This measure encourages evolution to find controllers that move the robot forward in a straight line. Thus, the robot must walk across the incline without climbing up or down, while avoiding the risk of tipping over or slipping down the incline.

Since the robot is the same as before with no morphological changes, the same hand-designed symmetries should apply. However, when the robot is on inclined ground, the direction of gravity is not aligned with its plane of symmetry, thus breaking the symmetry of its dynamics in a way that is difficult for a human designer to take into account. As a result, the appropriate controller symmetries for this task are expected to be different from those needed for walking on flat ground. Therefore, this task is a good test case to determine whether the fixed symmetry methods can evolve effective controllers when appropriate symmetries are difficult to design by hand. Moreover, the task will evaluate whether ENSO is more effective than random symmetry evolution at finding those symmetries.

The results of these experiments are shown in Figure 5.3b. ENSO produces significantly better fitness than random symmetry evolution (according to the Student's t-test, with $p < 0.002, df = 18$), which in turn produces significantly better fitness than evolution of
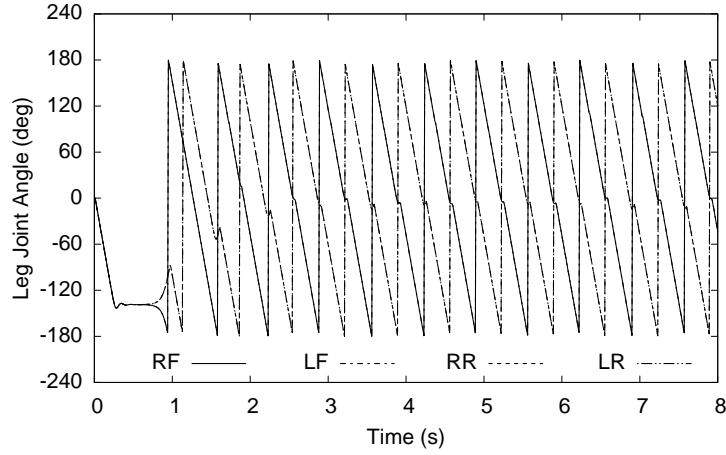
(a) ENSO (bound gait)
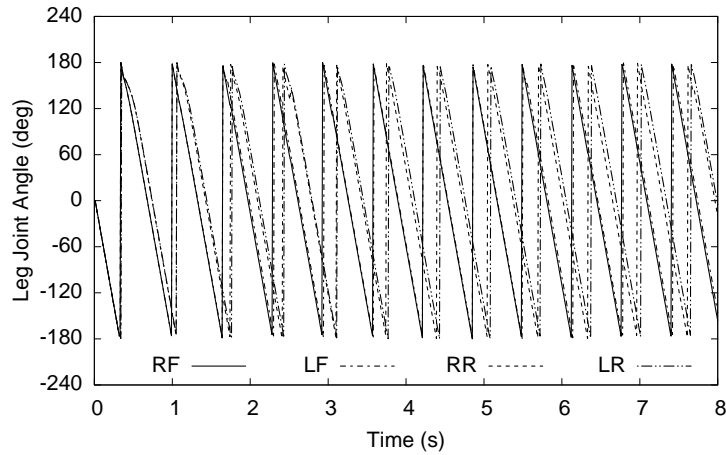
(b) Random symmetry evolution (gait resembling bound)

Figure 5.5: Example gaits of champion networks evolved by the different methods on flat ground. The graphs show the joint angles of the four legs of the robot in the first eight seconds of simulated time. The plot for ENSO was produced using the left phenotype graph in Figure 5.4a and that for random symmetry evolution was produced using the middle phenotype graph in Figure 5.4b. When the controllers reach a steady state, they maintain synchronicity and phase relations between legs. ENSO and the two fixed-symmetry methods evolve controllers that produce the well-defined gaits illustrated in Figure 1.1. However, random symmetry evolution typically evolves controllers that produce lesser-quality gaits. For example, in the bound-like gait of (b), the rear legs are poorly synchronized and the phase difference between the front and rear leg pairs is less than half-period. As a result, this gait is not as smooth as the gaits produced by ENSO and the fixed symmetry methods. Such smoothness is a major advantage in more challenging environments, as seen in Figure 5.7.

65
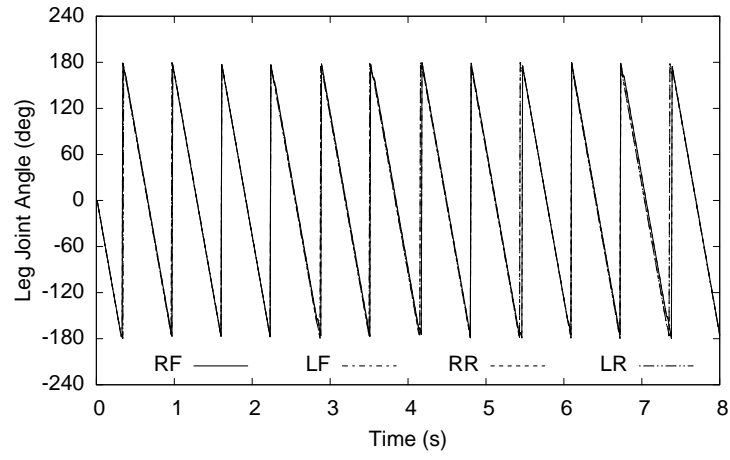
(c) Evolution with fixed $\mathcal{S}_4$ symmetry (pronk gait)
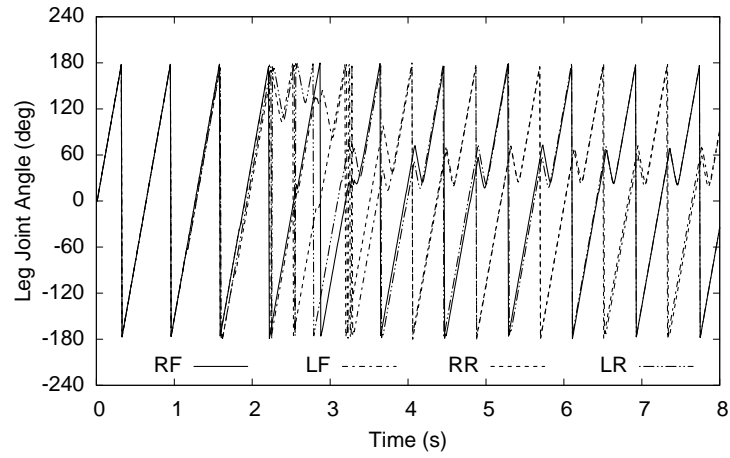
(d) Evolution with fixed $\mathcal{D}_2$ symmetry (trot gait)

Figure 5.5: (cont.)

fixed $\mathcal{D}_2$ symmetry ($p < 0.04, df = 18$). The differences between the two fixed-symmetry methods are not statistically significant ($p > 0.13, df = 18$). Since the only algorithmic difference between ENSO and random symmetry evolution is the way symmetries are broken, these results demonstrate that the group-theoretic symmetry mutations of ENSO are significantly better at evolving the appropriate symmetries than random symmetry mutations, i.e. ENSO's minimal symmetry breaking approach constrains search to promising symmetries more effectively. In addition, the results demonstrate that finding these symmetries is crucial for evolving effective controllers, since fixed symmetry evolution utilizing hand-designed symmetries performs significantly worse.

In this more challenging task, the phenotype graphs that ENSO evolves (Figure 5.6a) are often less symmetric than those it evolves on flat ground (Figure 5.4a). In particular, it evolves graphs that have two vertex colors, and therefore the corresponding controllers have two types of modules, making it possible for evolution to implement a different control function in each module. Different modules can implement different leg behaviors useful for walking effectively on inclined ground. Typically, two (or three) legs of the same module type remain nearly stationary to provide the support necessary for maintaining the robot's forward orientation, while the other legs make a full circle, propelling the robot forward without slipping.

The unsystematic symmetry mutations of random symmetry evolution are typically detrimental on inclined ground as well, and as a result many of the champion phenotype graphs retain their original $\mathcal{S}_4$ symmetry (Figure 5.6b). However, occasionally random symmetry evolution manages to discover symmetries that generate faster gaits than the fixed-symmetry methods. The gaits the fixed symmetry methods produce on inclined ground are similar to those they produce on flat ground because their gaits are constrained by symmetry. However, these gaits are not as effective on inclined ground, and the gaits discovered by ENSO are faster.

(a) ENSO (minimal symmetry breaking)

(b) Random symmetry breaking evolution
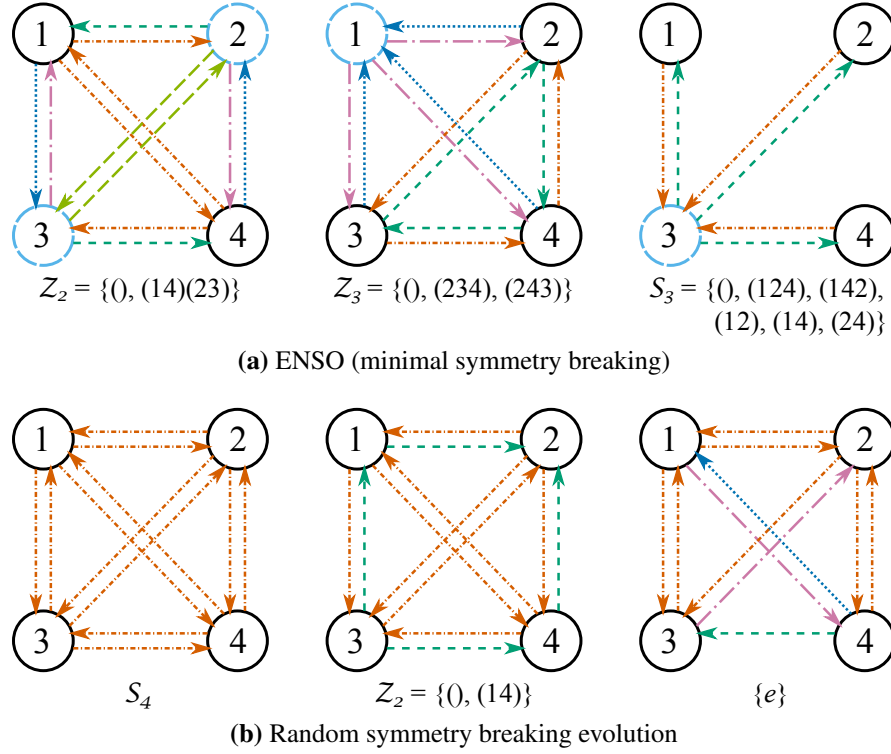
Figure 5.6: Phenotype graphs of typical champion networks evolved by ENSO and random symmetry evolution on inclined ground. (a) The graphs that produce effective gaits on inclined ground are often less symmetric than the graphs on flat ground (Figure 5.4a). They typically have two vertex colors, representing two types of controller modules that produce different leg behaviors for such gaits. (b) As on flat ground (Figure 5.4b), random symmetry evolution produces many graphs with the initial $\mathcal{S}_4$ symmetry, which produces less effective gaits on inclined ground. Other graphs it produces can generate faster gaits, but they are often slower than the gaits produced by ENSO. Thus the systematic symmetry search of ENSO is more effective when finding the right symmetry is more important.

Figure 5.7 illustrates the above observations by plotting leg angles of typical evolved controllers. The controller evolved by ENSO generates two types of waveforms, each corresponding to a different type of module and representing a different leg behavior. The first module type controls only the right rear leg, which powers the robot's forward motion. The second module type controls all the other legs and helps maintain the robot's orientation. The controllers for the other three methods have only one type of waveform because all legs are controlled by the same type of module. As on flat ground, the gaits evolved by random symmetry mutations are less regular than those evolved by the other methods. The controller evolved with the fixed $\mathcal{S}_4$ symmetry produces a new gait that is different from the four gaits discussed in Figure 1.1; it is similar to the walk, i.e. legs are quarter-period separated in phase, while the controller evolved with fixed $\mathcal{D}_2$ symmetry produces a trot gait. Comparing the periods of the plotted gaits indicates that the gait evolved by ENSO is faster than the other gaits.

Thus ENSO evolves more effective gaits on inclined ground than the other methods by finding symmetries that are better suited to the incline. Since ENSO adapts the gaits better to the environment, they should generalize better to changes in the environment as well. This hypothesis was tested by reducing the ground friction of the incline, as described next.

5.7 Generalization to Reduced Friction

Generalization of the champion controllers evolved by the different methods on inclined ground were tested by reducing the friction coefficient of the ground by 25%; all other simulation parameters remained the same. Making the ground slippery in this manner makes it harder for the robots to maintain their balance and orientation as they walk across the incline. However, controllers that evolved effective gaits for the incline should be able to maintain acceptable performance.
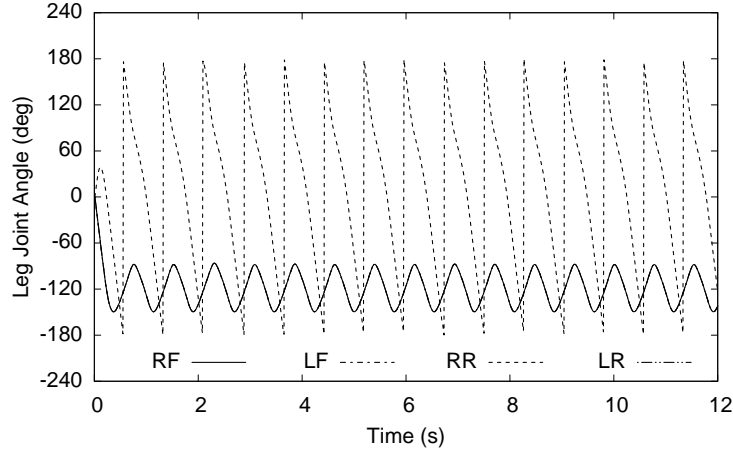
(a) ENSO
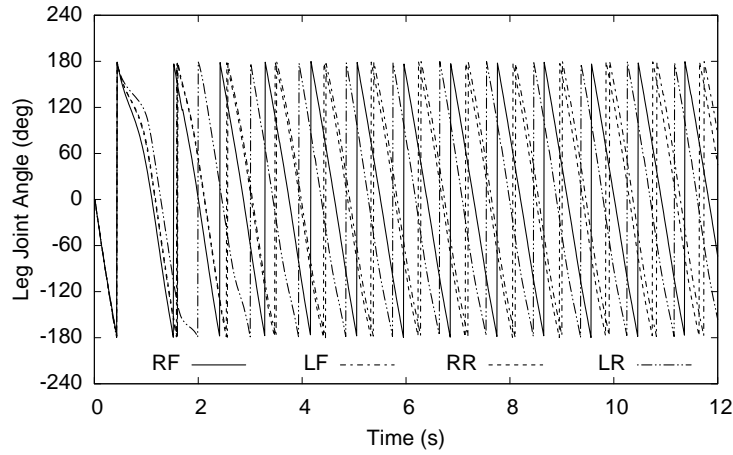
(b) Random symmetry evolution

Figure 5.7: Example gaits of champion networks evolved by the different methods on inclined ground. The graphs show the joint angles of the four legs of the robot in the first twelve seconds of simulated time. The plot for ENSO was produced using the middle phenotype graph in Figure 5.6a, and it shows the two waveforms corresponding to the two types of modules in the phenotype graph. The plot for random symmetry evolution was produced using the middle phenotype graph in Figure 5.6b, and it shows that this gait is less regular than the gaits produced by the other methods. Plots (c) and (d) show that evolving with fixed $\mathcal{S}_4$ and $\mathcal{D}_2$ symmetries produce the same gaits as on flat ground. However, they are significantly slower than the gait evolved by ENSO, as seen from the difference in gait periods.
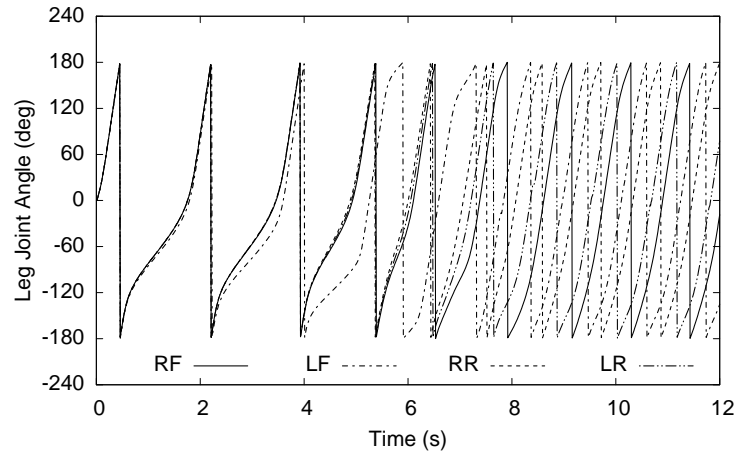
(c) Evolution with fixed $\mathcal{S}_4$ symmetry
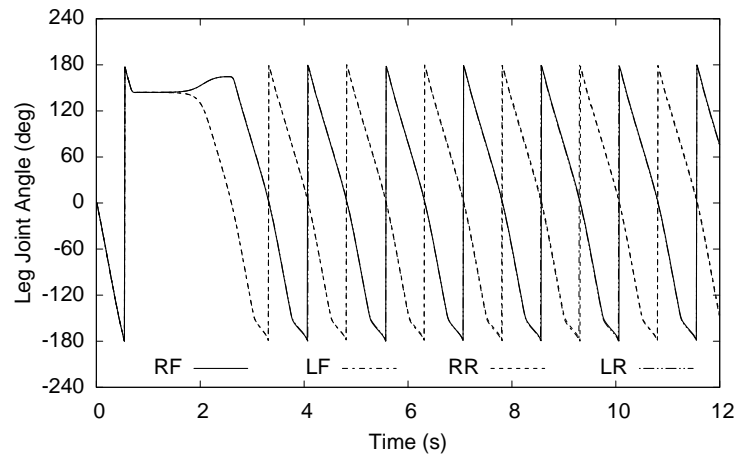
(d) Evolution with fixed $\mathcal{D}_2$ symmetry (trot gait)

Figure 5.7: (cont.)

71

Since the controllers evolved with fixed $\mathcal{S}_4$ and $\mathcal{D}_2$ symmetries and random symmetry mutations are ill-suited for inclines, the robot often ended up flipping over or moving downhill instead of walking across the incline, i.e. such controllers generalize poorly to slippery inclines. In contrast, the controllers that ENSO evolved make the robot walk nearly straight across the incline, slipping only a little. This behavior is possible because ENSO optimizes controllers to perform well on inclines, resulting in gaits that also generalize better. This type of generalization is crucial for transferring the controllers that ENSO evolves in simulation to physical robots, as discussed in the next chapter.

Together, these results demonstrate that utilizing the systematic symmetry search of ENSO focuses the search on better solutions, making it possible to find significantly more effective controllers than by utilizing random symmetry search or by designing the symmetry by hand. ENSO is therefore a promising approach for evolving distributed controllers for complex tasks, and in general, for designing complex modular systems with symmetries.

5.8   Conclusion

This chapter presented a novel evolutionary approach to design complex modular systems with symmetries. This approach, called Evolution of Network Symmetry and mOdularity (ENSO), utilizes group theory to search for symmetries systematically by breaking symmetry minimally. As a result, evolution progresses from simple, highly symmetric phenotypes to more complex, less symmetric phenotypes. This complexification gradually increases the variety of modules and their interconnections in the phenotype, constraining evolution to promising regions of the search space and thus making it effective. ENSO was evaluated by evolving neural network controllers for a quadruped robot in physically realistic simulations. In the difficult task of walking across an incline, ENSO discovered symmetries that produce significantly faster gaits that also generalize better than hand-designed symmetries and randomly evolved symmetries. The next chapter utilizes these capabilities of ENSO to evolve controllers for a physical robot.

Chapter 6

From Simulation to Reality

The ultimate goal of evolving controllers in simulation is to transfer them to real robots. In order to verify that ENSO can evolve controllers that transfer to the real world, I built a physical robot, similar to those targeted by the simulations, at the Cornell Computational Synthesis Lab (2010) of Prof. Hod Lipson. This chapter describes designing and building this robot and utilizing ENSO to evolve neural network controllers for it. The goal was to find out whether the robot would walk successfully and whether the gaits would be more robust against noise and faults than those that could be built by hand.

6.1 Evolving Controllers for Real Robots

It is possible to evolve controllers by evaluating their fitness directly on the real robot instead of in simulation (Floreano and Mondada, 1998, Hornby et al., 2000, Kohl and Stone, 2004b, Watson et al., 2002, Zykov et al., 2004, Section 3.2). However, performing thousands of such fitness evaluations in hardware may be impractical for the following reasons (Mataric and Cliff, 1996). First, hardware evaluations are slow, resulting in long evolutionary run times. Second, they cause wear and tear on the robot, making hardware failures likely and user intervention to repair them necessary. Third, the controllers created by evolution

through random variations may produce abnormal actuator signals that can crash or damage the robot.

Therefore, a good alternative is to evaluate controller fitness in simulation and then transfer only the final, evolved controller to the physical robot. However, transferring such controllers evolved in simulation to the physical robot is challenging (Brooks, 1992, Jakobi, 1998, Lipson et al., 2006, Mataric and Cliff, 1996). The main reason is that it is difficult to simulate physical properties such as friction and sensor and actuator characteristics with high enough fidelity to reproduce the simulated behaviors on real robots. In order to address this issue, researchers have developed several methods that improve the results of evolving in simulation by performing only a few experiments on the real robot.

A straightforward method is to fine-tune the controller behaviors evolved in simulation by continuing evolution on the real robot for a few more generations (Miglino et al., 1995, Nolfi et al., 1994). However, this method may be ineffective in correcting controller behaviors that have evolved to exploit flaws in the simulation. A better alternative is to make such behaviors less likely to evolve by incorporating transfer experiments from the beginning of evolution, e.g. by utilizing a multi-objective evolutionary algorithm that optimizes both a task-dependent controller fitness as well as a measure of how well the controller transfers from simulation to reality (Koos et al., 2010). In any given generation, this method chooses at most one controller based on behavioral diversity to be evaluated on the real robot, requiring only a small number of hardware evaluations.

Other methods utilize the information they gather from a few experiments on the real robot to build a more realistic simulator, typically in one of two ways: (1) Experiments are performed on the real robot before running evolution to collect samples of the real world by recording sensor activations (Miglino et al., 1995, Nolfi et al., 1994). When controllers are evaluated later during evolution, these samples are utilized to set the simulated sensor activations accurately. (2) Experiments are performed on the real robot during evolution to

co-evolve the simulator and the controller, making an initially crude simulation more and more accurate (Bongard and Lipson, 2004, Brooks, 1992, Zagal and Ruiz-Del-Solar, 2007).

In contrast to the above methods, the approach presented in this chapter bridges the simulation-reality gap by utilizing controllers that are robust to small discrepancies between simulation and reality. ENSO can evolve such controllers because they are coupled cell systems that provide theoretical guarantees of robustness to such small discrepancies (Section 2.3). Therefore, simulation accuracies sufficient for ENSO can be obtained easily by approximating the morphology and mass distribution of the real robot with cylindrical and rectangular blocks, without the need for any hardware experiments either before or during evolution (Section 6.3).

Evolving controllers in an accurate enough simulation is often insufficient to transfer them successfully to the real world because of uncertainties such as in sensor activations and actuator responses. Researchers have demonstrated that evolution can adapt controllers to such uncertainties by modeling them as noise in the simulation (Gomez and Miikkulainen, 2004, Jakobi et al., 1995, Miglino et al., 1995). The same idea is utilized in this chapter to evolve controllers that are robust against uncertainties in how the motors respond to control signals. The controllers evolved in the resulting simulation transfer successfully to the physical robot, producing the same behaviors both in simulation and on the physical robot. The design and fabrication of this robot are discussed next.

6.2   Parts and Design

The physical robot was designed with two constraints: (1) it must be similar to the model in Section 4.1 so that ENSO can evolve controllers for it in simulation without big modifications, and (2) it must be possible to prototype it quickly with parts that can be purchased or fabricated easily. While some parts of the robot such as the servo motors and the controller board to operate the motors were available commercially, other parts such as its body and legs were custom-designed and fabricated to fit the commercial parts.

Figure 6.1: Back and front views of the Dynamixel AX-12+ motor. Each motor's rotating output flange is attached to a robot leg. A quadruped robot therefore has four such motors and a hexapod has six, which are connected in a daisy chain using serial connectors. One end of the daisy chain is plugged into a CM-2+ microcontroller board (Figure 6.2) running an evolved neural network controller. This setup allows the neural network to communicate with all four motors and thus control the leg movements of the robot. Reprinted with permission from Robotis (2010); annotations added.

Each leg of the robot is attached to a Dynamixel AX-12+ servo motor (Figure 6.1) manufactured by Robotis (2010). The AX-12+ provides angular position feedback, and can be made to rotate continuously by specifying the desired angular velocity, making it suitable for use with the architecture of neural network controllers discussed in previous chapters. The neural network controlling the robot runs on a Robotis CM-2+ microcontroller circuit board (Figure 6.2), which provides an interface to communicate with the Dynamixel motors through a daisy-chain serial connection.

The AX-12+ motors are mounted on a rectangular body using a wedge-shaped piece to tilt their axes of rotation 20° from the vertical (Figure 6.3). The legs also slant 20° from their respective motor axes, making it possible for the robot to walk by rotating its legs continuously (as was described in Section 4.1). The body, the wedge, and the leg were designed using SolidWorks (2010), a program for computer aided design. The body was then cut from acrylic using a laser cutter and the wedges and the legs were fabricated in an Objet Eden 260V (2010) rapid-prototyping 3D printer. The circuit board is mounted on the
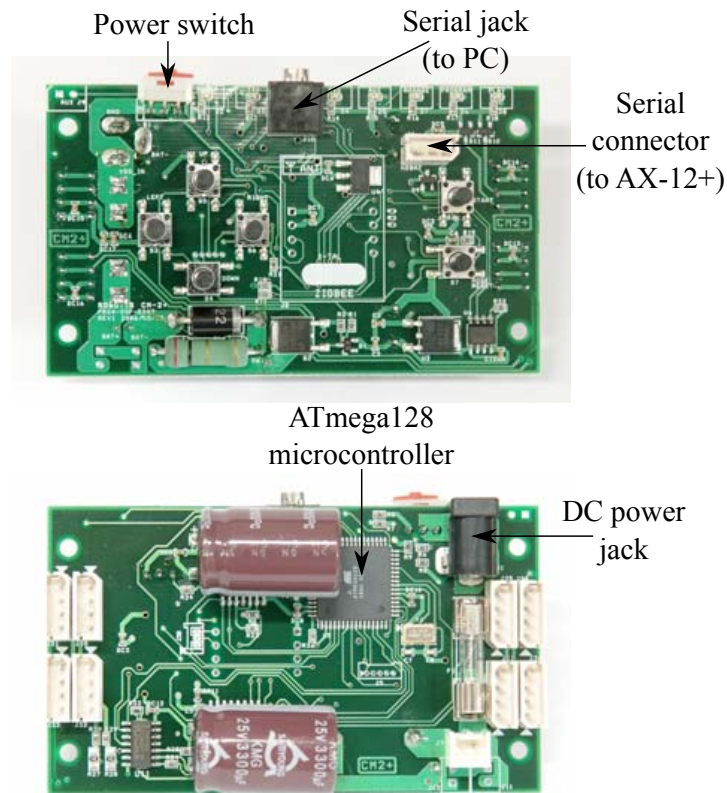
Figure 6.2: Top and bottom views of the CM-2+ circuit board. The CM-2+ board uses an ATmega128 microcontroller with 128KB flash memory and runs control programs for Dynamixel AX-12+ motors. The evolved neural network controllers are expressed in the C language and cross compiled for the ATmega128 using the GNU compiler toolchain. The compiled program is then downloaded to the CM-2+ via its RS-232 serial jack. The CM-2+ executes this program when it is switched on, sending control instructions to the Dynamixels connected in a daisy chain through its serial connector. Reprinted with permission from Robotis (2010); annotations added.
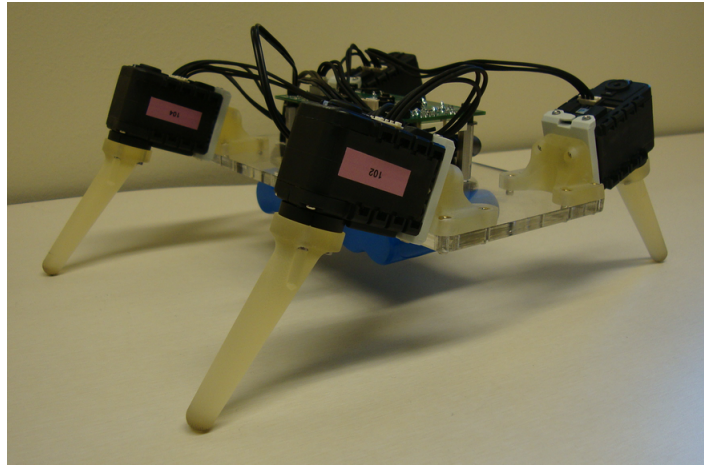
Figure 6.3: Assembled physical quadruped robot. The Dynamixel AX-12+ motors rotate the legs of the robot and are mounted on the four corners of its rectangular acrylic body, which has attachment points in the middle for a future hexapod extension. The legs make 20° with the axis of rotation of their respective motors, tracing trace cones as they rotate. The motor axes also have a 20° sideways tilt from the vertical. As a result, rotating the legs raises and lowers them and can produce locomotion when they make contact with the ground. A control program synchronizes the rotation of the legs to produce locomotion and runs on the CM-2+ circuit board mounted on top of the body. The board is powered by a 12V lithium-ion battery attached to the under-side of the body. Videos of experiments utilizing this robot can be seen at the website `http://nn.cs.utexas.edu/?enso-realrobots`

top side of the body and is powered by a 12V lithium-ion battery attached to its bottom side by Velcro.

Although the morphology and walking mechanism of this robot is similar to the model in previous simulations, it has more parts and it is more complex. Therefore, the simulation was extended to model the physical characteristics of the robot more accurately.

6.3 Extending the Simulation

The robot's legs are still modeled as cylinders with capped ends, but its body is now assembled from several rectangular boxes that approximate its different parts (Figure 6.4). These cylinders and boxes have the same dimensions and the same relative angles as the corresponding parts in the real robot. The leg angles used as controller input are measured
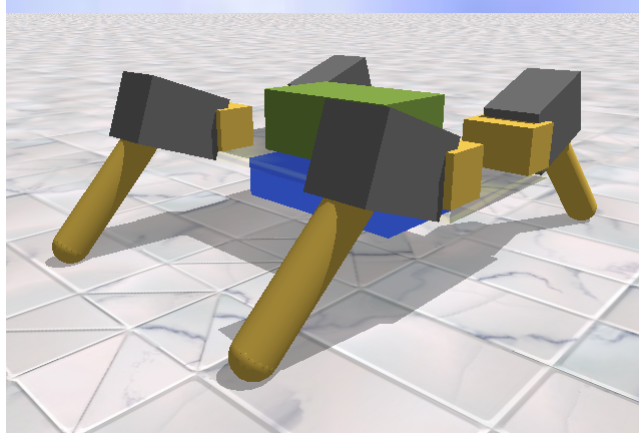
Figure 6.4: Simulation of the physical quadruped robot. The simulation model in Section 4.1 was extended to resemble the morphology and dynamics of the physical robot in Figure 6.3 more closely. The legs are modeled as capped cylinders and the other parts are approximated as rectangular boxes with the same dimensions. By assigning the weight of the corresponding parts to these shapes, this model represents the weight distribution of the physical robot with sufficient accuracy to simulate it realistically.

from the same vertical leg positions. Moreover, densities are assigned to parts such that they have the same mass in both simulation and the real robot. As a result, this simulation model has the same approximate morphology and mass distribution as the physical robot.

In addition to the morphology, the sensor and actuator characteristics of the AX-12+ motors are also modeled. The motor can sense its angular position if it is in the $[0, 300]$ degree range (Figure 6.5). However, it does not give valid position feedback for angles between 300° and 360°. Since the neural network controllers require angular positions as inputs, the sensor reading is interpolated when the motor is in this blind zone. In fact, the sensor reading is calculated the same way for all angles from an estimate of the angular velocity, which gets updated only when the angle is in the valid range. Exponential smoothing is applied to this estimate to filter out noise and discontinuities caused by any discrepancy between the estimated and actual angular velocities when the motor emerges from the blind zone.
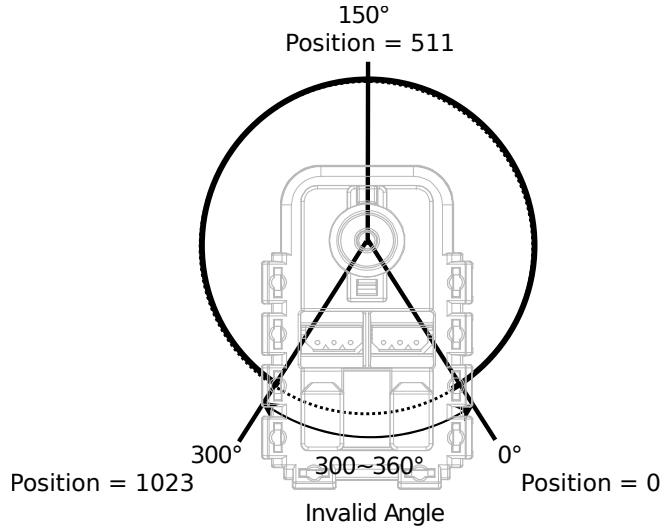
Figure 6.5: Angular position sensor readings of the Dynamixel AX-12+ motor. The angular position sensor of the motor provides an integer valued reading in the range $[0, 1023]$ when the motor is in the $[0, 300]$ degree range; angles outside this range produce invalid sensor readings and are therefore interpolated. Reprinted with permission from Robotis (2010); annotations edited.

The response of the motor to the angular velocity control signals from the neural network is more difficult to model accurately. In particular, the angular velocity of the motor drifts significantly over time for a constant control signal. This stochastic drift can change the periodic trajectory of the controller, thus disrupting the gait of the robot. Such uncertainties can be handled by adding noise to the simulation, making it possible for evolution to adapt the controllers suitably (Gomez and Miikkulainen, 2004, Lipson et al., 2006). Two types of Gaussian noise were added: The first type models fluctuations about the mean with standard deviation 2.5%. The second type of noise models drifts in the mean; it is therefore larger in magnitude (standard deviation 20%), but it is applied only a few times during evaluation.

The motor's inaccuracy in representing its angular position and velocity is also included in the simulation. The motor represents both variables with an integer value in the range $[0, 1023]$. Their precision in simulation is therefore downgraded from floating point precision to match the actual precision. Moreover, the neural network controller reads the

80

positions and updates the velocities at the same frequency in both simulation and the real robot.

The controller evolved in simulation in the above manner is transferred to the real robot by programming the CM-2+ circuit board with it, as will be described next.

6.4 Control Programs

The CM-2+ circuit board contains an ATmega128 CPU, which is an 8-bit microcontroller with 128KB of on-chip programmable flash memory. It can run programs stored in its memory for activating the motors of the robot. Therefore, the evolved neural network controller is converted to a C-language representation and is invoked from a control loop similar to that used in simulation for interfacing the network with the motors. This C program is then cross-compiled for the ATmega128 using the GNU compiler toolchain and downloaded to the CM-2+ board through an RS-232 serial connection.

This facility for writing control programs in C was also utilized to hand-code a baseline controller in order to compare hand-design with evolved controllers. The approach extends the hand-designed controller in Section 4.2: The neural network in the control loop is replaced with a PID controller of the leg angular velocities that utilizes feedback of leg positions. Thus, the hand-designed controller also benefits from the mechanism mentioned above for interpolating and smoothing sensor readings of leg positions. It generates a saw-tooth waveform for the desired leg positions as a function of time (Section 4.2) and uses this waveform as reference to compute error signals for PID control.

Experiments comparing this controller with evolved controllers are described in the following sections. The gaits produced by the evolved and hand-designed controllers were evaluated for walking on flat ground (1) when all four legs of the robot are functional and (2) when one leg is disabled to simulate a real-world motor failure. The controllers produced in the first experiment were evaluated further for generalization by reducing the maximum speed of the motors and by initializing one of the legs with a large error. In each

$\mathcal{D}_4 = \{(), (1243), (14),$
$(1342), (14)(23),$
$(23), (13)(24),$
$(12)(34)\}$
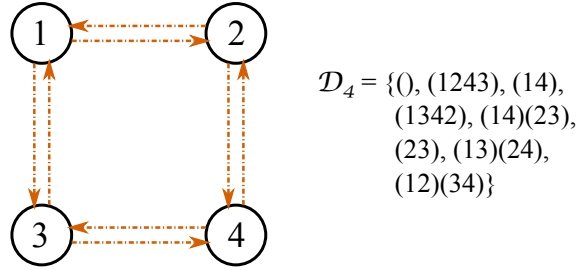
Figure 6.6: Phenotype graph of a champion neural network controller evolved by ENSO. This graph has symmetry group $\mathcal{D}_4$, making it similar to the graphs that ENSO evolved in Chapter 5 for a simpler robot model. As a result, it produces a trot gait, and it transfers well from simulation to the real robot (Figure 6.7).

experiment, generalization was also tested by placing the robot on different surfaces. In each case, ENSO evolved controllers utilizing the same experimental setup and parameters as discussed in Section 4.5. Videos of these experiments can be seen at the website `http://nn.cs.utexas.edu/?enso-realrobots`.

6.5 All Legs Enabled

Figure 6.6 shows the phenotype graph of a champion neural network controller that ENSO evolved to walk on flat ground utilizing the simulation model extended in this chapter. Its symmetry ($\mathcal{D}_4$) is similar to that of the graphs that ENSO evolved in Chapter 5 for the simpler robot model. Therefore, it also produces a similar trot gait (Figure 6.7a), demonstrating that ENSO can evolve symmetric controllers producing symmetric gaits even for a more complex robot model that is more realistic.

Transferring this controller to the real robot reproduces the same gait (Figure 6.7b). It is robust enough to walk smoothly in a straight line even on very different surfaces such as linoleum and carpet. These results demonstrate that ENSO can evolve controllers that transfer successfully from simulation to real robots.

The hand-designed controller was also tested on the real robot with a reference waveform for a trot gait having approximately the same period as the evolved controller
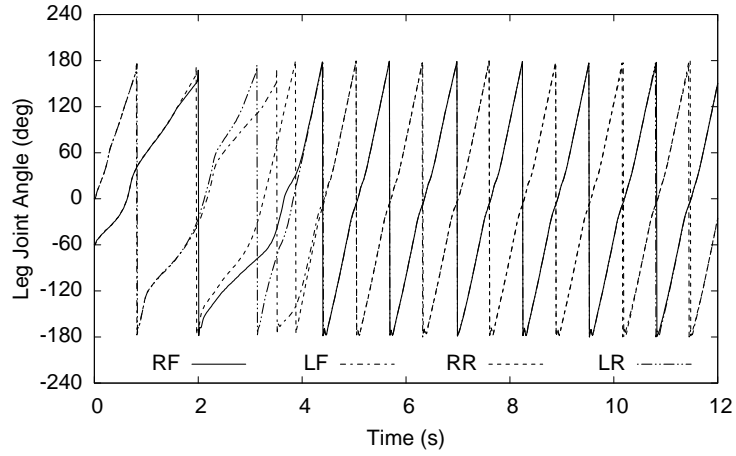
(a) Simulated robot
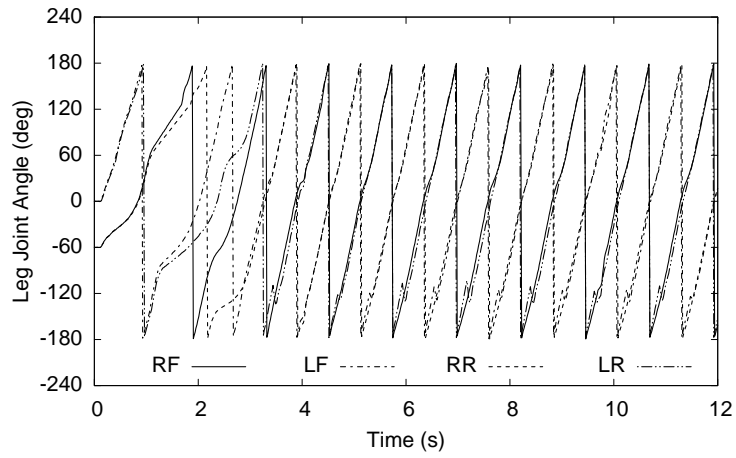
(b) Real robot

Figure 6.7: A trot gait evolved in simulation and transferred to the real robot. The plots show the four leg angles of the robot in the first twelve seconds. They were produced by the controller with the phenotype graph illustrated in Figure 6.6. In both plots, when the controller reaches a steady state, it maintains synchronicity and phase relations between the legs, producing a trot gait. This gait works on various surfaces robustly. Both plots are very similar, indicating that the controller produces the same walking behavior in both the simulated model and the real robot.

83
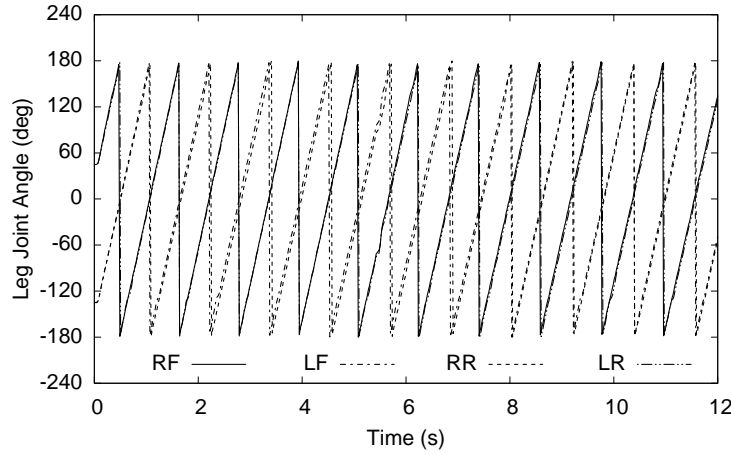
Figure 6.8: Trot gait produced by the hand-designed controller for the real robot. The plot shows the four leg angles of the robot in the first twelve seconds. This controller keeps the legs synchronized with a reference waveform for a trot gait by applying PID control to correct small errors in leg positions. Such controllers are difficult to design by hand in the general case.

(Figure 6.8). The legs are first positioned on the reference waveform so that there is no error for the controller to correct when it starts. Thereafter, the PID mechanism of the controller corrects small errors by speeding up or slowing down the legs to keep them aligned with the reference waveform. As a result, it produces a trot gait similar to the evolved controller. However, it is not as robust and does not generalize as well as the evolved controller as demonstrated by the experiments discussed next.

6.6 Generalization to Reduced Motor Speed

The maximum leg angular velocity that the motors can produce depends on the conditions in which the robot operates. For example, it decreases when the input voltage to the motor decreases as a result of e.g. low battery charge or temperature (Gao et al., 2002, Zhang et al., 2003). The challenge for the controller is to keep the legs synchronized and the robot walking effectively even in such conditions. Both the hand-designed and evolved

controllers were tested for their ability to generalize to such conditions by reducing the maximum angular velocity that the motors produce.

The hand-designed controller fails, losing leg synchronization, even for a small (10%) reduction in the maximum angular velocity (Figure 6.9a). It fails because the legs can no longer move fast enough to keep up with the reference waveform. Slowing down the waveform can correct the problem, but doing so in a way that produces the fastest possible gait robustly is difficult because it requires controlling both the waveform and the leg angular velocities simultaneously. In contrast, the evolved controller continues to function robustly even when the maximum angular velocity is reduced by 60% (Figure 6.9b). It achieves this robustness by slowing down the legs automatically and keeping them synchronized. Thus the evolved controller generalizes well to a range of motor speeds, while the hand-designed controller generalizes poorly.

6.7   Generalization to Different Leg Positions

Another situation in which the hand-designed controller performs poorly is when the error between the position of a leg and the reference waveform becomes too large, which could happen e.g. when the leg is obstructed by an obstacle. The larger the error, the longer it takes the PID mechanism of the hand-designed controller to correct the error. During this time, the leg may not be synchronized well enough with the other legs to produce a good gait. The worst such behavior occurs when the error is maximum, i.e. when the leg is 180° out-of-phase with the reference waveform.

In order to evaluate robustness against such errors, the legs were first positioned such that one leg (the left-rear leg) had the maximum error of 180° and the other legs had zero error. The controller was then initialized with these leg positions, making it possible to observe how quickly it corrects the error of the left-rear leg.

The hand-designed controller takes more than 30 seconds to correct this error (Figure 6.10a). During this time, the angular position of the left-rear leg overshoots and un-

85
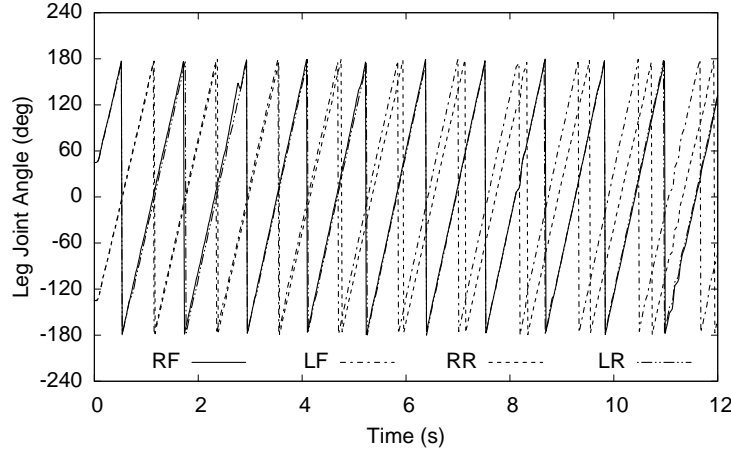
(a) Hand-designed controller for 10% reduction in maximum motor speed
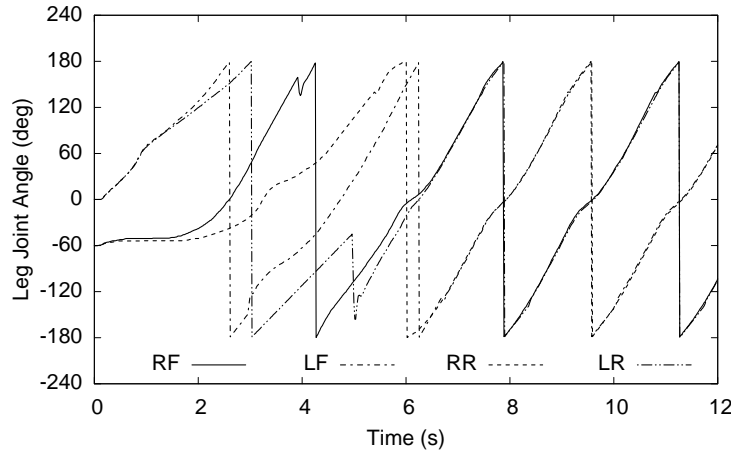
(b) Evolved controller for 60% reduction in maximum motor speed

Figure 6.9: Gaits produced by the hand-designed and evolved controllers on the real robot when the maximum speed of the motors is reduced. The plots show the four leg angles of the robot in the first twelve seconds. They were produced by the same hand-designed controller that produced the gait in Figure 6.8 and the same evolved controller that produced the gait in Figure 6.7 respectively. (a) Reducing the maximum speed of the motors even by 10% causes the hand-designed controller to lose leg synchronization quickly because it cannot keep up with the reference wave-form. (b) The evolved controller maintains leg synchronization and performs robustly even when the maximum speed of the motors is reduced by 60%. It does so by simply slowing down the gait automatically. Thus the hand-designed controller is less general than the evolved controller.

dershoots the reference waveform several times, synchronizing with the right-front leg to produce the original trot gait only gradually. Meanwhile, the other three legs that were initialized with zero error track their respective reference waveforms closely from the beginning. This behavior is the result of correcting the error of each leg separately without modifying the behavior of the other legs.

In contrast, the evolved controller takes only about two seconds to correct the same error (Figure 6.10b). Moreover, it synchronizes the legs without producing the undesirable overshooting and undershooting oscillations (ringing) that the hand-designed controller produces. This robust behavior is possible because the control module for each leg utilizes inputs from all legs. As a result, the evolved controller can adjust the behavior of all legs simultaneously, bringing them into the appropriate relative phases much quicker and smoother than the hand-designed controller.

Evolution utilizes this ability of one control module to influence the behavior of the other modules in the next experiment as well, producing a straight and effective gait even when a leg is disabled.

6.8   One Leg Disabled

An important requirement for many robots in the real world is fault tolerance (Ferrell, 1994). For example, hardware failures are likely in a robot operating in hostile environments or exploring another planet. In such applications, it is not always possible to replace a failed leg actuator with a new one. Walking with the same gait as before is also not an option because the asymmetric action of the remaining legs causes the robot to curve to one side, as was verified experimentally.

In such a situation, a new controller must be designed to make the robot walk effectively with its remaining legs, recovering as much performance as possible. Designing such a controller by hand is challenging for a quadruped with only one functional leg on one side. Designing the appropriate symmetry by hand for a neural network controller is
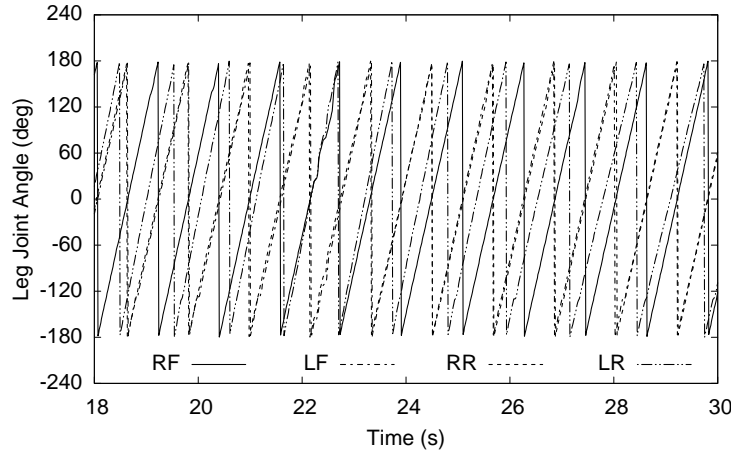
(a) Hand-designed controller
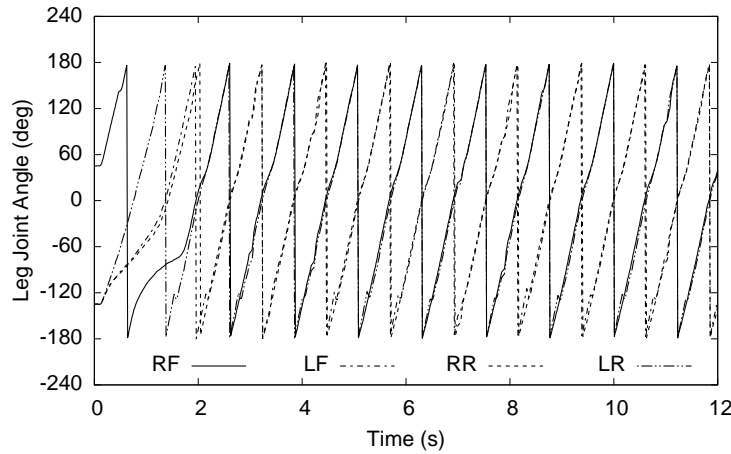
(b) Evolved controller

Figure 6.10: Gaits produced by the hand-designed and evolved controllers on the real robot when the left-rear leg is initialized with maximum angular position error. The plots show the variation of the four leg angles of the robot with time. They were produced by the same hand-designed controller that produced the gait in Figure 6.8 and the same evolved controller that produced the gait in Figure 6.7 respectively. In order to produce the original trot gaits, the controllers must correct the error by synchronizing the left-rear leg with the right-front leg. (a) The hand-designed controller adjusts only the behavior of the left-rear leg to correct the error. As a result, the left-rear leg leads and trails the right-front leg alternately, eventually synchronizing only after more than 30 seconds. (b) In contrast, the evolved controller adjusts the behaviors of multiple legs simultaneously, correcting the error and achieving synchronization smoothly in about two seconds. Thus the evolved controller generalizes well, while the hand-designed controller is less robust.

88

$$\mathcal{D}_2 = \{(), (12)(34),$$
$$(13)(24),$$
$$(14)(23)\}$$
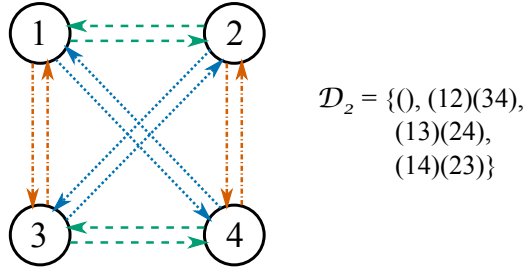
Figure 6.11: Phenotype graph of a champion neural network controller evolved with the left-rear leg disabled. The $\mathcal{D}_2$ symmetry group of this graph is surprising in that ENSO did not evolve a different module for the disabled leg; instead, it evolved the same module for all legs. As a result, it produces a gait resembling trot with the disabled leg not responding (Figure 6.12). ENSO adapted this gait to make the robot walk straight with only three legs.

also challenging because of the robot's asymmetry. In contrast, ENSO can evolve effective neural network controllers for it automatically by disabling the failed leg in simulation. The new controller can then be downloaded to the physical robot for a successful walk.

This hypothesis was tested by evolving controllers with the left-rear leg disabled in the simulation. Figure 6.11 illustrates the symmetry of a resulting champion controller. Surprisingly, it is still very symmetric, employing the symmetry group $\mathcal{D}_2$. In particular, it does not have $\mathcal{S}_3$ symmetry or any other symmetry that assigns a different module to the disabled leg. Instead, its $\mathcal{D}_2$ symmetry assigns the same module to all legs. Therefore, it produces a gait similar to a trot (Figure 6.12) and sends activation to the disabled leg also. Since the disabled leg does not respond, evolution adapted the gait accordingly to make the robot walk straight utilizing only three legs. When this controller is transferred to a similarly disabled physical robot, it produces the same gait on that robot as well, thus confirming successful transfer yet again.

6.9   Conclusion

This chapter demonstrated a method utilizing ENSO for designing controllers for a physical quadruped robot. It is based on evolving controllers for a detailed model of the robot
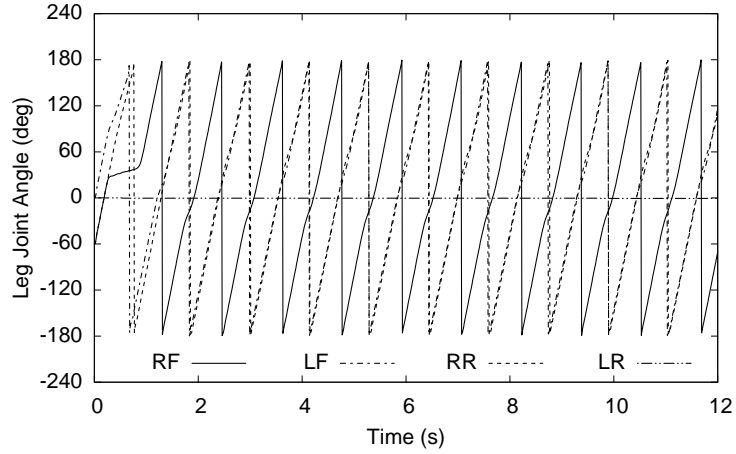
(a) Simulated robot
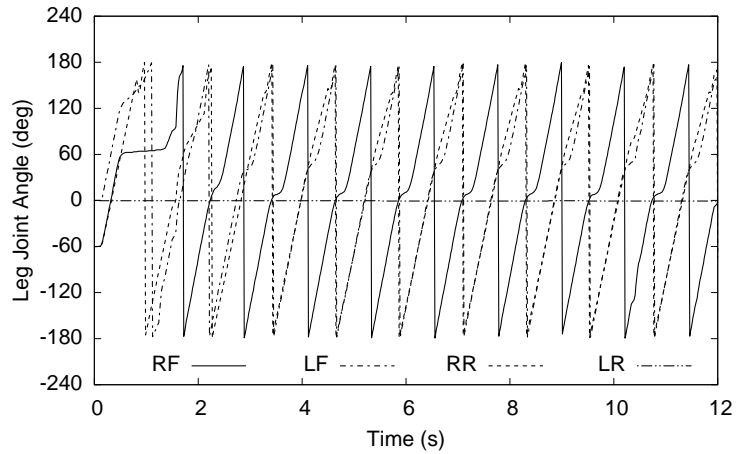
(b) Real robot

Figure 6.12: A gait evolved in simulation with the left-rear leg disabled and transferred to the similarly disabled real robot. The plots show the four leg angles of the robot in the first twelve seconds. They were produced by the controller with the phenotype graph illustrated in Figure 6.11. The disabled leg produces a flat line, while the other three legs maintain synchronous and phase-related oscillations resembling a trot gait. However, the synchronous lines for left-front and right-rear legs split slightly from each other between 0° and 180° and the line for the right-front leg curves a little around 0° indicating adaptation of the gait to produce a straight walk with only three legs. Again, this gait transfers well to the physical robot.

in simulation and then transferring the resulting controllers to the physical robot. ENSO's symmetry evolution makes this ordinarily challenging transfer process tractable by evolving symmetric neural network controllers. Since such controllers are actually coupled-cell systems, they produce stable gaits that are robust to small inaccuracies in the simulation and uncertainties in the real world. ENSO evolved such effective controllers both for a fully functional version of the robot and also for its fault-tolerant version with a disabled leg. Moreover, the results of generalization experiments suggest that they would be robust to common real-world challenges such as variations in battery performance and obstacles.

Chapter 7

Evolving Sorting Networks

Previous chapters demonstrated how the symmetry breaking approach can make evolutionary search more effective in designing controllers for multilegged robots. The same approach is also potentially useful in other applications with similar modular structure, e.g. distributed control systems, multiagent systems, and genetic regulatory networks. In other domains, the alternative process of building a desired symmetry step by step may be a more appropriate way to constrain search to promising regions. This chapter demonstrates this idea in one such problem: designing sorting networks with minimal number of comparators. I will begin by representing the network in terms of Boolean functions. I will then utilize this representation to express the symmetry of the network and thereby develop an approach for constructing minimal-size networks by building their symmetry in steps.

7.1 Boolean Function Representation

As described in Section 2.4, the zero-one principle can be utilized to express the inputs of a sorting network as Boolean variables and its outputs as functions of those variables. It simplifies the sorting problem to counting the number of inputs that have the value 1 and setting that many of the lowermost outputs to 1 and the remaining outputs to 0. In particular,
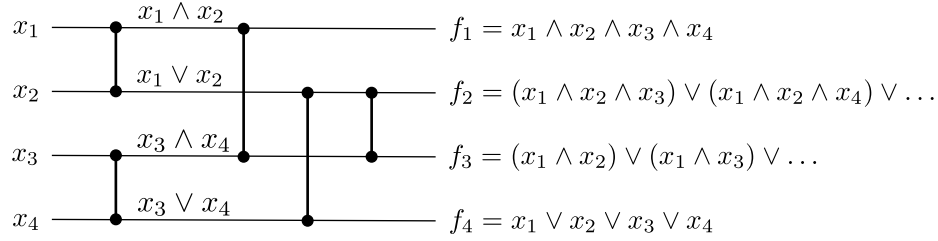
Figure 7.1: Boolean output functions of a 4-input sorting network. The zero-one principle can be utilized to represent the inputs of the network as Boolean variables. Each comparator produces the conjunction of its inputs on its upper line and their disjunction on its lower line. As a result, the functions at the outputs of the network are compositions of conjunctions and disjunctions of the input variables. In particular, the output function f_i at line i is the disjunction of all conjunctive terms with exactly $n + 1 - i$ variables. Therefore, a sorting network is a sequence of comparators that compute all its output functions from its input variables. This representation makes it possible to express the symmetry of the network in a way that is suitable for the symmetry-building approach.

the function $f_i(x_i, \ldots, x_n)$ at output i takes the value 1 if and only if at least $n+1-i$ inputs are 1. That is, f_i is the disjunction of all conjunctive terms with exactly $n + 1 - i$ variables.

Since these functions are implemented by the comparators in the network, the problem of designing a sorting network can be restated as the problem of finding a sequence of comparators that compute its output functions. Each comparator computes the conjunction (upper line) and disjunction (lower line) of their inputs. As a result, a sequence of comparators computes Boolean functions that are compositions of conjunctions and disjunctions of the input variables (Figure 7.1). Since the number of terms in these functions can grow exponentially as comparators are added, it is necessary to utilize a representation that makes it efficient to compute them and to determine whether all output functions have been computed.

Such functions computed utilizing only conjunctions and disjunctions without any negations are called *monotone Boolean functions* (Korshunov, 2003). Such a function f on n binary variables has the property that $f(\mathbf{a}) \leq f(\mathbf{b})$ for any distinct binary n-tuples $\mathbf{a} = a_1, \ldots, a_n$ and $\mathbf{b} = b_1, \ldots, b_n$ such that $\mathbf{a} \prec \mathbf{b}$, where $\mathbf{a} \prec \mathbf{b}$ if $a_i \leq b_i$ for $1 \leq i \leq n$. This property makes it possible to represent them efficiently utilizing the Boolean lattice of binary n-tuples, as illustrated in Figure 7.2 for functions of four variables.

(a) $f(x_1, x_2, x_3, x_4) = x_1$ **(b)** $f(x_1, x_2, x_3, x_4) = x_1 \vee (x_2 \wedge x_3)$
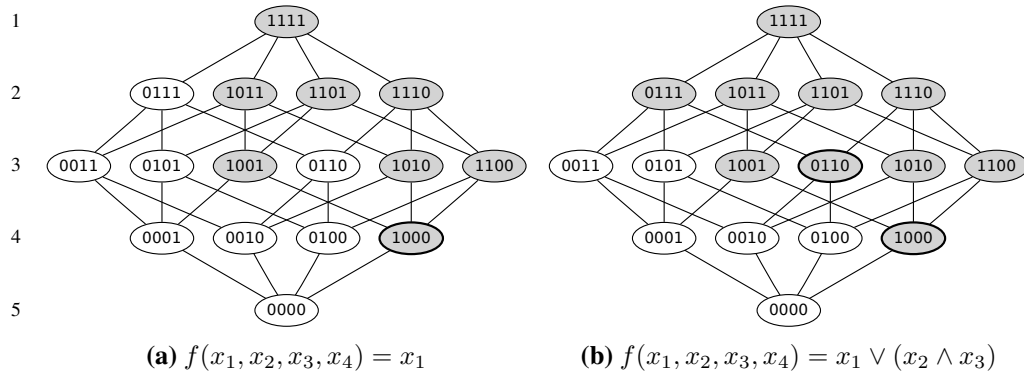
Figure 7.2: Representation of monotone Boolean functions on four variables in the Boolean lattice. The nodes of the lattice are organized in levels (numbered on the left), each containing the binary value assignments to the n-tuple $x_1 x_2 x_3 x_4$ with the same number of 1s. Therefore, the truth table for any Boolean function $f(x_1, x_2, x_3, x_4)$ can be represented in this lattice by shading all the nodes for which f takes the value 1. A node $b_1 b_2 b_3 b_4$ has a path to a lower node $a_1 a_2 a_3 a_4$ if $a_i \leq b_i$ for $1 \leq i \leq 4$. As a result, if node $a_1 a_2 a_3 a_4$ is shaded for a monotone function f, then all higher nodes reachable from it are also shaded, i.e. f is defined completely by the nodes in the lower boundary of its shaded region. This set of nodes (shown in bold) corresponds to the conjunctive terms in the disjunctive normal form of f. For example, it contains just the node 1000 for $f = x_1$ and two nodes 1000 and 0110 for $f = x_1 \vee (x_2 \wedge x_3)$. This representation makes it possible to compute such functions efficiently.

94

Any two nodes in this lattice are comparable if they can be ordered by $\prec$. Therefore, the nodes at which any monotone function f takes the value 1 are bounded at the top by 1111 and bounded below by a set of incomparable nodes (i.e. antichain) corresponding to the conjunctive terms in its disjunctive normal form, i.e. f is completely specified by the nodes in its boundary. Moreover, nodes in the same level i (numbered from the top of the lattice) have the same number $n + 1 - i$ of 1s, forming an antichain of incomparable nodes. They represent the boundary of the function f_i at output i of the sorting network since f_i is the disjunction of all conjunctive terms with exactly $n + 1 - i$ variables (Section 2.4). Therefore, f_i takes the value 1 for all nodes less than or equal to level i and the value 0 for all nodes greater than level i. This property makes it possible to verify efficiently whether f_i has been computed at output i. Thus, levels 1 to n of the lattice have a one-to-one correspondence with the output functions of the network.

Since a monotone Boolean function is completely determined by the nodes in its boundary, only those nodes need to be stored to represent the function. In a lattice of size 2^n, the maximum size of this representation is equal to the size of the longest antichain, which is only $\binom{n}{\lceil n/2 \rceil}$ nodes (by Stirling's approximation, $\binom{n}{\lceil n/2 \rceil} = \mathrm{O}\left(\frac{2^n}{\sqrt{n}}\right)$). However, computing conjunctions and disjunctions utilizing this representation is computationally expensive and produces a combinatorially large number of redundant, non-boundary nodes that have to be removed (Gunter et al., 1996). A more efficient representation is storing the values of the function in its entire truth table as a bit-vector of length 2^n. Its values are grouped according to the levels in its Boolean lattice so that values for any level can be retrieved easily. This representation also allows computing conjunctions and disjunctions efficiently as the bitwise AND and OR of the bit-vectors respectively. Moreover, efficient algorithms for bit-counting make it possible to determine if function f_i has been computed at output i.

This function representation is utilized by the symmetry-building approach to construct minimal-size sorting networks, as will be described next.

7.2 Symmetry-Building Approach

Finding a minimum sequence of comparators that computes all output functions of a sorting network through exhaustive search is a challenging combinatorial problem. It can be made more tractable by utilizing the symmetries of the network, represented in terms of the symmetries of its set of output functions. This representation of network symmetries makes it possible to develop a symmetry-building approach for constructing minimal-size sorting network.

7.2.1 Network Symmetries

Since each output function $f_i(x_i, \ldots, x_n)$ is the disjunction of all conjunctive terms with exactly $n + 1 - i$ variables, it is invariant to all $n!$ permutations of the variables. Therefore, the ordered set of all output functions f_i is itself invariant to all variable permutation, implying that the network has the symmetries represented by the group $\mathcal{S}_n$.

The network also has symmetries resulting from swapping the outputs of all its comparators to produce its dual network with the same set of output functions in the reverse order. Doing so swaps the conjunctions and disjunctions in the output functions of the primal network to produce the output functions of the dual network. Using the symbols $\wedge$ and $\vee$ to specify conjunctions and disjunctions, this duality can be expressed as $f_i(x_i, \ldots, x_n, \wedge, \vee) = f_{n+1-i}(x_i, \ldots, x_n, \vee, \wedge)$ for all $1 \leq i \leq n$. It is therefore possible to define symmetry operations σ_i for $1 \leq i \leq \lceil \frac{n}{2} \rceil$ that act on the network, swapping the dual functions f_i and f_{n+1-i} and also swapping the conjunctions and disjunctions in them. Applying these operations on the ordered set of output functions leaves the set invariant. Their compositions are also symmetries because σ_i and σ_j operate independently on different pairs of functions, leaving the set of outputs invariant. Therefore, this set of operations are closed under composition and they are associative. Moreover, each operation is its own inverse, producing the identity when applied twice in a row. Thus they satisfy all the group axioms and they therefore produce a group. Since every element of this group can be ex-

pressed as the composition of finitely many elements of the set $\Sigma = \{\sigma_1, \ldots, \sigma_{\lceil \frac{n}{2} \rceil}\}$, the group is said to be *generated* by Σ and it is denoted $\langle \Sigma \rangle$.

The full symmetry group of the network is the combined group of symmetries resulting from permuting the input variables and swapping the conjunctions and disjunctions in dual output functions. This group is obtained by taking the direct product of $\mathcal{S}_n$ and $\langle \Sigma \rangle$, denoted $\mathcal{S}_n \times \langle \Sigma \rangle$. Its set of elements is the Cartesian product of its component groups, i.e. the set of ordered pairs (g, ρ), where $g \in \mathcal{S}_n$ and $\rho \in \langle \Sigma \rangle$. Its group operation is the component-wise composition, $(g, \rho) \circ (h, \tau) = (g \circ h, \rho \circ \tau)$. Moreover, two of its subgroups $\{(g, e) : g \in \mathcal{S}_n\}$ and $\{(e, \rho) : \rho \in \langle \Sigma \rangle\}$, where e is the identity, are isomorphic to $\mathcal{S}_n$ and $\langle \Sigma \rangle$ respectively, confirming that $\mathcal{S}_n \times \langle \Sigma \rangle$ contains its component groups.

Therefore, the final symmetry group of the sorting network to be designed is already known, unlike the multilegged robot controllers in Chapter 5 that required the appropriate symmetries to be discovered by symmetry breaking. That is, any n-input sorting network has the symmetry group $\mathcal{S}_n \times \langle \Sigma \rangle$. Such a network can be constructed step by step through a sequence of subgoals corresponding to the subgroups of this symmetry group, as described next.

7.2.2 Defining Subgoal Sequence

The subgroups of $\mathcal{S}_n \times \langle \Sigma \rangle$ represent the symmetries of partial networks created in the intermediate stages of constructing a sorting network. In particular, computing pairs of dual output functions produces symmetries corresponding to a subgroup of $\langle \Sigma \rangle$ (Figure 7.3). Since the elements of Σ operate on different pairs of dual functions, any such subgroup can be written as $\langle \Gamma \rangle$, where Γ is a subset of Σ. Initially, before any comparators have been added, each line i in the network has the trivial monotone Boolean function x_i. As a result, the network does not have any symmetries, i.e. $\Gamma = \{\}$. Adding comparators to compute both the output function f_i and its dual f_{n+1-i} yields $\Gamma = \{\sigma_i\}$ for the resulting partial network. Adding more comparators to compute both f_j and its dual f_{n+1-j} creates

a new partial network with $\Gamma = \{\sigma_i, \sigma_j\}$, i.e. the new partial network is more symmetric. Continuing to add comparators until all output functions have been constructed produces a complete sorting network with $\Gamma = \Sigma$.

Thus adding comparators to the network in a particular sequence builds its symmetry in a corresponding sequence of subgroups $\langle \Gamma \rangle$ that extends from the bottom to the top of the subgroup lattice of $\langle \Sigma \rangle$. Conversely, building symmetry in a particular sequence constrains the possible comparator sequences. Symmetry can therefore be utilized to constrain the search space for designing networks with desired properties. In particular, the sequence of subgroups for building symmetry can represent a sequence of subgoals for minimizing the number of comparators in the network. Each subgoal is defined as the subgroup that can be produced from the previous subgoal by adding the least number of comparators.

Since $\Gamma = \{\}$ initially, the first subgoal is the symmetry that can be produced from the input variables by adding the least number of comparators (Figure 7.4). Producing this symmetry in turn requires computing its corresponding dual output functions. Since the dual functions $f_1 = x_1 \wedge \ldots \wedge x_n$ and $f_n = x_1 \vee \ldots \vee x_n$ have the least number of variable combinations, they can be computed by adding fewer comparators than any other pair of dual output functions. Therefore, the first subgoal is to produce the symmetry $\Gamma = \{\sigma_1\}$ by adding the least number of comparators.

After computing f_1 and f_n, the next pair of dual output functions with the least number of variable combinations are f_2 and f_{n-1}. Therefore, they are likely to be the next pair of dual functions that require the least number of comparators to compute, making the symmetry $\Gamma = \{\sigma_1, \sigma_2\}$ the next subgoal. The number of variable combinations in the output functions continues to increase from the outer lines to the middle lines of the network. Therefore, from any subgoal that adds the symmetry σ_k to Γ, the next subgoal adds the symmetry σ_{k+1} to Γ. This sequence of subgoals continues until all the output functions are computed, producing the final goal symmetry $\Gamma = \{\sigma_1, \ldots, \sigma_{\lceil \frac{n}{2} \rceil}\}$. The
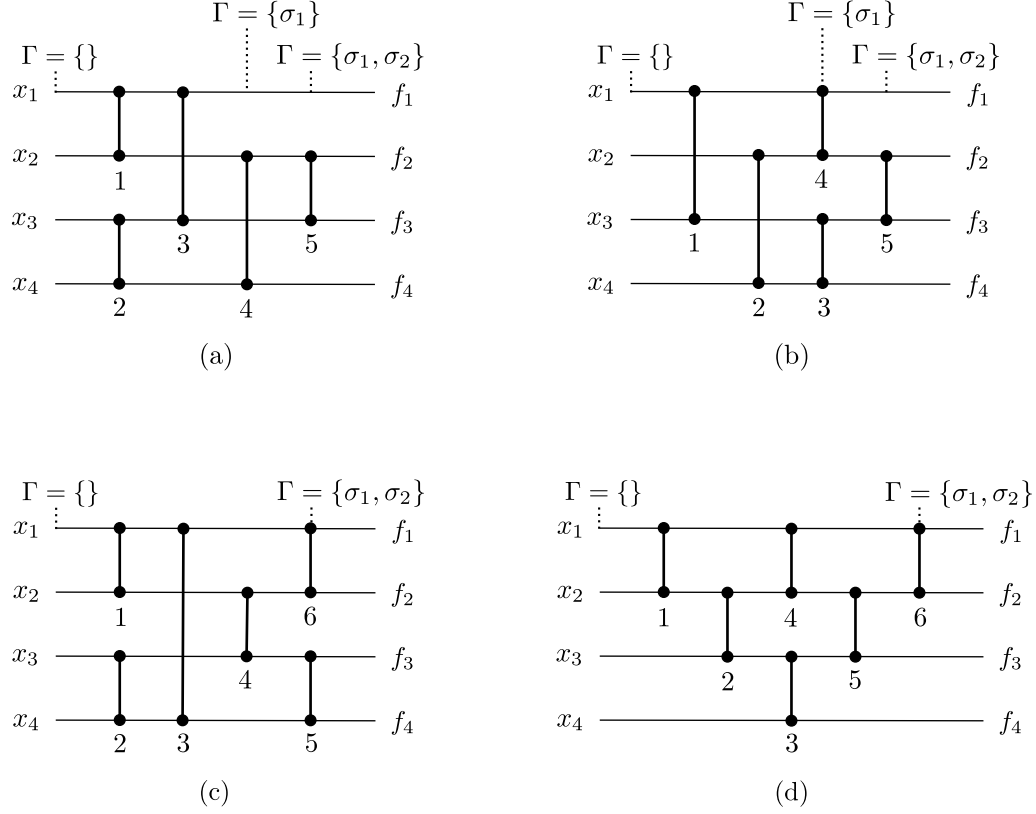
Figure 7.3: Symmetries of output function duals in 4-input sorting networks. The number below each comparator indicates the sequence in which it is added to construct the network. The last comparator touching horizontal line i completes computing the output function f_i for that line. Functions f_i and f_{n+1-i} form a dual, and computing them both gives the network the symmetry σ_i. In network (a), comparator 3 completes computing f_1 and when comparator 4 completes computing its dual f_4, the network gets the symmetry σ_1. Comparator 5 then completes computing both f_2 and its dual f_3, giving the network another symmetry σ_2. Network (b) also produces the same sequence of symmetries and has the same number of comparators. In network (c), comparator 5 completes computing both f_3 and f_4. However, it gets the symmetries σ_1 and σ_2 only when comparator 6 completes computing their duals f_1 and f_2. Network (d) is similar, and they both require one more comparator than networks (a) and (b). Thus the goal set of symmetries for a 4-input network is $\Gamma = \{\sigma_1, \sigma_2\}$, i.e. it is already known. Building this set of symmetries step by step corresponds to constructing such a network by adding comparators, some symmetry sequences requiring longer comparator sequences. Therefore, constructing the network in this manner through a suitable sequence of symmetries can be utilized to minimize its comparator requirement.

99
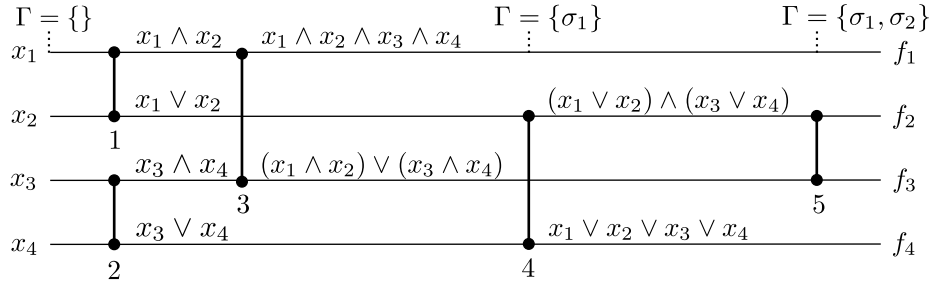
Figure 7.4: Subgoals for constructing a 4-input sorting network with minimum number of comparators. The final goal is to produce the symmetry group $\langle \Gamma \rangle$, where $\Gamma = \{\sigma_1, \sigma_2\}$, by computing all four output functions f_i with the minimum number of comparators. This goal can be decomposed into a sequence of subgoals specified as subgroups of the final symmetry group. At any stage in the construction, the next subgoal is the subgroup that can be produced by adding the least number of comparators. Initially, the network does not have any symmetries, i.e. $\Gamma = \{\}$. The dual functions f_1 and f_4 require fewer comparators than f_2 and f_3 to compute because they have fewer combinations of the input variables. Therefore, the first subgoal is to produce the symmetry $\Gamma = \{\sigma_1\}$. In order to reach this subgoal with the minimum number of comparators, the same comparators 1 and 2 compute parts of both f_1 and f_4. The second and final subgoal is to produce the symmetry $\Gamma = \{\sigma_1, \sigma_2\}$. The functions f_2 and f_3 that produce that symmetry have already been partially computed by comparators 3 and 4. Therefore, adding comparator 5 completes computing both f_2 and f_3. In this way, the number of comparators required to reach each subgoal can be optimized separately, making it tractable to search for minimum-size sorting networks with a large number of inputs.

number of comparators required to reach each of these subgoals is minimized as described next.

7.2.3 Minimizing Comparator Requirement

In order to reach the first subgoal, the same comparator can compute a conjunction for f_1 and also a disjunction for f_n simultaneously (Figure 7.4). Sharing the same comparator to compute dual functions in this manner reduces the number of comparators required in the network. However, such sharing between dual functions of the same subgoal is possible only in some cases. In other cases, it may still be possible to share a comparator with the dual function of a later subgoal. Constructing minimal-size sorting networks requires determining which comparators can be shared and then adding those comparators that maximize sharing.

The Boolean lattice representation of functions discussed in Section 7.1 can be utilized to determine whether sharing a comparator by computing parts of two functions simultaneously is possible (Figure 7.5). Assume that the current subgoal requires computing the output function f_i and its dual f_{n+1-i}. That is, functions for outputs less than i and greater than $n + 1 - i$ have already been computed. All the remaining output functions will need to have the value 1 for all nodes in levels less than or equal to i and the value 0 for all nodes in levels greater than $n + 1 - i$. Therefore, the current functions on lines $i \leq j \leq n + 1 - i$ are also guaranteed to have the same values for those levels. Otherwise, computing at least one of the output functions by adding comparators will be impossible (since conjunctions preserve 0s and disjunctions preserve 1s).

For the current subgoal, function f_i can be computed by setting its value for all nodes in level i to 1 and all nodes in level $i + 1$ to 0, thus defining its node boundary in the lattice. Its monotonicity then implies that its value for all nodes in levels less than i will be set to 1 automatically and its value at all nodes in levels greater than $i + 1$ will be set to 0 automatically. However, since f_i is computed from the current functions f'_j on lines

(a) x_1

(b) x_2

(c) $x_1 \wedge x_2$

(d) $x_1 \vee x_2$
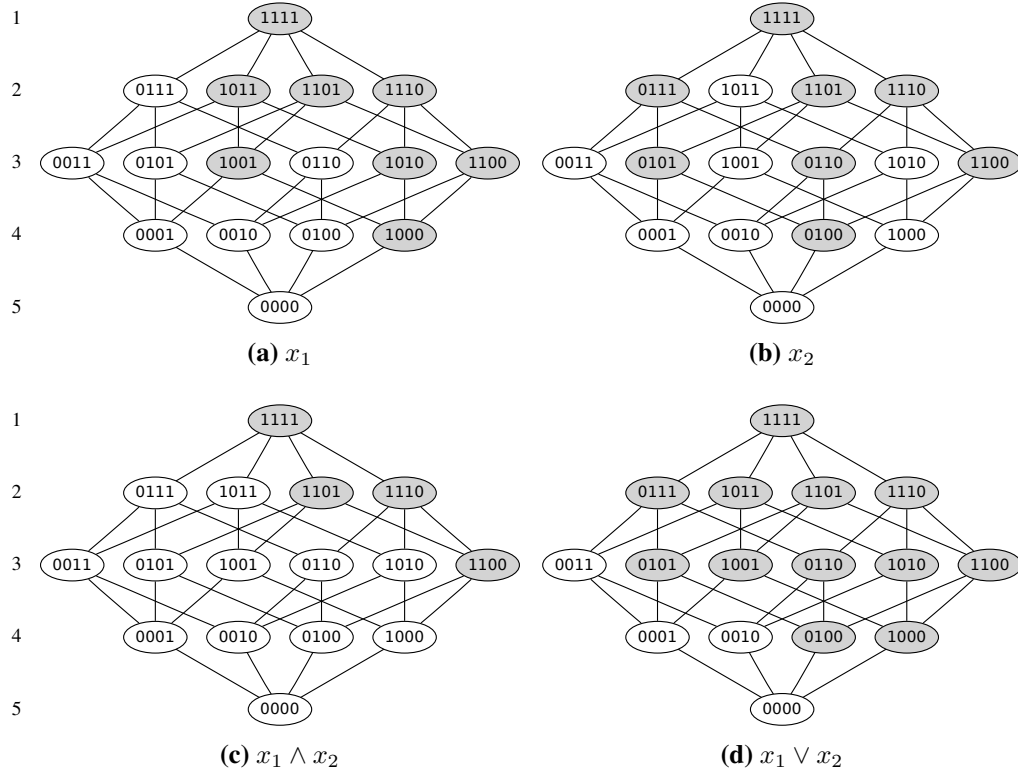
Figure 7.5: Comparator sharing to compute dual output functions in a 4-input sorting network. This figure illustrates the Boolean lattice representation of the functions computed by comparator 1 in Figure 7.4. The levels of the lattices are numbered on the left and the nodes for which the function value is 1 are shaded. Comparator 1 computes the conjunction (c) and the disjunction (d) of the functions (a) and (b) for the subgoal of computing the output functions $f_1 = x_1 \wedge x_2 \wedge x_3 \wedge x_4$ and $f_4 = x_1 \vee x_2 \vee x_3 \vee x_4$. Function f_1 can be computed by utilizing conjunctions to set the value for all nodes in level 2 of the lattice to 0. Similarly, f_4 can be computed by utilizing disjunctions to set the value for all nodes in level 4 to 1. Therefore, comparator 1 contributes to computing both f_1 and f_4 by setting the values of two nodes in level 2 of its conjunction to 0 and the values of two nodes in level 4 of its disjunction to 1. Such shared computation reduces the number of comparators required to construct sorting networks.

$i \leq j \leq n+1-i$ and they already have the value 1 for all nodes in levels less than or equal to i, the function f_i will also get the same value for those nodes automatically. Therefore, f_i can be computed just by setting the values for all nodes in level $i+1$ to 0.

The value for a particular node is set to 0 by utilizing a comparator that computes its conjunction with another function that already has the value 0 for that node. Moreover, the disjunction that the comparator also computes has the value 1 for all nodes in level $i+1$ as required for the other output functions that are yet to be computed. Therefore, exactly one of the functions f'_j already has the value 0 for any particular node in level $i+1$. Adding a comparator between a pair of such functions computes their conjunction with the 0-valued nodes from both functions. Repeating this process recursively collects the 0-valued nodes in level $i+1$ from all functions to the function on line i, thus producing f_i. Similarly, its dual function f_{n+1-i} can also be computed from the functions f'_j by utilizing disjunctions instead of conjunctions to set its values for all nodes in level $n+1-i$ to 1.

The leaves of the resulting binary recursion tree for f_i are the functions f'_j that have 0-valued nodes in level $i+1$ and its internal nodes are the comparators. Since the number of nodes of degree 2 in a binary tree is one less than the number of leaves (Mehta and Sahni, 2005), the number of comparators required depends only on the number of functions the recursion starts with, i.e. it is invariant to the order in which the recursion pairs the leaves. However, the recursion trees for f_i and f_{n+1-i} may have common leaves, making it possible to utilize the same comparator to compute a conjunction for f_i and a disjunction for f_{n+1-i}. Maximizing such sharing of comparators between the two recursion trees minimizes the number of comparators required for the current subgoal.

It may also be possible to share a comparator with a later subgoal, e.g. when it computes a conjunction for f_i and a disjunction for f_{n+1-k}, where $i < k \leq \left\lceil \frac{n}{2} \right\rceil$. In order to prioritize subgoals and determine which comparators maximize sharing, each pair of lines where a comparator can potentially be added is assigned a utility. Comparators that contribute to both f_i and f_{n+1-i} for the current subgoal get the highest utility. Comparators

that contribute to an output function for the current subgoal and an output function for the next subgoal get the next highest utility. Similarly, other possible comparators are also assigned utilities based on the output functions to which they contribute and the subgoals to which those output functions belong. Many comparators may have the same highest utility; therefore, one comparator is chosen randomly from that set and it is added to the network. Repeating this process produces a sequence of comparators that optimizes sharing within the current subgoal and between the current subgoal and later subgoals.

7.3   Evolving Minimal-Size Networks

Optimizing for each subgoal separately in the above manner constitutes a greedy algorithm that produces minimal-size networks with high probability for $n \leq 8$. However, for larger values of n, the number of subgoals is too many to find a global optimum reliably. In such cases, its performance can be improved by utilizing evolution to optimize the solutions further.

The most straightforward approach is to initialize evolution with a population of solutions that the greedy algorithm produces. The fitness of each solution is the negative of its number of comparators so that improving fitness will minimize the number of comparators. In each generation, two-way tournament selection based on this fitness measure is utilized to select the best individuals in the population for reproduction. Reproduction mutates the parent network, creating an offspring network in two steps: (1) a comparator is chosen from the network randomly to truncate the network, discarding all comparators that were added after it, and (2) the greedy algorithm is utilized to add comparators again, reconstructing a new offspring network. Since the greedy algorithm chooses a comparator with the highest utility randomly, this mutation explores a new combination of comparators that might be more optimal than the parent.

This straightforward approach restricts the search to the space of comparator combinations suggested by the greedy algorithm and assumes that it contains a globally minimal

network. But in some cases, the globally minimal networks may utilize comparators that are different from those suggested by the greedy algorithm. Therefore, a more powerful (but still brute force) approach is to let evolution utilize such comparators as well: With a low probability, the suggestions of the greedy algorithm are ignored and instead the next comparator to be added to the network is selected randomly from the set of all potential comparators.

A more effective way to combine evolution with such departures from the greedy algorithm is to utilize an Estimation of Distribution Algorithm (EDA) (Alden, 2007, Bengoetxea et al., 2001, Mühlenbein and Höns, 2005). The idea is to estimate the probability distribution of optimal comparator combinations and to utilize this distribution to generate comparator suggestions. The EDA is initialized as before with a population of networks generated by the greedy algorithm. In each generation, a set of networks with the highest fitness are selected from the population. These networks are utilized in three ways: (1) to estimate the distribution of optimal comparators for a generative model, (2) as elite networks passed unmodified to the next generation, and (3) as parent networks from which new offspring networks are created for the next generation.

The generative model of the EDA specifies the probability $P(C|S)$ of adding a comparator C to an n-input partial network with state S. The state of a partial network is defined in terms of the n Boolean functions that its comparators compute. These functions determine the remaining comparators that are needed to finish computing the output functions, making them a good representation of the partial network. However, storing the state as the concatenation of the n functions is computationally intractable since each function is represented as a vector of 2^n bits. Therefore, a condensed state representation is computed based on the observation that the greedy algorithm does not utilize the actual function values for the nodes in the Boolean lattice; it only checks whether the values in a given level are all 0s or all 1s. This information, encoded as $2(n+1)$ bits (Figure 7.6), is suitable as the state representation for the model as well.
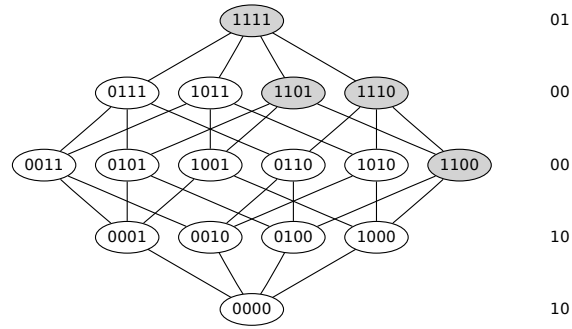
Figure 7.6: State representation of the function $x_1 \wedge x_2$ utilized in the EDA. The state (shown on the right) is a bit-string with two bits for each level of the Boolean lattice. The first bit is 1 only if the value of the function for all nodes in that level is 0 and the second bit is 1 only if its value for all nodes in that level is 1. This condensed representation of the function is based on the information utilized by the symmetry-building greedy algorithm and it is therefore useful for constructing minimal-size sorting networks.

Since the model is estimated from the set of the smallest networks in the population, it is likely to generate small networks as well. Although it can generate new networks from scratch, it is utilized as part of the above reproduction mechanism to reconstruct a new offspring network from the truncated parent network, i.e. it is utilized in step 2 of reproduction instead of the greedy algorithm. In this step, some comparators are also chosen randomly from the set of all potential comparators to encourage exploration of comparator combinations outside the model. Moreover, if the model does not generate any comparators for the current state, then the greedy algorithm is utilized to add a comparator. The resulting EDA finds smaller sorting networks than previous results, as demonstrated next.

7.4 Results

The EDA was run with a population size of 200 for 500 generations to evolve minimal-size networks for different input sizes. In each generation, the top half of the population (i.e. 100 networks with the least number of comparators) was selected for estimating the model. The same set of networks was copied to the next generation without modification.

Each of them also reproduced an offspring network to replace those in the bottom half of the population. A Gaussian probability distribution was utilized to select the comparator from which to truncate the parent network. The Gaussian was centered at the middle of its comparator sequence with a standard deviation of one-fourth its number of comparators. As a result, parent networks are more likely to be truncated near the middle than near the ends. When reconstructing the truncated network, the next comparator to add to the network is generated either by the estimated model (with probability 0.5) or is selected randomly from the set of all potential comparators (with probability 0.5).

The above experiments (variant 1) were repeated with a slight modification of the greedy algorithm used to initialize the population for the EDA. If the set of comparators with the highest utility contains a comparator that is symmetric with respect to another comparator already in the network, then it prefers that comparator (Graham and Oppacher, 2006). This modification (variant 2) makes the arrangement of comparators in the network more bilaterally symmetric about a horizontal axis through the middle of the network. Biasing the networks with this type of symmetry produced smaller networks for some input sizes. The source code for both variants is available from the website `http://nn.cs.utexas.edu/?sorting-code`.

Both variants were run 20 times, each time with a different random number seed. The least number of comparators that they found for each input size is listed in Table 7.1. For input sizes $n \leq 11$, the initial population of the EDA already contained networks with the smallest-known sizes for all 20 runs, i.e. the greedy algorithm was sufficient to find the smallest-known networks. As discussed in Section 3.3, optimality of such networks has been proven only for $n \leq 8$. For input sizes 12, 13, 14, 16, 21, and 23, the EDA evolved networks that have the same size as the best known networks. Moreover, it improved the previous best results for input sizes 17, 18, 19, 20, and 22 by one or two comparators. Examples of these networks are listed in Appendix A. Prospects of extending to $n > 24$ will be discussed in Chapter 8.

107

n	12	13	14	15	16	17	18	19	20	21	22	23	24
Previous best	Hand-design and END					Batcher's merge on smaller networks							
	39	45	51	56	60	73	80	88	93	103	110	118	123
EDA	*39*	*45*	*51*	57	*60*	**71**	**78**	**86**	**92**	*103*	**108**	*118*	125

Table 7.1: Sizes of the smallest networks for different input sizes found by the EDA. For input sizes $n \leq 11$, networks with the smallest-known sizes (Section 3.3) were already found in the initial population of the EDA, i.e. the greedy algorithm was sufficient. These sizes are therefore omitted from this table. For larger input sizes, evolution found networks that matched previous best results (indicated in *italics*) or improved them (indicated in **bold**). Appendix A lists examples of these networks. EDA variant 2 produced better results than variant 1 for input sizes 15, 17, 18, 20, 22, 23, and 24. Prospects of extending these results to input sizes greater than 24 will be discussed in Chapter 8. These results demonstrate that the symmetry-based EDA approach is effective at designing minimal-size sorting networks and has advanced the state-of-the-art.

The previous best results were obtained either by hand design or by the END evolutionary algorithm (Baddar, 2009, Juillé, 1995, Knuth, 1998). The END algorithm improved a 25-year old result for the 13-input case by one comparator and matched the best known results for other input sizes up to 16. However, it is a massively parallel search algorithm, requiring very large computational resources, e.g. it required a population size of 65,536 on 4096 processors to find minimal-size networks for 13 and 16 inputs. In contrast, the symmetry-based EDA algorithm finds such networks with much smaller resources (e.g. population size of 200 on a single processor in a similar number of generations), making it computationally feasible to solve larger problems.

7.5   Conclusion

Minimizing the number of comparators in a sorting network is a challenging optimization problem. This chapter presented an approach that converts it into the problem of building the symmetry of the network optimally. The resulting problem structure makes it possible to construct the network in steps and to minimize the number of comparators required for each step separately. This approach produces greedy solutions that are optimized further by evolution, exploring the neighborhood of these solutions in more detail. As with ENSO,

the resulting algorithm focuses search on promising regions of the search space, making it possible to find minimal-size networks efficiently. For several input sizes, these networks are smaller than the previous best results, thus advancing the state-of-the-art for designing minimal-size sorting networks.

Chapter 8

Discussion and Future Work

The work presented in previous chapters explored the hypothesis that symmetry can be utilized to constrain the design space meaningfully, making it possible to solve challenging engineering problems. For multilegged robots walking on flat ground, it was possible to constrain the controllers to a single hand-designed symmetry and evolve only the remaining parameters. Since it is not always possible to hand-design the appropriate symmetries, the ENSO approach was developed to evolve them automatically. ENSO utilizes group theory to break symmetry systematically, thereby constraining search to the most promising symmetries. The alternative process of building symmetry systematically was also useful in constraining the search space for finding minimal-size sorting networks. This chapter evaluates these results, discusses the insights gained from them, and proposes directions for future work.

8.1   Hand-Designed Symmetries

Modular neuroevolution with hand-designed symmetries produced controllers that were better than those produced by non-modular evolution with no symmetries in two respects: (1) they achieved a better fitness by travelling farther, and (2) they employed better gaits

that were symmetric, resembling those found in nature. Furthermore, this performance gap widened significantly in both respects when the number of legs or their degrees of freedom were increased. The symmetric controllers also demonstrated the capability to change gaits in response to changes in the environment. Changing gaits on an obstacle terrain made it easier for the robot to negotiate bumps. These results suggest that utilizing symmetries to constrain the search space makes it possible for modular neuroevolution to discover effective controllers.

In these experiments, the controllers were always evaluated by starting the robot from the same position. As a result, some evolved behaviors such as changing gaits to negotiate obstacles are not robust to different starting positions. They can be made more robust by averaging evaluations over multiple random starting positions or by adding noise to the simulation during evaluations as was done for the physical robot. Utilizing sensors that provide feedback about the environment may also improve robustness.

The controller symmetries were designed analytically using the theory of coupled cell systems. Hand-designing symmetries in this manner is too restrictive in the general case for two reasons. First, in the special case it was possible to replicate a single module for each leg because the legs were identical. In a more complex robot, more than one type of module may be needed, for example to control different types of front and rear legs. The resulting coupled cell system will have more than one type of cell and therefore different symmetries. Second, in the special case the coupling between the cells and the assignment of cells to legs was also determined by the hand-designed symmetries. More sophisticated behaviors may require different cell couplings and assignments that utilize different symmetries to explore a different part of the search space. Although hand-designing symmetries is possible in simple cases, it cannot (at least not as easily) be done in such complex, real-world cases.

Therefore, it is useful to evolve the appropriate symmetries automatically. However, the results of non-modular evolution suggests that it is too difficult to evolve symmetries in the unconstrained space of all possible symmetries. Consequently, a more constrained

111

approach that makes it possible to explore the space of symmetries in a meaningful way is necessary. The ENSO approach accomplishes this goal.

8.2 Symmetry Evolution with ENSO

Given the number of modules, ENSO's group-theory-based systematic symmetry search makes it possible to evolve the appropriate symmetry automatically. Demonstrating this capability, ENSO evolved gaits similar to those based on hand-designed symmetries on flat ground, and significantly faster gaits on inclined ground, for a quadruped robot. These gaits also generalized better when friction was reduced to make the ground slippery. As in the previous experiments with hand-designed symmetries, these gaits were evolved by starting the robot from the same position and orientation on the incline in every evaluation. More robust gaits can potentially be evolved by randomizing the initial orientation, by sensing the slope of the incline, or by adding noise to the simulation. Such robust gaits were indeed evolved for the physical robot in Chapter 6.

In order to verify that ENSO's symmetry-breaking approach is indeed a useful way to constrain search, it was compared with the less principled, random-symmetry-evolution approach. Random-symmetry evolution produces significantly worse gaits than ENSO because its unsystematic symmetry mutations often result in large changes in symmetry. In contrast, the group-theoretic mutations of ENSO result in only minimal changes in symmetry, making complexification possible (Section 2.1): Evolution starts with a highly symmetric (i.e. simple) controller and breaks the symmetry incrementally, producing gradual increases in complexity. As a result, evolution optimizes simpler controllers before elaborating on these by adding more parameters. Thus the complexification resulting from symmetry breaking provides ENSO with a smoother fitness gradient, making evolution easier.

In addition to these evolutionary advantages that group theory provides, the theory of coupled cell systems provides ENSO with guarantees on the behavior of evolved controllers. For example, if the symmetries of a coupled cell system admit a particular gait,

then there exists an instance of the system with an asymptotically stable periodic solution (i.e. limit cycle) implementing that gait (Golubitsky and Stewart, 2002). As a result, the gait is robust to small perturbations. ENSO constrains neuroevolution to find such an instance of the control system. When the dynamics of this system was perturbed manually (utilizing a visualization interface to the physical simulation) the gaits they generate were indeed found to be robust. Such robustness is useful in controllers of real-world robots because their interactions with environment are frequently perturbed.

As discussed in Section 2.3, the symmetries of coupled cell systems also makes it possible for the same controller to produce multiple gaits. Each gait is a stable limit cycle of the coupled cell system, and the system can transition from one limit cycle to another when perturbed. Sometimes small perturbations, caused by physical interaction with the environment, can trigger such a transition. Figure 5.5d shows an example of this phenomenon, where the robot changes from an initial pronk to a trot at about three seconds into the simulation. If the robot is prevented from interacting with the ground, then this change does not occur and the robot continues executing the pronk gait. The ability of controllers to generate such different gaits makes it possible to use the most effective gait for a given terrain, including those that allow it to go over obstacles (Section 4.7).

It is difficult to obtain the above properties in controllers evolved without such mathematical models. For example, oscillations required for generating gaits needed to be supplied as external inputs to quadruped controllers evolved using the HyperNEAT method (Clune et al., 2009). These properties were crucial in transferring the controllers that ENSO evolved in simulation to a physical robot.

These results suggest that ENSO is an effective approach for evolving locomotion controllers for multilegged robots. In the future, ENSO should be tested with more complex robots with more legs, more complex legs, and sensors that receive more varied stimuli from the environment. Their controllers can be modeled as coupled cell systems with more cells and cells receiving additional inputs. Utilizing such more sophisticated models should make

113

it possible for ENSO to evolve controllers that produce high-level behaviors such as path-following and foraging, in addition to generating regular gaits. ENSO is thus a promising approach for developing efficient, robust, and flexible controllers for multilegged robots in the real world.

ENSO breaks symmetry by utilizing the prior knowledge encoded in the subgroup lattice. In contrast, symmetry-breaking occurs spontaneously in nature when perturbations induce a physical system in a symmetric (but unstable) state to transition to a less symmetric (but stable) state with lower energy (Brading and Castellani, 2008, Kovacs, 1986). That is, the dynamics of natural phenomena encode the knowledge in the subgroup lattice implicitly. Nature can therefore utilize these phenomena to break symmetry in biological evolution. Whether modeling them in artificial evolution is an effective substitute for the constraints encoded explicitly in the subgroup lattice is an interesting question for future research.

8.3   Evolving Controllers for a Physical Robot

ENSO evolved controllers that produced the same gaits in the physical robot as they did in simulation. Moreover, these gaits were robust to uncertainties that commonly occur in the real world such as changes in ground friction between different surfaces, initial positions of legs from which the robot starts walking, and the maximum angular velocity that the motors can produce. The transfer was successful because of two factors: (1) ENSO was able to evolve robust controllers that produce stable gaits, and (2) it was possible to simulate the physical characteristics of the robot with sufficient accuracy.

It is often difficult to transfer controllers evolved in simulation to the real world because it is difficult to simulate the physical robot and its environment accurately (Gomez and Miikkulainen, 2004, Lipson et al., 2006). However, this requirement is less critical for the controllers that ENSO evolves because their robustness can compensate for small deviations from ideal behavior. For example, instead of detailed mesh models of the robot morphology, only a crude approximation of its weight distribution was required. Moreover,

it turned out sufficient to model the idiosyncratic properties of the motors and uncertainties in their behavior using interpolation and noise.

Evolving controllers in simulation and then transferring them to the real robot in this manner is an effective alternative to designing controllers by hand. Hand-design is difficult because it requires anticipating all possible operating conditions. Moreover, this laborious process has to be repeated whenever the configuration of the robot changes and it may even be impossible in some cases. In contrast, evolution can design a new controller automatically for the new configuration in simulation. For example, if a leg actuator fails on a quadruped robot during a remote mission, then it must continue the mission with minimum performance degradation by utilizing only the remaining three legs. ENSO evolved a straight and effective gait for such a three-legged configuration by disabling a leg in simulation. The resulting controller produced the same gait when transferred to the physical robot as well, suggesting that ENSO's symmetry-based approach can be utilized to design fault-tolerant robots for real-world applications.

The physical quadruped robot can be extended to a hexapod easily by adding two more legs to attachments in the middle. This extension should be able to demonstrate that the ENSO approach scales up for a physical robot with more legs. ENSO can also be tested on a robot with more complex legs by designing new legs with additional joints. Another interesting way to extend the robot is to attach Dynamixel AX-S1 sensors to measure distance Robotis (2010). Readings from these sensors can then be used as additional controller inputs, making it possible to evolve behaviors that respond effectively to obstacles in the environment. Such extensions can build up the sophistication necessary for real-world applications.

8.4 Utilizing Domain Knowledge in ENSO

ENSO can also evolve controllers for robots with more legs and more degrees of freedom per leg, such as those discussed in Chapter 4. These robots may have more joints per leg

such as a knee joint in addition to the hip joint. The controllers for such robots may need a different module for each type of joint. Moreover, the knee joint of one leg is not likely to influence the hip joint of another leg directly, allowing this domain knowledge to be used to restrict the connectivity of the graphs in the initial population of ENSO. In particular, each knee module is connected only to the hip module of the same leg, while the hip modules of all legs are fully interconnected as before. Utilizing domain knowledge in this manner to constrain the space of symmetries makes it easier for evolution to optimize the resulting controller.

The above robot morphology can be extended further by adding a foot joint to each leg, resulting in a controller with local interconnections between the hip, knee and foot modules. However, it is more convenient to represent such controllers using a two-level hierarchy instead of using a flat structure. The top level of the hierarchy contains the interconnection structure between leg modules. Each leg module is then decomposed into a second level, containing the interconnection structure between the hip, knee and foot modules for that leg. Such a hierarchical phenotype graph can be encoded by a hierarchical genotype tree (Figure 8.1). The vertex color in the top-level tree contains a special parameter that is a pointer to the bottom-level genotype tree. This hierarchical genotype allows the phenotype structure of each level to evolve independently. Moreover, it decomposes the phenotype graph into smaller graphs, whose symmetries can be evolved more easily because their automorphism groups are smaller.

Future experiments along these lines should demonstrate that (1) domain knowledge can be effectively incorporated into the ENSO approach by constraining the initial structure of the phenotype graph, and (2) the ENSO approach can design complex controller networks consisting of different modules and interconnection structures by evolving them together. These capabilities may be necessary to design controllers for complex robots, e.g. amphibious robots that can swim in water and walk on land, robotic manipulators that con-
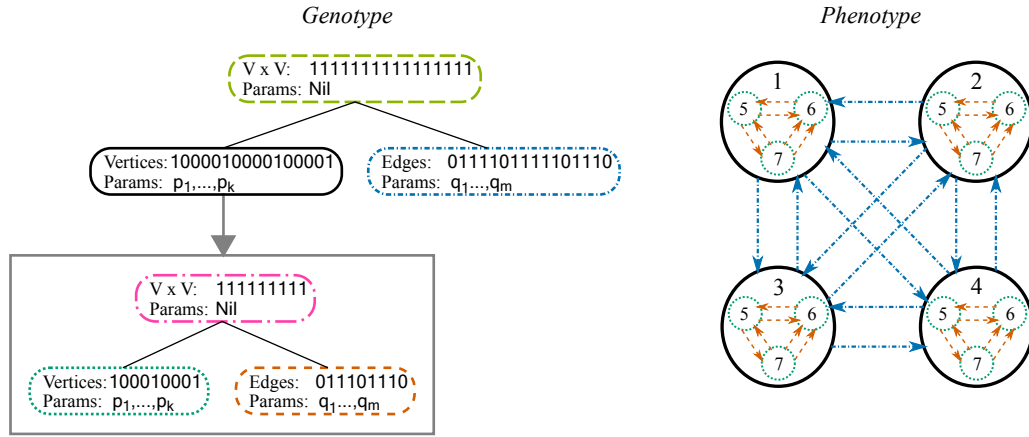
116

Figure 8.1: A two-level hierarchical genotype and phenotype. Modules of the top-level of the phenotype graph are decomposed into smaller interconnected modules, creating the bottom-level phenotype graphs. In the top-level of the corresponding genotype tree, the vertex color contains a special parameter that stores the genotype tree for the bottom-level phenotype graph. Decomposing the phenotype graph into smaller graphs in this manner should make it easier to evolve its symmetry, and constitutes an interesting direction of future work.

sist of several parts for use in industrial applications, and serpentine robots that move by flexing their spine.

8.5   Other Applications of ENSO

ENSO can also be used to evolve solutions for other control problems that are characterized by symmetry and modularity. For example, it can be used to design multiagent systems consisting of agents that interact with each other and with the environment, like those in online auctions and in robotic soccer (Stone and Veloso, 2000). The behavior of these agents can be represented as neural network modules and their interactions as (symmetric) connections between the modules. Another application is in designing distributed control systems for automated manufacturing processes (McFarlane, 1998). Such systems consist of controller modules interconnected by communication networks and they can therefore be implemented as modular neural networks. In both cases, identical modules and connections between them produce symmetries that ENSO can evolve to design effective control

systems. Similarly, ENSO can be used to design distributed computing systems such as a computer network of clients and servers by evolving the parameters and topology of those networks (Berryman et al., 2004).

Besides controllers for multilegged locomotion, coupled cell systems can also model other dynamical systems in nature as symmetric networks. As a result, ENSO can potentially be used to optimize them. For example, coupled cell systems have been used to study the formation of new species in nature (Golubitsky and Stewart, 2002), the role of structural symmetries of the visual cortex in inducing visual hallucinations (Golubitsky et al., 2003), and the properties of genetic regulatory networks (Edwards and Glass, 2000). ENSO can be used as a tool both for understanding such biological phenomena and for engineering artificial systems based on them.

8.6   Extending ENSO

Some of the above applications may require extending ENSO in various ways to improve its capabilities. First, modules with a fixed neural network architecture (i.e. network topology) was sufficient for the multilegged robot controllers that ENSO evolved in this dissertation. However, more complex applications may require more complex topologies. In such applications, ENSO can evolve the topology of the modules by utilizing techniques such as NEAT (Stanley and Miikkulainen, 2004).

Second, in many applications such as distributed controllers and multiagent systems, the number of modules remains fixed and is known. ENSO requires the user to specify this domain knowledge, making it possible to initialize evolution with the appropriate most general symmetries. However, in other applications such as biological networks (Kepes, 2007) and body-brain evolution (Bongard and Pfeifer, 2003), the modules may not be known a priori. If the number of modules is constant as in biological networks, then ENSO can potentially be extended with clustering algorithms to determine the modules au-

tomatically (Gao et al., 2009). If the number of modules changes as in body-brain evolution, then ENSO will have to change the subgroup lattice accordingly.

Third, crossover of genotypes to produce offspring is useful in applications that benefit from the building-block hypothesis: In such applications, it is possible to assemble functionally complementary blocks from different parents (Watson and Jansen, 2007). Therefore, in addition to the mutation operators that ENSO already implements, it should be extended to include crossover, e.g. by swapping subtrees that have the same structure and node colors. Such subtrees preserve symmetries in the offspring and are therefore likely to have similar roles in their parents, making crossover effective.

Fourth, although only the leaf nodes of the genotype trees represent the phenotype graph in the current implementation, an even more compact representation is possible. The child nodes could inherit one or more parameter values from their parent instead of specifying those parameter values repeatedly in each child node. This feature is useful for representing variations of similar elements compactly, which is a common theme in complex systems with regularities (Stanley, 2007, Stanley and Miikkulainen, 2003). Such elements can be constructed from leaf nodes that inherit some parameters from a common parent, but specify different values for other parameters in the leaf nodes. As a result, these elements have the same values for parameters inherited from the parent, while they differ in the values for parameters specified in the leaf nodes, i.e. they represent variations on a common theme such an extension would allow.

Fifth, ENSO utilizes the computational group theory functions of GAP (2007) to compute the subgroup lattice required for breaking symmetry. However, computing the subgroup lattice is combinatorially hard in the number of graph vertices. For evolving larger graphs, ENSO's scalability can be improved by approximating its group theory computations with fast graph computations. In particular, the orbital partitions of subgroups can be approximated with 2-stable colorings (Bastert, 2001). For a graph with vertex set v, this approximation will allow ENSO to search directly in the partition lattice of $V \times V$ instead

of in the subgroup lattice of $\mathcal{S}_{|V|}$, thus avoiding the computation of the subgroup lattice at the cost of visiting more points on the partition lattice. However, this additional cost is likely to be small because the stabilization algorithms used to compute 2-stable colorings produce orbital partitions in many favorable cases (Bastert, 2001).

These extensions would improve evolutionary search, potentially making it possible for ENSO to solve more difficult problems and a wider variety of problems.

8.7   Evolving Sorting Networks

The general principle on which ENSO is based, i.e. constraining search by utilizing symmetry, is broadly applicable, as demonstrated by evolving minimal-size sorting networks. Previous results on designing such networks automatically by search have been limited to small input sizes ($n \leq 16$) because the number of valid sorting networks near the optimal size is very small compared to the combinatorially large space that has to be searched (Juillé, 1995). The symmetry-building approach presented in Chapter 7 mitigates this problem by utilizing symmetry to focus the search on the space of networks near the optimal size. As a result, it was possible to search for minimal-size networks with more inputs ($n \leq 24$), improving the previous best results in five cases.

It should be possible to improve these results further and to scale them to larger values of n by extending this symmetry-based approach in the following ways. First, the greedy algorithm for adding comparators can be improved by evaluating the sharing utility of groups of one or more comparators instead of single comparators. Such groups having the highest average utility will then be preferred.

Second, the greedy algorithm can be made less greedy by considering the impact of current comparator choices on the number of comparators that will be required for later subgoals. This analysis will make it possible to optimize across subgoals, potentially producing smaller networks at the cost of additional computations.

120

Third, the state representation that the EDA algorithm utilizes contains only sparse information about the functions computed by the comparators. Extending it to include more relevant information should make it possible for the EDA to disambiguate overlapping states and therefore to model comparator distribution more accurately.

Fourth, the EDA generates comparators to add to the network only if the state of the network matches a state in the generative model exactly. Making this match fuzzy based on some similarity measure may produce better results by exploring similar states when an exact match is not found.

Fifth, evolutionary search can be parallelized, e.g. using the massively parallel END algorithm that has been shown to evolve the best known network sizes for $n \leq 16$ (Juillé, 1995). Utilizing the symmetry-building approach to constrain the search space should make it possible to run the END algorithm on networks with more inputs.

Sixth, the symmetry-building approach itself can be improved. For example, it utilizes only the symmetries resulting from the duality of the output functions. It may be possible to extend this approach by also utilizing the symmetries resulting from the permutations of the input variables.

Seventh, large networks can be constructed from smaller networks by merging the outputs of the smaller networks. Since smaller networks are easier to optimize, they can be evolved first and then merged by continuing evolution to add more comparators. This construction is similar to utilizing the odd-even merge (Batcher, 1968) to construct minimal networks for $n > 16$ from smaller networks.

In addition to finding minimal-size networks, the same symmetry-based approach can also be utilized to find minimal-delay networks. Instead of minimizing the number of comparators, it would now minimize the number of parallel steps into which the comparators are grouped. Both these objectives can be optimized simultaneously as well, either by preferring one objective over the other in the fitness function or by utilizing a multi-objective optimization algorithm such as NSGA-II (Deb et al., 2000).

Moreover, this approach can potentially be extended to design comparator networks for other related problems such as rank order filters (Chakrabarti and Wang, 1994, Chung and Lin, 1997, Hiasat and Hasan, 2003). A rank order filter with rank r selects the rth largest element from an input set of n elements. Such filters are widely used in image and signal processing applications, e.g. to reduce high-frequency noise while preserving edge information. Since these filters are often implemented in hardware, minimizing their comparator requirement is necessary to minimize their chip area. More generally, similar symmetry-based approaches may be useful for designing stack filters, i.e. circuits implementing monotone Boolean functions, which are also popular in signal processing applications (Hiasat and Hasan, 2003, Shmulevich et al., 1995). Furthermore, such approaches can potentially be used to design rearrangeable networks for switching applications as well (Seo et al., 1993, Yeh and Feng, 1992).

8.8   Conclusion

Utilizing symmetries to constrain evolutionary search improves search efficiency in problems as varied as designing controllers for multilegged robots and constructing minimal-size sorting networks. Depending on the nature of the problem, these constraints are applied either by breaking symmetries as in controller design or by building symmetries as in sorting network optimization. As discussed in this chapter, these methods may also benefit a variety of other problems with symmetries. Also, several proposed extensions should make it possible to solve even harder instances of these problems.

Chapter 9

Conclusion

Evolutionary search is a popular approach to automatically design complex systems that are difficult to design by hand. However, its effectiveness is often limited by the complexity and the size of the design space. Constraining the design space to promising solutions can improve the effectiveness of evolutionary search. This dissertation showed how such constraints can be applied when evolving systems with symmetries. This chapter summarizes the resulting contributions and evaluates their impact in evolutionary design.

9.1 Contributions

Sometimes it is possible to design the symmetries of the system by hand and utilize them to constrain evolutionary search. Chapter 4 explored this approach empirically by designing modular neural network controllers for simulated multilegged robots. The resulting controllers produced effective and symmetric gaits, resembling animal gaits in nature, and scaled well to more complex robots. In contrast, non-modular controllers, evolved without symmetry constraints, produced gaits resembling crippled animals that were less effective and did not scale. The conclusion is that constraining evolutionary search with appropriate symmetries is crucial for evolving effective controllers for multilegged robots.

Since designing such symmetries by hand is not always possible, Chapter 5 developed the ENSO approach to evolve the symmetries together with the neural network modules. In order to search the space of symmetries effectively, ENSO utilizes group theory to break symmetry systematically, thus constraining evolution to promising symmetries. Repeating the previous experiments with ENSO showed that it evolves controllers that are as effective as those with hand-designed symmetries. Moreover, when the appropriate symmetries are difficult to design by hand (such as for inclined ground), ENSO evolves specialized gaits that are significantly faster and generalizes better. That is, ENSO is effective at designing modular neural network controllers together with their symmetries.

Chapter 6 extended this capability to a physical quadruped robot. Utilizing a detailed simulation of the robot, ENSO evolved controllers that were shown to work equally well when transferred to the physical robot. These controllers are robust and generalize well to common variations in the real world. Further experiments on this robot with a disabled leg showed that ENSO also allows building extremely fault-tolerant systems by evolving effective controllers even for such challenging configurations.

The principle of utilizing symmetry to constrain evolutionary search can be generalized to develop new approaches for solving structural design problems as well. Chapter 7 demonstrated this generality by building symmetries for minimal-size sorting networks. Minimizing such networks is a hard combinatorial optimization problem with practical applications. The resulting algorithm scales evolution to larger networks than was previously possible, discovering several now minimal networks.

9.2 Conclusion

Evolutionary design of complex systems is challenging because such systems have large search spaces. This dissertation presented an approach that utilizes symmetry to constrain evolution to promising regions of the search space, thus making search more effective. In particular, the ENSO method was developed to design symmetric modular systems such

as controllers for multilegged robots. However, the principle of utilizing symmetries to constrain evolutionary search is more general, finding applications in structural design as well, including sorting networks.

The approach was primarily developed with engineering design in mind, and such applications are where this dissertation can potentially have its largest impact. However, ENSO was inspired by symmetry-breaking in natural evolution, i.e. simple, symmetric organisms evolving into complex, less symmetric organisms. By utilizing symmetry as the organizing principle, it is also able to represent other common properties of developmental systems such as modularity and reuse. Therefore, this research can also potentially contribute to a deeper understanding of biology by building artificial systems to simulate and validate hypotheses about natural phenomena.

Appendix A

Evolved Sorting Networks

This appendix lists examples of minimal-size sorting networks evolved by the algorithm described in Chapter 7. For each example, the sequence of comparators is illustrated in a figure and also listed as pairs of horizontal lines numbered from top to bottom.
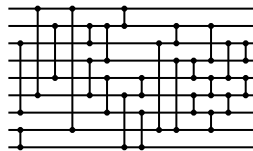

Figure A.1: Evolved 9-input network with 25 comparators: [3, 7], [1, 6], [2, 5], [8, 9], [1, 8], [2, 3], [4, 6], [5, 7], [6, 9], [2, 4], [7, 9], [1, 2], [5, 6], [3, 8], [4, 8], [4, 5], [6, 7], [2, 3], [2, 4], [7, 8], [5, 6], [3, 5], [6, 7], [3, 4], [5, 6].
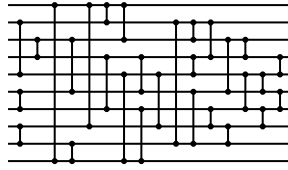
Figure A.2: Evolved 10-input network with 29 comparators: [2, 5], [8, 9], [3, 4], [6, 7], [1, 10], [3, 6], [1, 8], [9, 10], [4, 7], [5, 10], [1, 2], [1, 3], [7, 10], [4, 6], [5, 8], [2, 9], [4, 5], [6, 9], [7, 8], [2, 3], [8, 9], [2, 4], [3, 6], [5, 7], [3, 4], [7, 8], [5, 6], [4, 5], [6, 7].
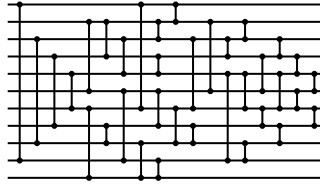

Figure A.3: Evolved 11-input network with 35 comparators: [1, 10], [3, 9], [4, 8], [5, 7], [2, 6], [2, 4], [3, 5], [7, 11], [8, 9], [6, 10], [1, 7], [2, 3], [9, 11], [10, 11], [1, 2], [6, 8], [4, 5], [7, 9], [3, 7], [2, 6], [8, 9], [5, 10], [3, 4], [9, 10], [2, 3], [5, 7], [4, 6], [7, 8], [8, 9], [3, 4], [5, 7], [6, 7], [4, 5], [7, 8], [5, 6].
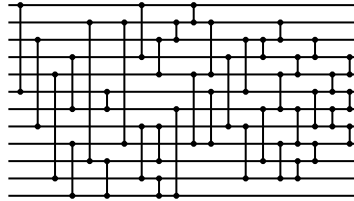

Figure A.4: Evolved 12-input network with 39 comparators: [1, 6], [3, 8], [5, 11], [4, 7], [9, 12], [2, 10], [6, 7], [2, 9], [1, 4], [3, 5], [10, 12], [8, 11], [8, 10], [11, 12], [2, 3], [7, 12], [1, 2], [5, 9], [6, 9], [2, 5], [4, 8], [3, 6], [8, 11], [7, 10], [3, 4], [5, 7], [9, 11], [2, 3], [10, 11], [7, 9], [4, 5], [9, 10], [3, 4], [6, 8], [5, 6], [7, 8], [8, 9], [6, 7], [4, 5].
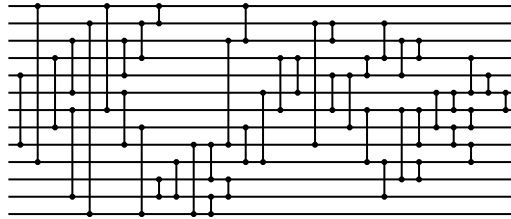

Figure A.5: Evolved 13-input network with 45 comparators: [5, 9], [1, 10], [4, 8], [3, 6], [7, 12], [2, 13], [1, 7], [3, 5], [6, 9], [8, 13], [2, 4], [11, 12], [10, 12], [1, 2], [9, 13], [9, 11], [3, 9], [12, 13], [1, 3], [8, 10], [6, 10], [4, 7], [4, 6], [2, 9], [5, 7], [5, 8], [11, 12], [7, 10], [4, 5], [2, 3], [10, 12], [2, 4], [7, 11], [3, 5], [3, 4], [10, 11], [7, 9], [6, 8], [6, 7], [8, 9], [4, 6], [9, 10], [5, 6], [7, 8], [6, 7].
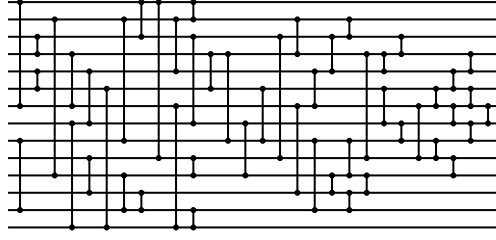
127

Figure A.6: Evolved 14-input network with 51 comparators: [1, 7], [3, 4], [9, 13], [5, 6], [2, 11], [8, 14], [10, 12], [4, 7], [5, 8], [6, 14], [2, 9], [11, 13], [1, 3], [12, 13], [1, 10], [2, 5], [7, 14], [13, 14], [1, 2], [3, 8], [4, 6], [10, 11], [4, 9], [8, 11], [6, 9], [3, 10], [7, 12], [5, 7], [9, 13], [2, 4], [11, 12], [3, 5], [12, 13], [2, 3], [9, 11], [4, 10], [4, 5], [3, 4], [11, 12], [6, 8], [8, 9], [7, 10], [6, 7], [5, 6], [9, 10], [7, 8], [10, 11], [4, 5], [6, 7], [8, 9], [7, 8].
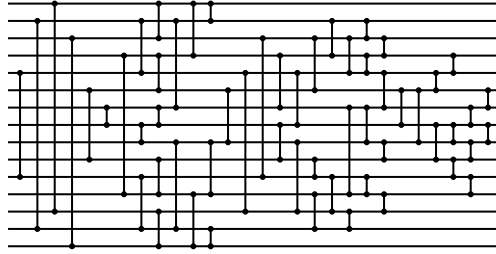

Figure A.7: Evolved 15-input network with 57 comparators: [5, 11], [2, 14], [1, 13], [3, 15], [6, 10], [7, 8], [4, 12], [8, 9], [2, 5], [11, 14], [4, 6], [10, 12], [1, 3], [13, 15], [7, 8], [2, 7], [9, 14], [1, 4], [12, 15], [9, 12], [1, 2], [6, 9], [14, 15], [5, 13], [3, 11], [8, 10], [4, 7], [9, 13], [5, 8], [10, 11], [3, 6], [2, 4], [12, 14], [11, 13], [13, 14], [3, 5], [2, 3], [7, 12], [4, 5], [7, 9], [11, 12], [5, 7], [9, 10], [12, 13], [3, 4], [6, 8], [6, 9], [8, 10], [5, 6], [10, 11], [11, 12], [4, 5], [8, 9], [9, 10], [7, 8], [6, 7], [8, 9].
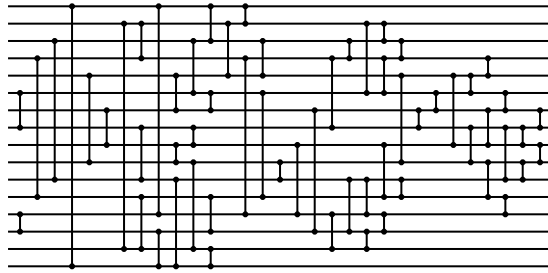

Figure A.8: Evolved 16-input network with 60 comparators: [13, 14], [6, 8], [4, 12], [3, 11], [1, 16], [5, 10], [7, 9], [2, 15], [12, 15], [2, 4], [8, 11], [1, 13], [5, 7], [3, 6], [9, 10], [14, 16], [11, 16], [1, 3], [10, 15], [2, 5], [1, 2], [15, 16], [6, 7], [8, 9], [12, 14], [4, 13], [6, 12], [10, 11], [9, 13], [3, 5], [7, 14], [4, 8], [3, 4], [13, 15], [11, 14], [2, 6], [14, 15], [2, 3], [4, 6], [11, 13], [13, 14], [3, 4], [9, 12], [5, 10], [11, 12], [7, 8], [6, 7], [5, 9], [8, 10], [5, 6], [10, 12], [12, 13], [4, 5], [7, 9], [8, 11], [10, 11], [6, 7], [8, 9], [9, 10], [7, 8].
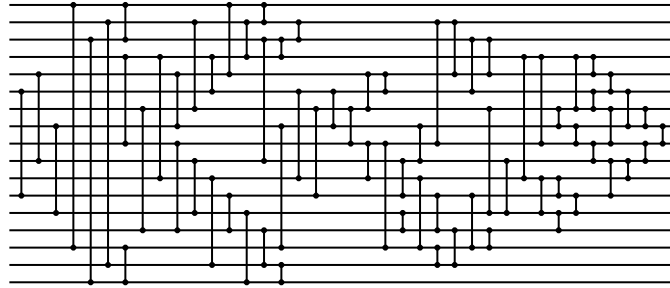
128

Figure A.9: Evolved 17-input network with 71 comparators: [6, 12], [5, 10], [8, 13], [1, 15], [3, 17], [2, 16], [4, 9], [7, 14], [4, 11], [9, 14], [5, 8], [10, 13], [1, 3], [15, 17], [2, 7], [11, 16], [4, 6], [12, 14], [1, 5], [13, 17], [2, 4], [14, 16], [1, 2], [16, 17], [3, 10], [8, 15], [6, 11], [7, 12], [6, 8], [7, 9], [9, 11], [3, 4], [9, 15], [10, 12], [13, 14], [5, 7], [11, 15], [5, 6], [8, 10], [12, 14], [2, 3], [15, 16], [2, 9], [14, 16], [2, 5], [3, 6], [12, 15], [14, 15], [3, 5], [7, 13], [10, 13], [4, 11], [4, 9], [7, 8], [11, 13], [4, 7], [4, 5], [13, 14], [11, 12], [6, 7], [12, 13], [5, 6], [8, 9], [9, 10], [7, 9], [10, 12], [6, 8], [7, 8], [10, 11], [9, 10], [8, 9].
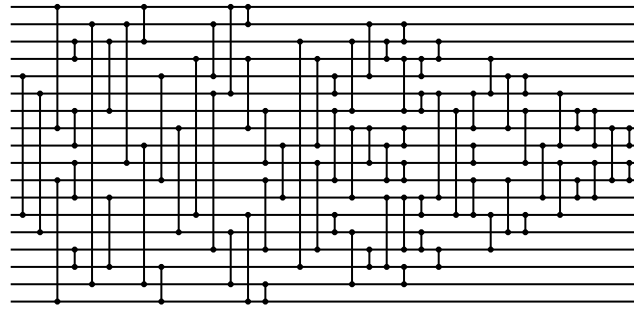

Figure A.10: Evolved 18-input network with 78 comparators: [5, 13], [6, 14], [1, 8], [11, 18], [3, 4], [15, 16], [7, 9], [10, 12], [2, 17], [3, 7], [12, 16], [2, 10], [9, 17], [5, 11], [8, 14], [4, 13], [6, 15], [1, 3], [16, 18], [2, 5], [14, 17], [1, 6], [13, 18], [1, 2], [17, 18], [4, 8], [11, 15], [7, 10], [9, 12], [3, 16], [4, 9], [10, 15], [5, 6], [13, 14], [7, 11], [3, 7], [8, 12], [2, 5], [14, 17], [15, 16], [3, 4], [12, 16], [16, 17], [2, 3], [12, 15], [4, 7], [14, 15], [4, 5], [15, 16], [3, 4], [6, 7], [12, 13], [8, 10], [9, 11], [10, 11], [8, 9], [6, 12], [7, 13], [11, 13], [6, 8], [13, 15], [4, 6], [11, 14], [5, 8], [13, 14], [5, 6], [9, 10], [7, 10], [9, 12], [10, 13], [6, 9], [7, 8], [11, 12], [7, 9], [10, 12], [8, 11], [10, 11], [8, 9].
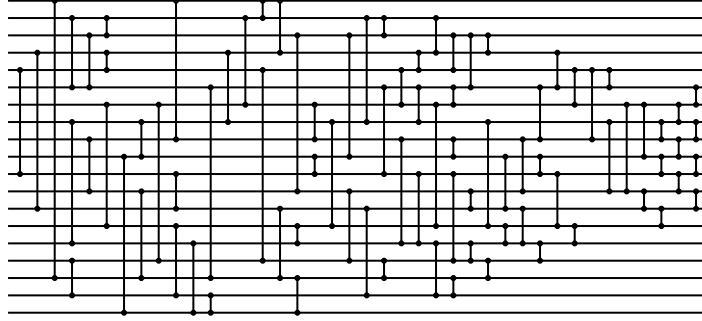
Figure A.11: Evolved 19-input network with 86 comparators: [5, 11], [4, 13], [1, 17], [8, 15], [9, 12], [7, 14], [16, 18], [2, 6], [10, 19], [3, 6], [12, 17], [8, 10], [2, 3], [7, 16], [11, 13], [4, 5], [14, 18], [1, 9], [15, 19], [6, 17], [4, 8], [18, 19], [2, 7], [5, 16], [1, 2], [13, 17], [1, 4], [17, 19], [3, 12], [10, 11], [14, 15], [7, 9], [8, 14], [3, 10], [12, 16], [2, 8], [6, 11], [13, 18], [9, 15], [5, 7], [11, 15], [4, 5], [16, 17], [2, 3], [15, 18], [2, 4], [17, 18], [6, 8], [7, 14], [6, 7], [11, 16], [3, 5], [15, 16], [3, 6], [12, 13], [16, 17], [3, 4], [9, 10], [8, 14], [10, 13], [9, 12], [10, 11], [14, 15], [6, 9], [13, 15], [15, 16], [4, 6], [5, 7], [11, 14], [5, 9], [5, 6], [14, 15], [8, 12], [7, 12], [7, 10], [8, 9], [12, 13], [7, 8], [13, 14], [6, 7], [10, 11], [11, 12], [12, 13], [9, 10], [8, 9], [10, 11].
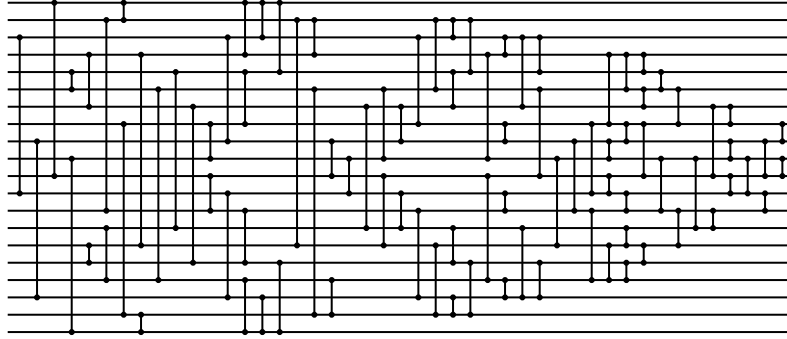

Figure A.12: Evolved 20-input network with 92 comparators: [3, 12], [9, 18], [1, 11], [10, 20], [5, 6], [15, 16], [4, 7], [14, 17], [2, 13], [8, 19], [4, 15], [6, 17], [1, 2], [19, 20], [5, 14], [7, 16], [8, 10], [11, 13], [3, 9], [12, 18], [5, 8], [13, 16], [1, 4], [17, 20], [1, 3], [18, 20], [1, 5], [16, 20], [2, 15], [6, 19], [9, 11], [10, 12], [7, 14], [6, 10], [11, 15], [2, 4], [17, 19], [7, 9], [12, 14], [3, 8], [13, 18], [2, 6], [2, 3], [15, 19], [5, 7], [14, 16], [18, 19], [16, 19], [2, 5], [4, 10], [11, 17], [3, 4], [17, 18], [14, 18], [3, 7], [16, 18], [3, 5], [8, 9], [12, 13], [6, 11], [10, 15], [9, 13], [8, 12], [4, 8], [13, 17], [4, 6], [15, 17], [16, 17], [4, 5], [6, 7], [14, 15], [15, 16], [5, 6], [11, 12], [9, 10], [12, 13], [8, 9], [8, 11], [10, 13], [6, 8], [13, 15], [10, 14], [7, 11], [7, 8], [11, 12], [13, 14], [9, 10], [10, 12], [12, 13], [9, 11], [8, 9], [10, 11].
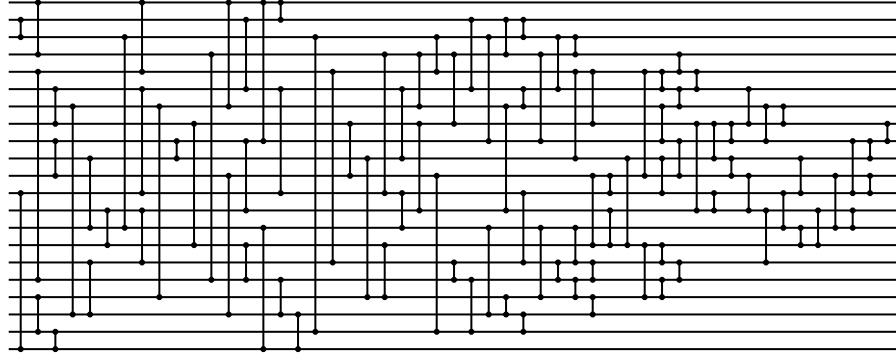
130

Figure A.13: Evolved 21-input network with 103 comparators: [12, 21], [2, 3], [5, 17], [9, 11], [18, 20], [6, 8], [7, 19], [10, 14], [13, 15], [1, 4], [3, 14], [1, 5], [20, 21], [16, 19], [6, 12], [13, 16], [7, 18], [9, 10], [8, 15], [4, 17], [11, 19], [9, 13], [15, 17], [1, 7], [14, 21], [2, 6], [1, 9], [17, 19], [19, 21], [1, 2], [6, 12], [3, 20], [5, 16], [8, 11], [10, 18], [4, 12], [6, 10], [12, 14], [8, 13], [15, 18], [4, 7], [11, 20], [3, 5], [16, 17], [4, 8], [2, 6], [17, 20], [3, 9], [14, 19], [2, 4], [18, 19], [19, 20], [2, 3], [7, 13], [12, 16], [6, 7], [14, 18], [16, 17], [4, 9], [17, 18], [3, 6], [18, 19], [3, 4], [14, 16], [11, 15], [5, 10], [5, 8], [11, 12], [13, 15], [10, 15], [5, 11], [5, 6], [16, 17], [15, 18], [17, 18], [4, 5], [7, 9], [10, 12], [6, 7], [9, 11], [15, 16], [5, 6], [16, 17], [8, 13], [12, 13], [8, 10], [10, 11], [11, 13], [8, 9], [6, 8], [13, 16], [12, 14], [7, 9], [14, 15], [7, 8], [13, 15], [10, 12], [11, 14], [9, 12], [9, 10], [8, 9], [11, 12], [13, 14].
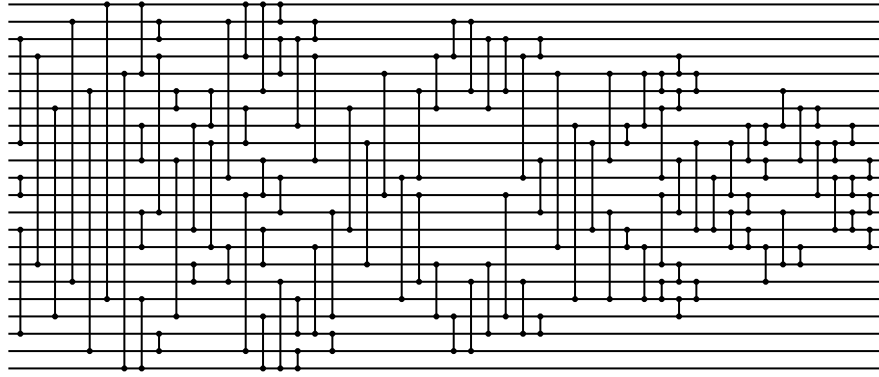

Figure A.14: Evolved 22-input network with 108 comparators: [11, 12], [3, 9], [14, 20], [4, 16], [7, 19], [2, 17], [6, 21], [1, 18], [5, 22], [8, 10], [13, 15], [1, 5], [18, 22], [4, 13], [10, 19], [2, 3], [20, 21], [8, 14], [9, 15], [6, 7], [16, 17], [6, 8], [15, 17], [2, 11], [12, 21], [1, 4], [19, 22], [1, 6], [17, 22], [1, 2], [21, 22], [7, 9], [14, 16], [3, 5], [18, 20], [10, 12], [11, 13], [3, 8], [15, 20], [4, 10], [13, 19], [7, 14], [9, 16], [5, 12], [11, 18], [6, 11], [12, 17], [4, 7], [16, 19], [2, 3], [20, 21], [2, 4], [19, 21], [2, 6], [17, 21], [3, 7], [16, 20], [12, 19], [3, 6], [17, 20], [4, 11], [3, 4], [19, 20], [10, 13], [5, 15], [8, 18], [9, 14], [13, 18], [5, 10], [14, 15], [8, 9], [5, 8], [15, 18], [5, 6], [17, 18], [18, 19], [4, 5], [7, 11], [12, 16], [6, 7], [16, 17], [5, 6], [17, 18], [10, 13], [9, 14], [11, 14], [9, 12], [8, 10], [13, 15], [8, 9], [14, 15], [15, 17], [6, 8], [10, 11], [12, 13], [7, 10], [13, 16], [15, 16], [7, 8], [9, 12], [11, 14], [9, 10], [13, 14], [8, 9], [14, 15], [11, 12], [12, 13], [10, 11].
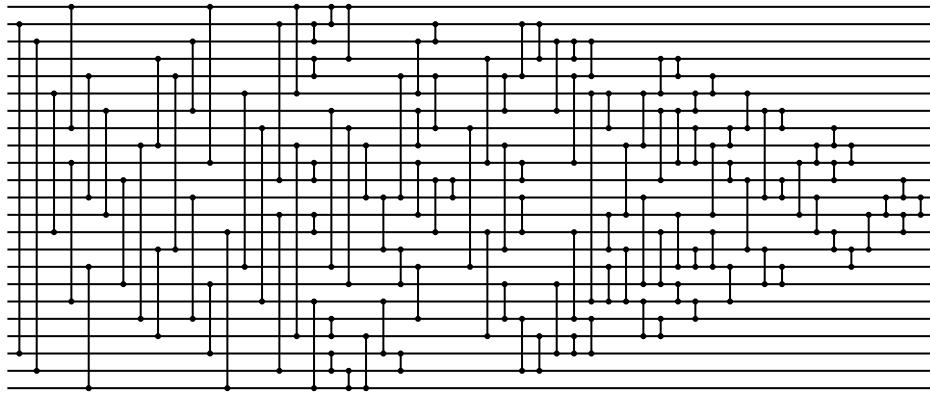
131

Figure A.15: Evolved 23-input network with 118 comparators: [2, 21], [3, 22], [6, 14], [10, 18], [1, 8], [16, 23], [5, 12], [7, 13], [11, 17], [9, 19], [15, 20], [4, 9], [5, 15], [12, 19], [3, 7], [17, 21], [1, 10], [14, 23], [6, 16], [8, 18], [2, 11], [13, 22], [9, 20], [18, 23], [1, 6], [21, 22], [2, 3], [19, 20], [4, 5], [22, 23], [1, 2], [20, 23], [1, 4], [13, 14], [10, 11], [7, 16], [8, 17], [9, 12], [12, 15], [5, 12], [7, 9], [15, 17], [18, 21], [3, 6], [10, 13], [11, 14], [16, 19], [11, 12], [5, 8], [21, 22], [2, 3], [8, 16], [4, 10], [14, 20], [17, 19], [9, 15], [5, 7], [19, 22], [2, 5], [20, 22], [2, 4], [10, 11], [12, 14], [3, 7], [17, 21], [5, 10], [14, 19], [20, 21], [3, 4], [19, 21], [3, 5], [6, 18], [13, 15], [9, 13], [6, 8], [16, 18], [6, 9], [15, 18], [4, 6], [18, 20], [4, 5], [19, 20], [7, 11], [12, 17], [14, 17], [7, 10], [17, 18], [6, 7], [5, 6], [8, 10], [18, 19], [13, 16], [15, 16], [9, 13], [8, 9], [14, 16], [16, 18], [6, 8], [10, 11], [11, 15], [7, 12], [15, 17], [16, 17], [7, 8], [11, 12], [10, 13], [12, 14], [14, 15], [9, 10], [8, 9], [15, 16], [10, 11], [9, 10], [13, 15], [12, 13], [13, 14], [11, 12], [12, 13].
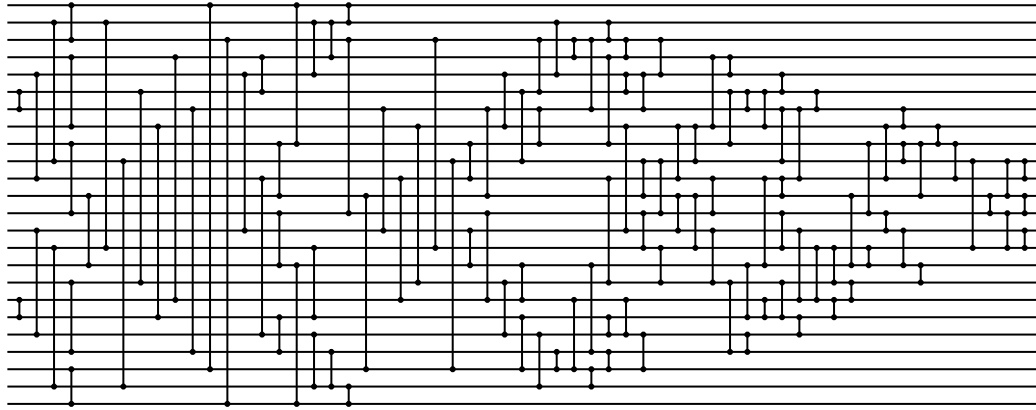
Figure A.16: Evolved 24-input network with 125 comparators: [6, 7], [18, 19], [5, 11], [14, 20], [2, 10], [15, 23], [9, 13], [12, 16], [4, 8], [17, 21], [1, 3], [22, 24], [2, 15], [10, 23], [6, 17], [8, 19], [4, 18], [7, 21], [1, 22], [3, 24], [5, 14], [11, 20], [9, 12], [13, 16], [4, 6], [19, 21], [1, 9], [16, 24], [2, 5], [20, 23], [2, 4], [21, 23], [15, 19], [1, 2], [23, 24], [3, 13], [12, 22], [7, 14], [11, 18], [8, 17], [3, 15], [10, 22], [9, 11], [14, 16], [7, 12], [13, 18], [5, 8], [17, 20], [6, 10], [19, 22], [3, 6], [2, 5], [20, 23], [16, 18], [7, 9], [21, 22], [3, 4], [18, 22], [3, 7], [2, 3], [22, 23], [16, 21], [4, 9], [5, 6], [19, 20], [18, 20], [5, 7], [21, 22], [3, 4], [20, 22], [3, 5], [11, 17], [8, 14], [10, 12], [13, 15], [10, 13], [15, 17], [8, 11], [12, 14], [12, 15], [14, 17], [8, 10], [4, 8], [17, 21], [4, 5], [20, 21], [6, 9], [16, 19], [18, 19], [6, 7], [17, 19], [6, 8], [19, 20], [5, 6], [7, 10], [11, 13], [11, 16], [13, 15], [14, 18], [11, 12], [7, 11], [15, 18], [18, 19], [6, 7], [15, 17], [12, 16], [9, 13], [8, 11], [17, 18], [7, 8], [15, 16], [9, 10], [13, 14], [9, 12], [14, 16], [16, 17], [8, 9], [9, 11], [10, 15], [12, 13], [10, 12], [13, 15], [14, 15], [12, 13], [10, 11].

Bibliography

Ajtai, M., Komlós, J., and Szemerédi, E. (1983). Sorting in $c \log n$ parallel steps. *Combinatorica*, 3(1):1–19.

Alden, M. E. (2007). *MARLEDA: Effective Distribution Estimation Through Markov Random Fields*. PhD thesis, Department of Computer Sciences, The University of Texas at Austin. Technical Report AI07-349.

Baddar, S. W. A. (2009). *Finding Better Sorting Networks*. PhD thesis, Kent State University.

Bastert, O. (2001). *Stabilization Procedures and Applications*. PhD thesis, Technische Universität Müchen.

Batcher, K. E. (1968). Sorting networks and their applications. In *AFIPS Spring Joint Computing Conference*, 307–314.

Beer, R. D., Chiel, H. J., and Sterling, L. S. (1989). Heterogeneous neural networks for adaptive behavior in dynamic environments. In *Advances in Neural Information Processing Systems 1*, 577–585. San Francisco, CA, USA: Morgan Kaufmann Publishers Inc.

Beer, R. D., and Gallagher, J. C. (1992). Evolving dynamical neural networks for adaptive behavior. *Adaptive Behavior*, 1(1):91–122.

Beineke, L., Wilson, R., and Cameron, P. (2004). Introduction. In Beineke, L. W., and Wilson, R. J., editors, *Topics in Algebraic Graph Theory*, 1–29. New York, NY, USA: Cambridge University Press.

Bengoetxea, E., Larranaga, P., Bloch, I., and Perchant, A. (2001). Estimation of distribution algorithms: A new evolutionary computation approach for graph matching problems. In *Energy Minimization Methods in Computer Vision and Pattern Recognition*, 454–469. Springer.

Berryman, M. J., Allison, A., and Abbott, D. (2004). Optimizing genetic algorithm strategies for evolving networks. In White, L. B., editor, *Noise in Communication*, vol. 5473 of *Proceedings of SPIE*, 122–130. Bellingham, WA, USA: SPIE.

Billard, A., and Ijspeert, A. J. (2000). Biologically inspired neural controllers for motor control in a quadruped robot. In *Proceedings of the International Joint Conference on Neural Networks (IJCNN 2000)*, 637–641.

Boers, E. J. W., and Kuiper, H. (1992). *Biological Metaphors and the Design of Modular Artificial Neural Networks*. Master's thesis, Departments of Computer Science and Experimental and Theoretical Psychology at Leiden University, The Netherlands.

Bongard, J. C., and Lipson, H. (2004). Once more unto the breach: Co-evolving a robot and its simulator. In *Proceedings of the Ninth International Conference on the Simulation and Synthesis of Living Systems (ALIFE9)*, 57–62. MIT Press.

Bongard, J. C., and Pfeifer, R. (2001). Repeated structure and dissociation of genotypic and phenotypic complexity in artificial ontogeny. In Spector, L., Goodman, E. D., Wu, A., Langdon, W. B., Voigt, H.-M., Gen, M., Sen, S., Dorigo, M., Pezeshk, S., Garzon, M. H., and Burke, E., editors, *Proceedings of the Genetic and Evolutionary Computation Conference*, 829–836. San Francisco: Morgan Kaufmann.

Bongard, J. C., and Pfeifer, R. (2003). Evolving complete agents using artificial ontogeny. In *Morpho-Functional Machines: The New Species (Designing Embodied Intelligence)*, 237–258. Springer-Verlag, Berlin.

Brading, K., and Castellani, E. (2008). Symmetry and symmetry breaking. In Zalta, E. N., editor, *The Stanford Encyclopedia of Philosophy*. The Metaphysics Research Lab, Center for the Study of Language and Information, Stanford University.

Brooks, R. A. (1989). A robot that walks; emergent behaviors from a carefully evolved network. Technical Report AIM-1091, Massachusetts Institute of Technology, Cambridge, MA, USA.

Brooks, R. A. (1992). Artificial life and real robots. In *Proceedings of the First European Conference on Artificial Life*, 3–10. MIT Press.

Brooks, R. A., and Maes, P., editors (1994). *Proceedings of the Fourth International Workshop on the Synthesis and Simulation of Living Systems (Artificial Life IV)*. Cambridge, MA: MIT Press.

Bull, L., Fogarty, T. C., and Snaith, M. (1995). Evolution in multi-agent systems: Evolving communicating classifier systems for gait in a quadrupedal robot. In *Proceedings of the 6th International Conference on Genetic Algorithms*, 382–388. San Francisco, CA, USA: Morgan Kaufmann Publishers Inc.

Cangelosi, A., Parisi, D., and Nolfi, S. (1994). Cell division and migration in a 'genotype' for neural networks. *Network: Computation in Neural Systems*, 5:497–515.

Chakrabarti, C., and Wang, L.-Y. (1994). Novel sorting network-based architectures for rank order filters. *IEEE Transactions on Very Large Scale Integration (VLSI) Systems*, 2(4):502–507.

Chan, A., and Godsil, C. (1997). Symmetry and eigenvectors. In Hahn, G., and Sabidussi, G., editors, *Graph Symmetry: Algebraic Methods and Applications*, 75–106. Springer.

Chauvin, Y., and Rumelhart, D. E., editors (1995). *Backpropagation: Theory, Architectures, and Applications*. Hillsdale, NJ: Erlbaum.

Chung, K.-L., and Lin, Y.-K. (1997). A generalized pipelined median filter network. *Signal Processing*, 63(1):101 – 106.

Clark, J. E. (2004). *Design, Simulation, and Stability of a Hexapedal Running Robot*. PhD thesis, Department of Mechanical Engineering, Stanford University.

Clune, J., Beckmann, B. E., Ofria, C., and Pennock, R. T. (2009). Evolving coordinated quadruped gaits with the HyperNEAT generative encoding. In *Proceedings of the Eleventh conference on Congress on Evolutionary Computation (CEC'09)*, 2764–2771. Piscataway, NJ, USA: IEEE Press.

Collins, J. J., and Stewart, I. N. (1993). Coupled nonlinear oscillators and the symmetries of animal gaits. *Journal of Nonlinear Science*, 3(1):349–392.

Cornell Computational Synthesis Lab (2010). Cornell Computational Synthesis Lab (CCSL). `http://ccsl.mae.cornell.edu/`.

Deb, K., Agrawal, S., Pratab, A., and Meyarivan, T. (2000). A fast elitist non-dominated sorting genetic algorithm for multi-objective optimization: NSGA-II. *PPSN VI*, 849–858.

Dellaert, F., and Beer, R. D. (1996). A developmental model for the evolution of complete autonomous agents. In Maes, P., Mataric, M. J., Meyer, J.-A., Pollack, J., and Wilson, S. W., editors, *From Animals to Animats 4: Proceedings of the Fourth International Conference on Simulation of Adaptive Behavior*. Cambridge, MA: MIT Press.

Edwards, R., and Glass, L. (2000). Combinatorial explosion in model gene networks. *Chaos*, 10:691–704.

Fahlman, S. E., and Lebiere, C. (1990). The cascade-correlation learning architecture. In Touretzky (1990), 524–532.

Ferrell, C. (1994). Failure recognition and fault tolerance of an autonomous robot. *Adaptive Behavior*, 2(4):375–398.

Filliat, D., Kodjabachian, J., and Meyer, J.-A. (1999). Evolution of neural controllers for locomotion and obstacle avoidance in a six-legged robot. *Connection Science*, 11(3/4):225–242.

Floreano, D., and Mondada, F. (1998). Evolutionary neurocontrollers for autonomous mobile robots. *Neural Networks*, 11:1461–1478.

Gao, L., Liu, S., and Dougal, R. A. (2002). Dynamic lithium-ion battery model for system simulation. *IEEE Transactions on Components and Packaging Technologies*, 25(3):495 – 505.

Gao, L., Sun, P., and Song, J. (2009). Clustering algorithms for detecting functional modules in protein interaction networks. *Journal of Bioinformatics and Computational Biology*, 07(01):217.

GAP (2007). GAP – groups, algorithms, and programming. `http://www.gap-system.org`.

Garcia-Bellido, A. (1996). Symmetries throughout organic evolution. *PNAS*, 93(25):14229–14232.

Golubitsky, M., Shiau, L. J., and Török, A. (2003). Bifurcation on the visual cortex with weakly anisotropic lateral coupling. *SIAM Journal on Applied Dynamical Systems*, 2(2):97–143.

Golubitsky, M., and Stewart, I. (2002). Patterns of oscillation in coupled cell systems. In Newton, P., Holmes, P., and Weinstein, A., editors, *Geometry, Mechanics, and Dynamics: Volume in Honor of the 60th Birthday of J. E. Marsden*, chapter 8, 243–286. Springer.

Gomez, F., and Miikkulainen, R. (2004). Transfer of neuroevolved controllers in unstable domains. In *Proceedings of the Genetic and Evolutionary Computation Conference*. Berlin: Springer.

Graham, L., and Oppacher, F. (2006). Symmetric comparator pairs in the initialization of genetic algorithm populations for sorting networks. *IEEE Congress on Evolutionary Computation, 2006 (CEC 2006)*, 2845–2850.

Gruau, F. (1994a). Automatic definition of modular neural networks. *Adaptive Behavior*, 3(2):151–183.

Gruau, F. (1994b). *Neural Network Synthesis Using Cellular Encoding and the Genetic Algorithm*. PhD thesis, Ecole Normale Superieure de Lyon, France.

Gruau, F., and Whitley, D. (1993). Adding learning to the cellular development of neural networks: Evolution and the Baldwin effect. *Evolutionary Computation*, 1:213–233.

Gruau, F., Whitley, D., and Pyeatt, L. (1996). A comparison between cellular encoding and direct encoding for genetic neural networks. In Koza, J. R., Goldberg, D. E., Fogel, D. B., and Riolo, R. L., editors, *Genetic Programming 1996: Proceedings of the First Annual Conference*, 81–89. Cambridge, MA: MIT Press.

Gunter, C. A., Ngair, T.-H., and Subramanian, D. (1996). Sets as anti-chains. In *ASIAN '96: Proceedings of the Second Asian Computing Science Conference on Concurrency and Parallelism, Programming, Networking, and Security*, 116–128. London, UK: Springer-Verlag.

Heylighen, F. (1999). The growth of structural and functional complexity during evolution. In Heylighen, F., Bollen, J., Riegler, A., and Riegler, A., editors, *The Evolution of Complexity: The Violet Book of 'Einstein Meets Magritte'*, chapter 2, 17–44. Springer.

Hiasat, A., and Hasan, O. (2003). Bit-serial architecture for rank order and stack filters. *Integration, the VLSI Journal*, 36(1-2):3 – 12.

Hillis, W. D. (1991). Co-evolving parasites improve simulated evolution as an optimization procedure. In Farmer, J. D., Langton, C., Rasmussen, S., and Taylor, C., editors, *Artificial Life II*. Reading, MA: Addison-Wesley.

Holmes, P., Full, R. J., Koditschek, D., and Guckenheimer, J. (2006). The dynamics of legged locomotion: Models, analyses, and challenges. *SIAM Review*, 48(2):207–304.

Hornby, G. S., Fujita, M., Takamura, S., Yamamoto, T., and Hanagata, O. (1999). Autonomous evolution of gaits with the sony quadruped robot. In *Proceedings of the Genetic and Evolutionary Computation Conference (GECCO)*, 1297–1304.

Hornby, G. S., and Pollack, J. B. (2002). Creating high-level components with a generative representation for body-brain evolution. *Artificial Life*, 8(3).

Hornby, G. S., Takamura, S., Yokono, J., Hanagata, O., Yamamoto, T., and Fujita, M. (2000). Evolving robust gaits with AIBO. In *Proceedings of the IEEE International Conference on Robotics and Automation*, vol. 3, 3040–3045.

Ijspeert, A. J. (2008). Central pattern generators for locomotion control in animals and robots: A review. *Neural Networks*, 21(4):642–653.

Jakobi, N. (1998). *Minimal Simulations for Evolutionary Robotics*. PhD thesis, School of Cognitive and Computing Sciences, University of Sussex.

Jakobi, N., Husbands, P., and Harvey, I. (1995). Noise and the reality gap: The use of simulation in evolutionary robotics. In Moran, F., Moreno, A., Merelo, J., and Chacon, P., editors, *Advances in Artificial Life*, vol. 929 of *Lecture Notes in Computer Science*, 704–720. Springer Berlin / Heidelberg.

Juillé, H. (1995). Evolution of non-deterministic incremental algorithms as a new approach for search in state spaces. In *Proceedings of the 6th International Conference on Genetic Algorithms*, 351–358. San Francisco, CA, USA: Morgan Kaufmann Publishers Inc.

Kauffman, S. A. (1993). *The Origins of Order*. New York: Oxford University Press.

Kepes, F., editor (2007). *Biological Networks*. World Scientific.

Kimura, H., Akiyama, S., and Sakurama, K. (1999). Realization of dynamic walking and running of the quadruped using neural oscillator. *Autonomous Robots*, 7(3):247–258.

Kipfer, P., Segal, M., and Westermann, R. (2004). Uberflow: A gpu-based particle engine. In *HWWS '04: Proceedings of the ACM SIGGRAPH/EUROGRAPHICS conference on Graphics hardware*, 115–122. New York, NY, USA: ACM.

Kitano, H. (1990). Designing neural networks using genetic algorithms with graph generation system. *Complex Systems*, 4:461–476.

Knuth, D. E. (1998). *Art of Computer Programming: Sorting and Searching*, vol. 3. Addison-Wesley Professional. Second edition.

Koditschek, D. E., Full, R. J., and Buehler, M. (2004). Mechanical aspects of legged locomotion control. *Arthropod Structure and Development*, 33(3):251–272.

Kodjabachian, J., and Meyer, J.-A. (1998). Evolution and development of modular control architectures for 1D locomotion in six-legged animats. *Connection Science*, 10:211–237.

Kohl, N., and Stone, P. (2004a). Machine learning for fast quadrupedal locomotion. In *Nineteenth National Conference on Artificial Intelligence*.

Kohl, N., and Stone, P. (2004b). Policy gradient reinforcement learning for fast quadrupedal locomotion. In *Proceedings of the IEEE International Conference on Robotics and Automation*, vol. 3, 2619–2624.

Koos, S., Mouret, J.-B., and Doncieux, S. (2010). Crossing the reality gap in evolutionary robotics by promoting transferable controllers. In *GECCO '10: Proceedings of the 12th annual conference on Genetic and evolutionary computation*, 119–126. New York, NY, USA: ACM.

Korenek, J., and Sekanina, L. (2005). Intrinsic evolution of sorting networks: A novel complete hardware implementation for FPGAs. In *Evolvable Systems: From Biology to Hardware*, 46–55. Springer.

Korshunov, A. D. (2003). Monotone boolean functions. *Russian Mathematical Surveys*, 58(5):929.

Kovacs, A. (1986). Spontaneous symmetry breaking in biological systems. *Origins of Life and Evolution of Biospheres*, 16:429–430.

Koza, J. R., Goldberg, D. E., Fogel, D. B., and Riolo, R. L., editors (1996). *Genetic Programming 1996*. Cambridge, MA: MIT Press.

Koza, J. R., Koza, J. R., Forest H. Bennett, I., Forest H. Bennett, I., Hutchings, J. L., Bade, S. L., Keane, M. A., and Andre, D. (1998). Evolving computer programs using rapidly reconfigurable field-programmable gate arrays and genetic programming. In *FPGA '98: Proceedings of the 1998 ACM/SIGDA Sixth International Symposium on Field Programmable Gate Arrays*, 209–219. New York, NY, USA: ACM.

le Cun, Y., Denker, J. S., and Solla, S. A. (1990). Optimal brain damage. In Touretzky (1990), 598–605.

Leighton, T., and Plaxton, C. G. (1990). A (fairly) simple circuit that (usually) sorts. In *SFCS '90: Proceedings of the 31st Annual Symposium on Foundations of Computer Science*, 264–274 vol.1. Washington, DC, USA: IEEE Computer Society.

Lindenmayer, A. (1968). Mathematical models for cellular interaction in development parts I and II. *Journal of Theoretical Biology*, 18:280–299 and 300–315.

Lipson, H., Bongard, J., Zykov, V., and Malone, E. (2006). Evolutionary robotics for legged machines: From simulation to physical reality. In *Proceedings of the 9th International Conference on Intelligent Autonomous Systems.*, 11–18.

Luke, S., and Spector, L. (1996). Evolving graphs and networks with edge encoding: Preliminary report. In Koza, J. R., editor, *Late-Breaking Papers of Genetic Programming 1996*. Stanford Bookstore.

Martindale, M. Q., and Henry, J. Q. (1998). The development of radial and biradial symmetry: The evolution of bilaterality. *American Zoologist*, 38(4):672–684.

Mataric, M., and Cliff, D. (1996). Challenges in evolving controllers for physical robots. *Robotics and Autonomous Systems*, 19(1):67–83.

McFarlane, D. (1998). Modular distributed manufacturing systems and the implications for integrated control. In *IEE Colloquium on Choosing the Right Control Structure for Your Process (Digest No. 1998/280)*.

Mehta, D. P., and Sahni, S. (2005). *Handbook of data structures and applications*. CRC Press.

Miglino, O., Lund, H. H., and Nolfi, S. (1995). Evolving mobile robots in simulated and real environments. *Artificial Life*, 2:417–434.

Miller, J. F. (2004). Evolving a self-repairing, self-regulating, French flag organism. In *Proceedings of the Genetic and Evolutionary Computation Conference (GECCO-2004)*. Berlin: Springer Verlag.

Mühlenbein, H., and Höns, R. (2005). The estimation of distributions and the minimum relative entropy principle. *Evolutionary Computation*, 13(1):1–27.

Murtagh, F. (2002). Clustering in massive data sets. In Abello, J., Pardalos, P. M., and Resende, M. G. C., editors, *Handbook of Massive Data Sets*, chapter 14, 501–543. Norwell, MA, USA: Kluwer Academic Publishers.

Nolfi, S., Floreano, D., Miglino, O., and Mondada, F. (1994). How to evolve autonomous robots: Different approaches in evolutionary robotics. In Brooks and Maes (1994), 190–197.

Objet Eden 260V (2010). Objet Eden 260V. `http://www.objet.com/3D-Printer/Eden260V/`.

ODE (2007). ODE: Open dynamics engine. `http://www.ode.org/`.

OGRE (2007). OGRE: Object-oriented graphics rendering engine. `http://www.ogre3d.org/`.

OPAL (2007). OPAL: Open physics abstraction layer. `http://opal.sourceforge.net/`.

Open BEAGLE (2007). Open BEAGLE. `http://beagle.gel.ulaval.ca/`.

Palmer, A. R. (2004). Symmetry breaking and the evolution of development. *Science*, 306:828–833.

Pinto, C. M. A., and Golubitsky, M. (2006). Central pattern generators for bipedal locomotion. *Journal of Mathematical Biology*, 53(3):474–489.

Raibert, M. H. (1986). Legged robots. *Communications of the ACM*, 29(6):499–514.

Raibert, M. H., Chepponis, M., and H. Benjamin Brown, J. (1986). Running on four legs as though they were one. *IEEE Journal of Robotics and Automation*, 2(2):70–82.

Righetti, L., and Ijspeert, A. J. (2008). Pattern generators with sensory feedback for the control of quadruped locomotion. In *Proceedings of the 2008 IEEE International Conference on Robotics and Automation (ICRA 2008)*, 819–824.

Robotis (2010). Robotis. `http://www.robotis.com/`.

Rumelhart, D. E., Hinton, G. E., and Williams, R. J. (1986). Learning internal representations by error propagation. In Rumelhart, D. E., and McClelland, J. L., editors, *Parallel Distributed Processing: Explorations in the Microstructure of Cognition, Vol. 1: Foundations*, 318–362. Cambridge, MA: MIT Press.

Seo, K., and Slotine, J. J. E. (2007). Models for global synchronization in CPG-based locomotion. In *Proceedings of the 2007 IEEE International Conference on Robotics and Automation*, 281–286.

Seo, S.-W., yun Feng, T., and Kim, Y. (1993). A simulation scheme in rearrangeable networks. In *Proceedings of the 36th Midwest Symposium on Circuits and Systems*, 177 – 180 vol. 1.

Shastri, S. V. (1997). A biologically consistent model of legged locomotion gaits. *Biological Cybernetics*, 76(6):429–440.

Shmulevich, I., Sellke, T. M., Gabbouj, M., and Coyle, E. J. (1995). Stack filters and free distributive lattices. In *Proceedings of the 1995 IEEE Workshop on Nonlinear Signal and Image Processing*, 927–930. IEEE Computer Society.

Siebel, N. T., and Sommer, G. (2007). Evolutionary reinforcement learning of artificial neural networks. *International Journal of Hybrid Intelligent Systems*, 4(3):171–183.

Sims, K. (1994a). Evolving 3D morphology and behavior by competition. In Brooks and Maes (1994), 28–39.

Sims, K. (1994b). Evolving 3D morphology and behavior by competition. In Brooks, R. A., and Maes, P., editors, *Proceedings of the Fourth International Workshop on the Synthesis and Simulation of Living Systems (Artificial Life IV)*, 28–39. Cambridge, MA: MIT Press.

SolidWorks (2010). SolidWorks. `http://www.solidworks.com/`.

145

Stanley, K. (2007). Compositional pattern producing networks: A novel abstraction of development. *Genetic Programming and Evolvable Machines*, 8(2):131–162.

Stanley, K. O., D'Ambrosio, D. B., and Gauci, J. (2009). A Hypercube-Based encoding for evolving Large-Scale neural networks. *Artificial Life*, 15(2):185–212.

Stanley, K. O., and Miikkulainen, R. (2003). A taxonomy for artificial embryogeny. *Artificial Life*, 9(2):93–130.

Stanley, K. O., and Miikkulainen, R. (2004). Competitive coevolution through evolutionary complexification. *Journal of Artificial Intelligence Research*, 21:63–100.

Steiner, T., Jin, Y., and Sendhoff, B. (2009). Vector field embryogeny. *PLoS ONE*, 4(12):e8177.

Stone, P., and Veloso, M. (2000). Multiagent systems: A survey from a machine learning perspective. *Autonomous Robots*, 8(3):345–383.

Téllez, R. A., Angulo, C., and Pardo, D. E. (2006). Evolving the walking behaviour of a 12 DOF quadruped using a distributed neural architecture. In *Biologically Inspired Approaches to Advanced Information Technology*, Lecture Notes in Computer Science 3853, 5–19. Berlin: Springer.

Touretzky, D. S., editor (1990). *Advances in Neural Information Processing Systems 2*. San Francisco: Morgan Kaufmann.

Watson, R. A., Ficici, S. G., and Pollack, J. B. (2002). Embodied evolution: Distributing an evolutionary algorithm in a population of robots. *Robotics and Autonomous Systems*, 39(1):1 – 18.

Watson, R. A., and Jansen, T. (2007). A building-block royal road where crossover is provably essential. In *Proceedings of the 9th annual conference on Genetic and evolutionary computation (GECCO '07)*, 1452–1459. New York, NY, USA: ACM.

Yeh, Y.-M., and Feng, T.-y. (1992). On a class of rearrangeable networks. *IEEE Transactions on Computers*, 41(11):1361–1379.

Zagal, J. C., and Ruiz-Del-Solar, J. (2007). Combining simulation and reality in evolutionary robotics. *Journal of Intelligent and Robotic Systems*, 50(1):19–39.

Zhang, S. S., Xu, K., and Jow, T. R. (2003). The low temperature performance of li-ion batteries. *Journal of Power Sources*, 115(1):137 – 140.

Zykov, V., Bongard, J., and Lipson, H. (2004). Evolving dynamic gaits on a physical robot. In *Proceedings of the Genetic and Evolutionary Computation Conference, Late-Breaking Papers*.

Vita

Vinod K. Valsalam entered the Indian Institute of Technology (IIT), Madras, India in 1992 and graduated with a Bachelor of Technology degree in Aerospace Engineering in 1996. After graduating from IIT, he moved to Starkville, Mississippi, where he studied Computational Engineering at Mississippi State University, eventually graduating with a Master of Science degree in 1998. Thereafter, he worked as a researcher in Computer Science at Mississippi State University. In 2002, he entered the University of Texas at Austin, Texas to pursue a doctorate degree in Computer Science.

Permanent Address: Department of Computer Sciences

1 University Station

C0500

Austin, TX 78712

This dissertation was typeset with LATEX 2$_\varepsilon$[1] by the author.

---

[1]LATEX 2$_\varepsilon$ is an extension of LATEX. LATEX is a collection of macros for TEX. TEX is a trademark of the American Mathematical Society. The macros used in formatting this dissertation were written by Dinesh Das, Department of Computer Sciences, The University of Texas at Austin, and extended by Bert Kay, James A. Bednar, and Ayman El-Khashab.